Universitat Politècnica de Catalunya
Facultat de Matemàtiques i Estadística

Master in Advanced Mathematics and Mathematical Engineering

Master's thesis

A Study on the Generation of Chaos due to the Presence of Smale Horseshoes in Dynamical Systems with a Homoclinic Orbit

Pol Deulofeu Matas

Supervised by Inma Baldomá Barraca and Pau Martín de la Torre

June, 2020

I would like to thank Inma and Pau, my thesis supervisors, for their patience and guidance. I would also like to thank my family and friends for their unconditional support.

Abstract

One of the fundamental problems in dynamical systems is the detection and characterisation of chaotic behaviours. In this work we will focus on chaos induced by what is called the Smale horseshoe. Smale horseshoes frequently appear, but not exclusively, in the hyperbolic context and in what is known as the Sil'nikov Phenomenon. We will also present a generalization of the described phenomenons to systems with parabolic points.

Keywords

Dynamical systems, chaos, Smale horseshoe Sil'nikov variables, hyperbolic points, parabolic points.

1. Introduction

When working with differential equations or discrete dynamical systems one may come across some fascinating and unique behaviours. It is possible that the reader may have come across at some point with an illustrative quote by Edward Norton Lorenz.

When a butterfly flutters its wings in one part of the world, it can eventually cause a hurricane in another.

It is no coincidence that Lorenz ended up making such a statement. When studying systems of differential equations used to model atmospheric phenomenons in 1961, Lorenz unexpectedly stumbled upon a mathematical property that had never been described before. In one occasion, he was using a computer to simulate weather patterns with his differential equation models. He wanted to see a sequence of data again and to save time he started the simulation in the middle of its course, expecting similar results. He did this by entering data that corresponded to conditions in the middle of the original simulation. Surprisingly, the new computations showed a completely different prediction from the previous one. What happened was that the computer printout rounded variables up to the third digit, for instance, 0.687341 was printed as 0.687. This almost insignificant difference would generally be accepted to have no practical effect. However, Lorenz discovered that small changes in initial conditions can produce massive changes on a long-term basis. This discovery allowed Lorenz to state that in general it is not possible to make precise long-term weather predictions. This is the idea behind the butterfly quote and it is currently known as chaos. One may perceive that chaos has a very deep impact when studying flows induced by differential equations or discrete dynamical systems induced by maps. This is why many results have been developed and different situations have been explored in order to detect chaos and the mechanisms that produce it. One of the mechanisms that generate chaos in dynamical systems was discovered by Stephen Smale. Smale proved that when we have a region in our system that is stretched in one direction and then compressed in another direction and after that it is folded onto itself, then the dynamics in a subset of that region is chaotic, in a very precise sense. This stretching, compressing and folding is what is known as a horseshoe map or Smale horseshoe (Figure 1), due to its resemblance with a real-life horseshoe. The procedure used to

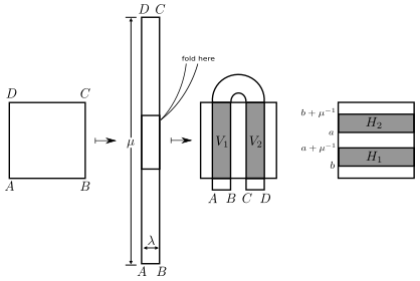

Figure 1: Stretch, compression and folding of a square.

show that chaos exists when a dynamical system has a horseshoe is absolutely brilliant. It is done by first denoting each "side" of the horseshoe with a symbol. Then, by following the journey a point of the region undertakes under the iteration of the horseshoe map, we can create a sequence with the chosen symbols that will represent this journey. Then, it can be proved that the set of all of these sequences is a metric space. In this metric space we can then define a dynamical system induced by a map called the *shift*. This shift map is then proved to be chaotic and by showing that the dynamics of the shift are equivalent to the dynamics of the points inside the horseshoe, we have that the region that contains the horseshoe also

contains chaos. Therefore, it is important to learn how to detect when a system may have a horseshoe. The existence of horseshoes is often related to the interaction between two manifolds that exist within a dynamical system, the stable and the unstable manifolds of hyperbolic fixed points. The orbits of points in these manifolds tend to the fixed point when time goes to positive infinity in the case of the stable manifold and negative infinity in the case of the unstable manifold. When looking for chaos induced by horseshoes, it is crucial to detect when the intersection between the stable and the unstable manifold is non-empty. We distinguish between two different situations. If these two manifolds meet transversally, we get what is known as a homoclinic tangle. This means that if the stable and unstable manifolds intersect, then, the orbits of points near them fold intersecting one of the manifolds infinitely many times. This event

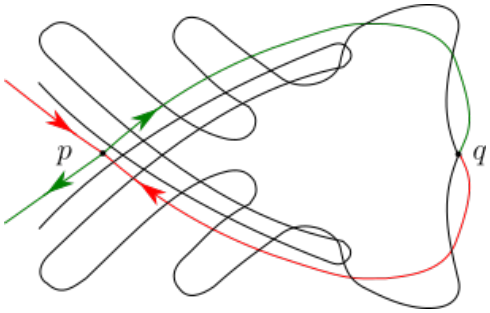

Figure 2: A case of two entangled manifolds

leads to the existence of horseshoes in a region of the dynamical system and therefore chaos. Another interesting situation happens when the intersection between the two manifolds is not transversal, but one of them is contained inside the other. This work focuses around a particular case of this situation which is when in dimension 3, the unstable manifold is contained inside the stable manifold. We will study in depth a result given by Russian mathematician Kirill Alexandrovitch Sil'nikov in 1965. Sil'nikov proved that for a system with a fixed point and a one-dimensional unstable manifold contained into a two-dimensional stable manifold could lead to chaos. This kind of relationship between the two manifolds gives way to the existence of a homoclinic orbit, which is an orbit that at positive infinity tends to the fixed point as well as at negative infinity. When this occurs, if the system satisfies certain conditions on the tangent space

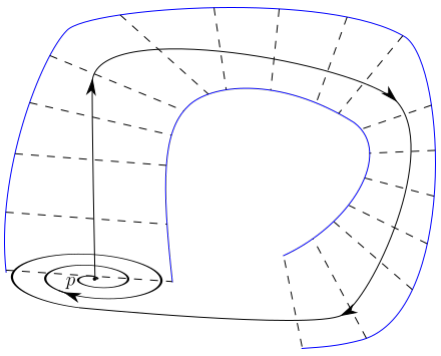

Figure 3: A system with a homoclinic orbit. The one dimensional stable manifold (pointing upwards from the fixed point p) is contained inside the two-dimensional stable manifold (tangent to the fixed point p).

of the fixed point, then there is a transversal section at the homoclinic orbit that contains a countable set of horseshoes. It is important to stress the fact that in this case, the number of horseshoes is *countable*.

This means that it is a much more chaotic situation in comparison to the case of the homoclinic tangle, where we can only assure that there is one region with *one* horseshoe. The proof of this result by Sil'nikov can be found in Guckenheimer and Holmes [7]. The proof shows that by following the orbits of points near the homoclinic orbit one can build a return map on a transversal section of the homoclinic orbit that contains a countable set of horseshoes (see Section 5). However, this proof requires a very precise analysis of the trajectories that flow close to the fixed point so in Guckenheimer and Holmes in order to simplify the proof, the authors assume that the system (which is thought as a generic system) can be turned into a linear system of differential equations. This is not true in general and further bibliographical research is required.

At this point, a key idea at understanding systems with homoclinic orbits is introduced in the form of a change of variables. Instead of thinking the problem in the usual cartesian variables, we consider two transversal sections and we take as a variable the time that the orbit of a point needs to go from one of the sections to the other (See Figure 4). This idea of considering two sections and taking the time a point needs

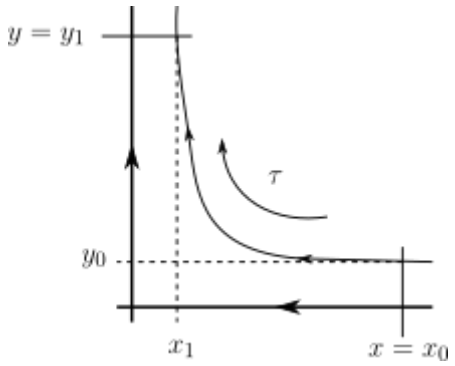

Figure 4: To exemplify the idea, in dimension 2 we consider two sections. The time τ that a point needs to go from one section to the other is thought of as a variable

to reach the top section as a variable is presented by Bo Deng in [3]. Due to their relevance, in this work we follow the results that appear in his work (See Section 6). Going back to the proof by Guckenheimer and Holmes, the work of Deng turns out to be very convenient. At some point, Deng introduces an expansion of the solutions that allows us to give an unpublished proof of the result by Sil'nikov (Section 8). It is worth mentioning that the work of Deng is for arbitrary dimension (Sil'nikov's results are in dimension 3) and he even proves a similar result to the one by Sil'nikov in arbitrary dimension too. We expose this result in Section 7 and, due to its high complexity, we only give a brief sketch of the proof.

All the results on systems with homoclinic orbits that we have referred to up to now assume that the differential matrix of the fixed point is hyperbolic, which means that it has a of non-degeneracy property with respect to the real part of the matrix eigenvalues. There is no bibliography about what happens when the fixed point is parabolic, which means that one of the eigenvalues has real part equal to 0. This is why in this work we have devoted a section to the study of some examples of this kind of situation (Section 9). We look at cases that can be transformed to non-degenerate systems by means of a change of time and systems that can be explicitly integrated. This allows us to discuss when does the system present chaos or not. It is difficult to identify any kind of behaviour pattern with these few examples. This leaves a very wide opening for future research.

This sections in this work are organized as follows. In Section 2 we give an introduction of the idea of chaos and how it is rigorously defined. In Section 3 we present a central object in this work, the Smale

horseshoe. In Section 4 we introduce the idea of structural stability and the bifurcation problem that we will study, the Sil'nikov bifurcation. In Section 5 we dive into the proof of the existence of horseshoes in the Sil'nikov bifurcation. Section 6 shows Bo Deng's approach to the Sil'nikov problem which will later be a fundamental part in the proof of the Sil'nikov Theorem in arbitrary dimension showed in Section 7. We then use Deng's ideas in Section 8 to make a new unpublished proof of Sil'nikov's Theorem. To end up with, Section 9 is devoted to an innovative generalization of the Sil'nikov Theorem to parabolic cases.

2. Introduction to Chaos

This work is concerned with the detection of chaos in dynamical systems. It is true that the word "chaos" is very illustrative when describing a certain behaviour but, how do we define it rigorously? In this section we will follow the course notes from Inma Baldomá Barraca and Pau Martín [2] except for the last subsection, Subsection 2.5 which follows the development by Guckenheimer and Holmes [7]. We will introduce notions of dynamical systems which will enable us to understand a first fundamental example, the Logistic Map. What we call the Logistic Map is in fact a uniparametric family of maps that present extremely rich dynamics. We will see that this family of maps presents a cascade bifurcation (Figure 5). Although the cascade bifurcation is a very attractive object to study, at least visually, we will focus on another aspect of the Logistic Map. This is the fact that for certain parameters we can codify the dynamics of points with symbols. This codification is the key idea that will open the door to understanding what is a chaotic behaviour and how chaos can be precisely defined.

2.1 A First Example of Chaos

In this section we will introduce the reader to a simple yet illustrative example of chaotic behaviour, the *Logistic Map*, a map designed to model population growth. First of all, we give some fundamental definitions.

Definition 2.1. Consider X to be a topological space, let $f : X \to X$ be a diffeomorphism. The orbit of a point $x \in X$ under the iteration of f is

$$\bigcup_{i\in\mathbb{Z}} f^i(x). \tag{1}$$

A point $x^* \in X$ is an n-periodic point for f if

$$f^n(x^*) = x^* \quad \text{for some } n \in \mathbb{N}. \tag{2}$$

A 1-periodic point ($f(x^*) = x^*$) is called a fixed point.

The expression of the Logistic Map is the following.

$$f_\mu(x) = \mu x(1-x) \quad x \in [0,1] \quad \text{and} \quad \mu > 1 \tag{3}$$

where μ is a parameter that represents the reproduction ratio of the population. We can see that if x is small, the map is approximately $f_\mu(x) = \mu x$. If x increases, there are less resources available which means that either mortality increases or births decrease. Observe that the units of population are such that the maximum is 1. This map has fixed points $x = 0$, which corresponds to extinction and $x = (\mu - 1)/\mu$. The behaviour of this map changes with μ in very interesting ways. For instance, when $2 \leq \mu < 4$, the

bifurcation diagram of periodic points has a cascade structure. Figure 5 shows this cascade bifurcation. For every μ, each value on the vertical axis represents a point in a periodic orbit. At first glance, it looks like there is no pattern and in fact, it is yet unknown. It is important though to notice that for some values of μ (≈ 3.61 for instance), we have a 3-periodic orbit. Due to a theorem by the Ukranian mathematician Sarkovskii, it is known that if a discrete dynamical system has a 3-periodic orbit, then there are periodic points of any period. This is clearly an erratic behaviour. For $\mu \geq 4$ we encounter a surprising behaviour.

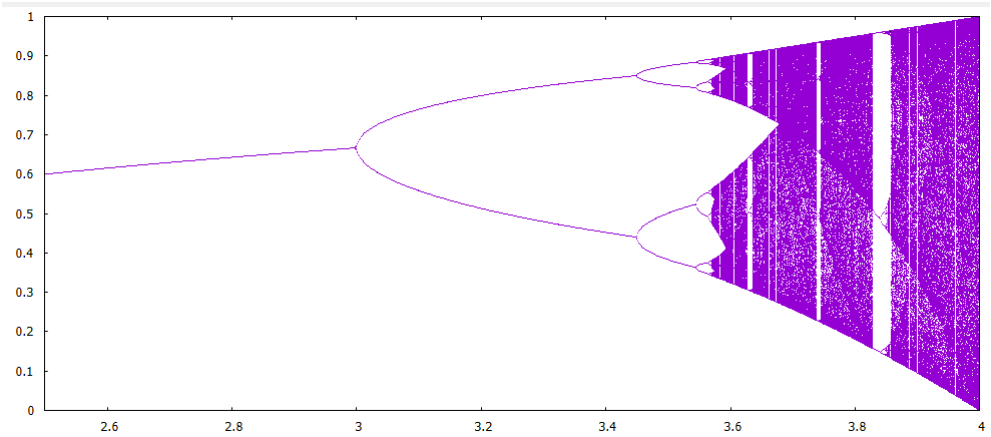

Figure 5: As μ increases (horizontal axis), the number of periodic points bifurcate in the form of a cascade.

Start by considering what happens when $\mu = 4$ which is the last value for which the map maps the interval [0,1] onto itself. We will first take a look to what happens when we follow orbits which are close together $x_0 = 0.1$ and $x_1 = 0.10000001$.

x_0	x_1
$f_4(x_0) = 0.36$	$f_4(x_1) = 0.3600000319999996$
$f_4^2(x_0) = 0.9216$	$f_4^2(x_1) = 0.9216000358399954$
$f_4^3(x_0) = 0.2890137599999997$	$f_4^3(x_1) = 0.2890136391188584$
$\vdots$	$\vdots$
$f_4^{20}(x_0) = 0.8200138734368849$	$f_4^{20}(x_1) = 0.8332436027386397$
$f_4^{21}(x_0) = 0.5903644832316856$	$f_4^{21}(x_1) = 0.5557948049350867$
$f_4^{22}(x_0) = 0.9673370406810817$	$f_4^{22}(x_1) = 0.9875477589690225$
$f_4^{23}(x_0) = 0.1263843616297959$	$f_4^{23}(x_1) = 0.0491887308971359$
$f_4^{24}(x_0) = 0.4416454190608994$	$f_4^{24}(x_1) = 0.1870767985994601$
$f_4^{25}(x_0) = 0.9863789715336878$	$f_4^{25}(x_1) = 0.6083162801009485$
$\vdots$	$\vdots$
$f^{50}(x_0) = 0.4960128314016922$	$f^{50}(x_1) = 0.1218180732050873$
$f^{51}(x_0) = 0.9999364099462746$	$f^{51}(x_1) = 0.4279137209827491$
$f^{52}(x_0) = 0.0002543440401217$	$f^{52}(x_1) = 0.9792142735097882$
$\vdots$	$\vdots$

Figure 6: Orbits of $x_0 = 0.1$ and $x_1 = 0.10000001$ under the map f_4

In first place, we notice that neither the iterates of x_0 or x_1 seem to have any kind of limit or period.

The following figure shows a graph of how many times the iterates of $f_4(x_0)$ visit each interval of length 10^{-3}. So it is unclear whether the iteration under f_4 of these points has any kind of limit. Also, notice that

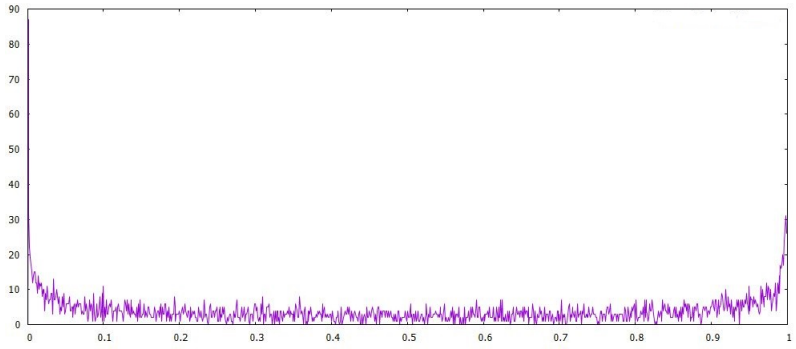

Figure 7: Graph showing the number of times $f_4^n(x_0)$ visits each partition of [0,1]

although x_0 and x_1 are fairly close together, after only 25 iterations of the map, the values of the iterates for these points are completely different. This is known as *sensitivity with respect to initial conditions* and it is characteristic of a chaotic dynamical system.

As we have already said, for values of μ smaller than 4, the dynamics of f_μ consist of periodic points which bifurcate in the form of a cascade, but what is truly relevant to this work are the cases when $\mu > 4$. Assume $\mu > 4$. We now have that $f_\mu([0,1]) \subset [0,1]$ is no longer true. It is clear that points $x \in [0,1]$ for which their image is above 1 end up at $-\infty$. Denote by A_0 this set of points. Then, $A_1 = f_\mu^{-1}(A_0) = \{x \in [0,1] | f_\mu(x) \in A_0\}$ is the set of points that abandon [0,1] after two iterations of f_μ. Inductively we define $A_k = f_\mu^{-1}(A_{k-1}) = \{x \in [0,1] | f_\mu^k(x) \in A_0\}$, the set of point that abandon $[0,1]$ after $k+1$ iterations. Therefore, $\cup_{n\geq 0} A_k$ are the points that leave $[0,1]$ at some point. Thus, we can consider

$$\Lambda = [0,1] \setminus \left(\bigcup_{k\geq 0} A_k\right) \tag{4}$$

which is the set of points in [0,1] whose orbits never leave [0,1].

We will now proceed to describe Λ. We start by observing that A_0 is an open interval centered at $1/2$ and $[0,1] \setminus A_0$ consists of two intervals I_0 and I_1, one at each side of A_0. Moreover, f_μ is non-constant at both I_0 and I_1. Also, $f_\mu(I_0) = f_\mu(I_1) = [0,1]$. Hence, $A_1 = f_{-\mu}^{-1}(A_0)$ consists of four open intervals, contained in I_0 and I_1. Again, f_μ^2 of each of these intervals is [0,1] and in general we can induce that A_n consists of 2^n disjoint open intervals. Also, f_μ^{n+1} sends each of these intervals monotonously to all of [0,1]. This is, the graph of f_μ^{n+1} has 2^n maxima above 1 and 2^{n-1} minima beneath 0, which means that the graph of $f^n\mu$ crosses the diagonal at least 2^n times. Hence, f_μ has at least 2^n periodic points.

This inductive construction of Λ may remind the reader of the construction of the middle-third Cantor Set, which is precisely what we are going to prove now. Recall the definition of a Cantor Set,

Definition 2.2. A set $\Gamma \subset I = [0,1]$ is a Cantor Set if it is a closed, nowhere dense and perfect subset of I. A set is nowhere dense if it does not contain open intervals and it is perfect if every point is a accumulation point of the set.

We have the following theorem.

Theorem 2.3. *If $\mu > 2 + \sqrt{5}$, the set Λ is Cantor Set.*

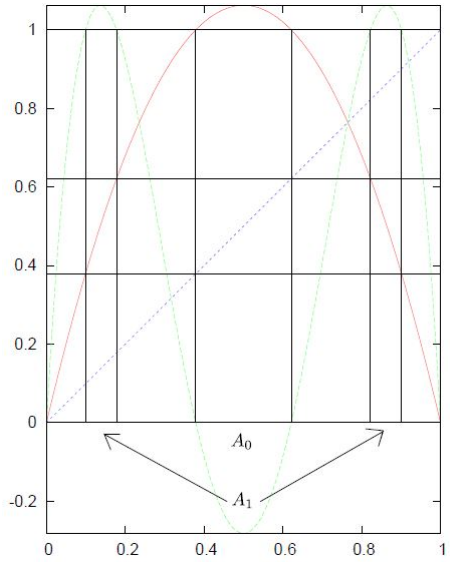

Figure 8: Graph of $f_\mu(x) = \mu x(1-x)$, f_μ^2 and $y = x$ for $\mu = 4.25$. We also show the sets A_0 and A_1.

Proof. We define

$$\Lambda_n = [0,1] \setminus (\bigcup_{k\geq}^{n} A_k). \tag{5}$$

We can induce that $\Lambda_{n+1} = \Lambda_n \setminus A_{n+1} = \Lambda_n \cap A_{n+1}^C$ (where A^C denotes the complementary of a set). We can clearly see that Λ_{n+1} is a closed set and that $\Lambda_{n+1} \subset \Lambda_n$. Hence, as $\Lambda \subset \cap_{k\geq 0}\Lambda_k$, we have that Λ is a nonempty closed set. Observe that for this part we only need that $\mu > 4$.

If $\mu > 2+\sqrt{5}$, we can immediately check that $|f'_\mu(x)| > 1$ for any $x \in I_0 \cup I_1$. Hence, there exists $\lambda > 1$ such that $|f'_\mu(x)| > \lambda$ for any $x \in \Lambda$. The chain rule allows us to assure that $|f'_\mu(x)| > \lambda^n$ for any $x \in \Lambda$ and $n \geq 1$. To prove that Λ does not contain intervals, we will force a contradiction. Assume that Λ does contain an interval $[x,y] \subset \Lambda$. Since $\lambda > 1$, we can choose n such that $\lambda^n|x-y| > 1$. Then, by the Mean Value Theorem, we have that $|f_\mu^n(x) - f_\mu^n(y)| \geq \lambda^n|x-y| > 1$, which means that either $f_\mu^n(x)$ or $f_\mu^n(y)$ are outside of $[0,1]$, which contradicts the fact that $x, y \in \Lambda$.

Finally, we prove that Λ is perfect. First we observe that the endpoints of the open intervals A_k belong to Λ, as their image under f_μ^{k+1} is 1 and therefore, the rest of the orbit will be 0. Assume now that p is an isolated point of Λ. This means that every point in a neighbourhood of p leaves the interval $[0,1]$. Therefore, it belongs to some A_k. Hence, there are two possibilities, either there is a neighbourhood U of p such that $U \setminus \{p\}$ is contained in one of the A_k or p is the limit of endpoints of sets A_k. In the latter case, as the endpoints of A_k belong to Λ, we have found a sequence in Λ which tends to p. In the first case, we have that $f_\mu^{k+1}(U \setminus \{p\}) > 1$, which implies that $f_\mu^{k+1}(p) = 1$. Then $f_\mu^{k+1}(U \setminus \{p\}) < 0$ and $f_\mu^{k+1}(p) = 0$. This is, f_μ^{k+1} has a maximum at p and therefore, $(f_\mu^{k+1})'(p) = 0$ and, by the chain rule, $f'_\mu(f_\mu^j(p)) = 0$ for some $1 \leq j \leq k+1$. We then have that $f_\mu^j(p) = 1/2$ and $f_\mu^{j+1}(p) > 1$ which contradicts the fact that $p \in \Lambda$. Also, observe that for this part of the argument we do not require $\mu > 2+\sqrt{5}$ either. □

Remark 2.4. For $\mu > 4$ the set Λ is also a Cantor set, but the proof is more involved. See the book by Devaney [6].

With the example of the logistic map, we have seen an example where we encounter an invariant set of points with a highly complex structure, the Cantor set. It is possible though, to obtain information on the dynamics of the map f_μ on these points through a surprising, yet extremely useful tool. This tool that we refer to is known as *Symbolic Dynamics* and it will help us to understand complex behaviours in a simple and visual way.

2.2 Symbolic Dynamics

In Theorem 2.3 we have described the topology of Λ. We now want to describe the dynamics in Λ under the iteration of f_μ. In order to do so, we will use a brilliant idea which is to give a *symbolic* description to Λ which we will later prove to be equivalent to the iteration of f_μ. This symbolic description will allow us to understand better the behaviour of f_μ.

Definition 2.5. We define the space of two symbol sequences Σ as

$$\Sigma = \{\mathbf{a} = (a_0, a_1, ...) | a_i = 0 \text{ or } 1\}.$$

Note that in this definition of Σ, 0 and 1 are treated as symbols, not as numbers. We could choose any other couple of symbols for Σ.

We consider Σ with the product topology. Since it is a metrizable space we can give an equivalent distance. Let $\mathbf{a}$ and $\mathbf{b} \in \Sigma$, the distance between these two points is

$$d(\mathbf{a}, \mathbf{b}) = \sum_{i \geq 0} \frac{|a_i - b_i|}{2^i}. \tag{6}$$

Proposition 2.6. *The function d defines a metric over Σ.*

Proof. It is quite straightforward that $d(\mathbf{a}, \mathbf{b}) \geq 0$, $d(\mathbf{a}, \mathbf{b}) = d(\mathbf{b}, \mathbf{a})$ and $d(\mathbf{a}, \mathbf{b}) = 0$ if and only if $\mathbf{a} = \mathbf{b}$. From $|a_i - b_i| \leq |a_i - c_i| + |c_i - b_i|$ for $\mathbf{c} \in \Sigma$, we deduce that $d(\mathbf{a}, \mathbf{b}) \leq d(\mathbf{a}, \mathbf{c}) + d(\mathbf{c}, \mathbf{b})$ □

The following proposition allows us to determine if two sequences in Σ are close to each other.

Proposition 2.7. *Let $\mathbf{a}, \mathbf{b} \in \Sigma$ such that $a_i = b_i$ for every $0 \leq i \leq n$. Then $d(\mathbf{a}, \mathbf{b}) \leq 1/2^n$.*

Reciprocally, if $d(\mathbf{a}, \mathbf{b}) < 1/2^n$, then $a_i = b_i$ for $0 \leq i \leq n$.

Proof. If $a_i = b_i$ for $0 \leq i \leq n$,

$$d(\mathbf{a}, \mathbf{b}) = \sum_{i=0}^{n} \frac{|a_i - b_i|}{2^i} + \sum_{i \geq n+1} \frac{|a_i - b_i|}{2^i} \leq \sum_{i \geq n+1} \frac{1}{2^i} = \frac{1}{2^n}.$$

And, if $a_i \neq b_i$ for some $i \leq n$, then

$$d(\mathbf{a}, \mathbf{b}) \geq \frac{1}{2^i} \geq \frac{1}{2^n}.$$

Hence, if $d(\mathbf{a}, \mathbf{b}) \leq 1/2^n$, then $a_i = b_i$ for $0 \leq i \leq n$. □

Once we have defined the metric space Σ, we now define a map which will define a dynamical system in Σ that will model the dynamic of f_μ in Λ through an homeomorphism.

Definition 2.8. The shift map is a map $\sigma : \Sigma \to \Sigma$ that shifts indices in the sense that,

$$\sigma(a_0, a_i, a_2, ...) = (a_1, a_2, ...).$$

This is, $\sigma(\mathbf{a})$ discards a_0 and relocates the other components of the sequence one place to the left.

Proposition 2.9. *The shift map σ is continuous.*

Proof. Let $\mathbf{a} \in \Sigma$ and $\varepsilon > 0$. Take $n > 0$ such that $1/2^n < \varepsilon$ and $\delta = 1/2^{n+1}$. Then if $d(\mathbf{a}, \mathbf{b}) < \delta$, Proposition 2.7 assures us that $a_i =_i$ for $0 \leq i \leq n+1$. Hence, $\sigma(\mathbf{a})_i = a_{i+1} = b_{i+1} = \sigma(\mathbf{b})_i$, for $0 \leq i \leq n$ and again, by Proposition 2.7, $d(\sigma(\mathbf{a}), \sigma(\mathbf{b})) < 1/2^n < \varepsilon$. □

The following Proposition presents the important dynamical features induced by σ.

Proposition 2.10.
1. *A sequence $\mathbf{a} \in \Sigma$ is a periodic point of σ if and only if there exists $n \geq 0$ such that $a_i = a_{i+n}$ for every $i \geq 0$. The period of $\mathbf{a}$ is n.*
2. *The number of n-periodic points of σ is 2^n.*
3. *The periodic points of σ are dense in Σ.*
4. *There is a dense orbit in Σ.*

Proof. Let $\sigma : \Sigma \to \Sigma$ be the shift map. Then, Item 1 is a consequence of $\sigma^n(\mathbf{a})_i = a_{i+n}$. Item 2 is directly derived from 1.

Item 3 is due to the definition of the distance in Σ. Indeed, given any sequence $\mathbf{a} \in \Sigma$, consider for every $n > 0$ the periodic sequence $\mathbf{a}_n$ such that $(\mathbf{a}_n)_i = a_i$ if $i \leq n$. Then, from Proposition 2.7, we have

$$d(\mathbf{a}, \mathbf{a}_n) \leq \frac{1}{2^n} \xrightarrow[n\to\infty]{} 0.$$

Finally, for the last item, it is enough to consider the sequence

$$\mathbf{s} = (01\,|\,00\,01\,10\,11\,|\,000\,001\,010\,100\,011\,101\,110\,111\,|\,...)$$

composed of all the blocks of length n, for all $n \geq 1$ laid consecutively. For any $\mathbf{a} \in \Sigma$ and any $\varepsilon > 0$, there is an $n \geq 0$ such that $d(\sigma^n(\mathbf{s}), \mathbf{a}) < \varepsilon$. Indeed, let m be such that $\frac{1}{2^m} < \varepsilon$. Then there exists n_m such that $\sigma^{n_m}(\mathbf{s}) = (a_1, \dots, a_m, ...)$. Then by Proposition 2.7 $d(\sigma^{n_m}(\mathbf{s}), \mathbf{a}) \leq \frac{1}{2^m} \leq \varepsilon$. □

In Σ periodic points under σ have a regular dynamic. If an initial condition is in a periodic orbit, it remains inside the periodic orbit. Point 2 in Proposition 2.10 tells us that the subset of points in Σ that have a regular behaviour is dense. On the other hand, Point 3 contemplates an orbit that is dense in Σ, which depicts a behaviour far from regular.

2.3 Topological Conjugacy with the Shift Map

We will now establish the precise meaning of what we informally claimed before by announcing that the dynamics of f_μ in Λ are modelled by the shift map σ in Σ.

Recall that $\Lambda \subset I_0 \cup I_1$ is the set of points for which its orbit under f_μ (defined in (3)), with $\mu > 4$ remains in [0,1] for all n. See Formula (5) and Figure 8.

Now we assign to every $x \in \Lambda$ a sequence in Σ.

Definition 2.11. We identify the itinerary of a point $x \in \Lambda$ with a sequence $S(x) = (s_0, s_1, s_2, ...)$ where $s_i = 0$ if $f_\mu^i(x) \in I_0$ and $s_i = 1$ if $f_\mu^i(x) \in I_1$.

With this definition, $S(x)$ contains the itinerary that x follows between I_0 and I_1. Also, due to its construction, $S : \Lambda \to \Sigma$ satisfies that

Theorem 2.12. $S \circ f_\mu = \sigma \circ S$.

Proof. Assume that $S(x)_i = \ell$, where $\ell \in \{0, 1\}$. By definition, this happens if and only if $f_\mu^i(x) \in I_\ell$. Hence $(\sigma \circ S(x))_{i-1} = \ell$, but as $f_\mu^{i-1}(f_\mu(x)) = f_\mu^i(x) \in I_\ell$ we have that $S(f_\mu(x))_{i-1} = \ell$. □

Observe that, at first glance, Theorem 2.12 does not tell us much. For instance, we know nothing of the set $S(\Lambda)$ that could potentially be small. Also, we have no information about the relationship that S establishes between the dynamics of f_μ and σ. The following theorem answers this question.

Theorem 2.13. *If $\mu > 2 + \sqrt{5}$, then $S : \Lambda \to \Sigma$ is a homeomorphism.*

Proof. We first prove that S is injective. Let $x, y \in \Lambda$ and suppose that $S(x) = S(y)$. This is, for all n, $f_\mu^n(x)$ and $f_\mu^n(y)$ are at the same side of $1/2$. As f_μ is nonconstant at each of these sides, we also have that f_μ is nonconstant at the interval between $f_\mu^n(x)$ and $f_\mu^n(y)$ for all n. This implies that this interval remains in $I_0 \cup I_1$ which is a contradiction with the fact that Λ is nowhere dense. Hence, S is injective.

We now check that S is surjective. Recall that f_μ has a maximum at $x = 1/2$ and that $f_\mu(x) = f_\mu(1-x)$. Hence, if $J \subset [0, 1]$ is an interval, $f_\mu^{-1}(J)$ consists of two disjoint intervals, one in I_0 and the other in I_1.

Now, let $\mathbf{s} = (s_0, s_1, s_2, ...) \in \Sigma$. Define

$$\begin{aligned} I_{s_0,\dots,s_n} &= \{x \in [0, 1] | x \in I_{s_0},\ f_\mu(x) \in I_{s_1}, \dots, f_\mu^n \in I_{s_n}\} \\ &= I_{s_0} \cap f_\mu^{-1}(I_{s_1}) \cap \cdots \cap f_\mu^{-n}(I_{s_n}). \end{aligned}$$

From this definition we get that

$$I_{s_0,\dots,s_n} = I_{s_0} \cap f_\mu^{-1}(I_{s_1}, \dots, s_n) = I_{s_0,\dots,s_{n-1}} \cap f_\mu^{-n}(I_{s_n}).$$

We can see that the sets $I_{s_0,\dots,s_n}$ form a sequence of closed fitted intervals. We prove it by induction. Case $n = 0$ is clear. Assume that $I_{s_1,\dots,s_n}$ is nonempty. Then, $f_\mu^{-1}(I_{s_1,\dots,s_n})$ consists of two disjoint closed intervals, one contained in I_0 and the other in I_1. Hence, if $I_{s_0} \cap f_\mu^{-1}(I_{s_1,\dots,s_n})$ is a nonempty closed interval. We then have that

$$I_{s_0,\dots,s_n} = I_{s_0,\dots,s_{n-1}} \cap f_\mu^{-n}(I_{s_n}) \subset I_{s_0,\dots,s_{n-1}}.$$

Hence, $\cap_{n\geq 0} I_{s_0,\dots,s_n} \neq \emptyset$. Furthermore, if $x \in \cap_{n\geq 0} I_{s_0,\dots,s_n}$, $x \in I_{s_0}$, $f_\mu(x) \in I_{s_1}$ and so on. This means that $S(x) = (s_0, s_1, ...)$, hence S is surjective.

Now we prove that S is continuous. Let $x \in \Lambda$ and $\varepsilon > 0$. Let $\mathbf{s} = S(x)$. Choose $n > 0$ so that $1/2^n < \varepsilon$. For this n, we consider all the intervals $I_{t_0,\dots,t_n}$, where $(t_0, \dots, t_n) \in \{0, 1\}^n$. There is a finite number of these intervals and $I_{s_0,\dots,s_n}$ is one of them and $x \in I_{s_0,\dots,s_n}$. These intervals are disjoint and Λ is contained inside the union of all of them. As there are a finite number and they are disjoint, there exists $\delta > 0$ such that if $y \in \Lambda$ and $|x - y| < \delta$. Then, $y \in I_{s_0,\dots,s_n}$. This is, $S(x)_i = S(y)_i$ for $0 \leq i \leq n$. From Proposition 2.7,

$$d(S(x), S(y)) < \frac{1}{2^n} < \varepsilon$$

Hence, S is continuous.

We are left to check that S^{-1} is also continuous, but S is a continuous bijective map between two compact sets, hence its inverse is also continuous. □

The fact that S is an homeomorphism that conjugates f_μ and σ, namely $S \circ f_\mu = \sigma \circ S$, gives as us a great amount of information about the dynamics of f_μ. The following theorem is a corollary of Theorems 2.12, 2.13 and Proposition 2.10.

Theorem 2.14. *If $\mu > 2 + \sqrt{5}$, we have the following:*

1. *To every orbit in Λ corresponds a unique sequence in Σ. Also, as periodic orbits correspond to periodic sequences, to every periodic sequence there corresponds a periodic orbit.*
2. *To every sequence in Σ, corresponds a unique orbit in Λ. This is, for any imaginable itinerary between I_0 and I_1, there is an orbit that performs it.*
3. *For any given $n > 0$, the number of n-periodic orbits of f_μ is exactly 2^n*
4. *Since the periodic sequences for σ are dense in Σ and S satisfies that $S \circ f_\mu = \sigma \circ S$, periodic orbits for f_μ are dense in Λ*
5. *There is a dense orbit for f_μ in Λ.*

2.4 Chaos

To sum up, we introduce the concept of a *chaotic* dynamical system and we will also discuss the chaotic behaviour of f_μ.

The definition of chaos that we consider has three ingredients. One of them is that periodic orbits must be dense. The other two are the following.

Definition 2.15. A map $f : I \to I$ is topologically transitive if for any open sets $U, V \subset I$, there exists $k > 0$ such that $f^k(U) \cap V \neq \emptyset$.

This means that for a given point, the images of any neighbourhood of this point visit the whole space. Observe that if the system has a dense orbit, then it topologically transitive.

Definition 2.16. A map $f : I \to I$ has sensitive dependence with respect to initial conditions if there exists $\delta > 0$ such that, for any $x \in I$ and for any neighbourhood U of x, there exists $y \in U$ and $n \geq 0$ such that $|f^n(x) - f^n(y)| > \delta$.

Note that in this definition we do not ask that the orbits of any two points separate. The definition requires that for arbitrarily small neighbourhoods of a point, we may find at least another point arbitrarily close to x whose orbit separates from the orbit of x.

With this definition and with the appearance of the Cantor Set in its dynamics, we have plenty of reasons to suspect that the map f_μ is chaotic. In fact, we have that

Proposition 2.17. *Let $\mu > 2+\sqrt{5}$. The map f_μ has sensitive dependence with respect to initial conditions.*

Proof. Let δ be smaller than the length of the set $A_0 = \{x \in [0,1] | f_\mu(x) > 1\}$ that abandon [0,1] after one iteration of f_μ. Let $x, y \in \Lambda$ and $x \neq y$. Since $S(x) \neq S(y)$, this means that there is n such that $S(x)_n \neq S(y)_n$. By the definition of S, this means that $f_\mu^n(x)$ and $f_\mu^n(y)$ are at opposite sides of A_0 and, therefore,

$$|f_\mu^n(x) - f_\mu^n(y)| > \delta$$

□

In general, we define a chaotic map as

Definition 2.18. Let V be a set. A map $f : V \to V$ is chaotic in V if

1. f has sensitive dependence with respect to initial conditions,
2. f is topologically transitive and
3. periodic points are dense in V.

With the results in the previous section we obtain that

Corollary 2.19. *If $\mu > 2 + \sqrt{5}$ de map $f_\mu : \Lambda \to \Lambda$ is chaotic.*

Remark 2.20. Even when Λ is a "small" set in $[0,1]$, we can prove chaos rigorously for f/Λ.

2.5 λ-Lemma and the Homoclinic Smale Theorem

Previously in this section we have introduced the notion of sensitivity with respect to initial conditions and chaos with an example, the Logistic map. We will now concern ourselves with the study of certain structures present in discrete dynamical systems which induce chaos. To start with, we will look at homoclinic tangles. This is, we will pay attention to certain trajectories emanating from a fixed point that cross each other, this known as a homoclinic tangle. When this happens we have behaviours similar to what we observed with the Logistic map. These behaviours are expressed in the form of results. We will see some of them in this section, such as the λ-lemma or the Homoclinic Smale-Birkhoff Theorem.

Definition 2.21. Let $U \subset \mathbb{R}^n$ be an open subset and $f : U \to \mathbb{R}^n$ be a diffeomorphism. A hyperbolic fixed point $p \in U$ is a point such that $f(p) = p$ and $Df(p)$ has no eigenvalues with modulus different from 1, namely $\text{spec}(Df(p)) \subset \{\lambda \in \mathbb{C}; \quad |\lambda| \neq 1\}$. For each hyperbolic point $p \in U$, the tangent space $T_p\mathbb{R}^n$ and $T_p\mathbb{R}^n = E_p^u \oplus E_p^s$ is a direct sum splitting of this vector space into subspaces of dimensions u and s ($u + s = n$). The vector space E_p^u is generated by the eigenvectors corresponding to eigenvalues greater than 1. Respectively, E_p^s is generated by the eigenvectors corresponding to eigenvalues smaller than 1.

Theorem 2.22. *Let $f : U \to \mathbb{R}^n$ be a diffeomorphism with a hyperbolic fixed point at $p \in U$. Then on a sufficiently small neighbourhood $N \subseteq U$ of p there exist local stable and unstable manifolds,*

$$\begin{aligned} W_{loc}^s(p) &= \{x \in N | f^n(x) \to p \text{ as } n \to \infty\}, \\ W_{loc}^u(p) &= \{x \in N | f^n(x) \to p \text{ as } n \to -\infty\}, \end{aligned} \tag{7}$$

of the same dimensions as E_p^s and E_p^u for $Df(p)$ and tangent to them at p.

Definition 2.23. Two smooth manifolds M, $N \subset \mathbb{R}^n$ such that $M \cap N \neq \emptyset$ intersect transversally if for each point p of the intersection, the tangent spaces at p satisfy that $\dim T_pM \cup T_pN = n$. In particular, this means that there exist n linearly independent vectors that are tangent to at least one of these manifolds at any intersection point.

Remark 2.24. If either $\dim E^s_p = 0$ ($\dim E^u_p = 0$ respectively), then $W^s(p) = \emptyset$ ($W^u(p) = \emptyset$ respectively).

Theorem 2.22 has global repercussions because it allows us to define global stable and unstable manifolds at p by

$$\begin{aligned} W^s(p) &= \bigcup_{m\in\mathbb{Z}^+} f^{-m}(W^s_{loc}(p)) \\ W^u(p) &= \bigcup_{m\in\mathbb{Z}^+} f^{m}(W^u_{loc}(p)). \end{aligned} \tag{8}$$

The behaviour of $W^s(p)$ and $W^u(p)$ is extremely relevant, specially when they intersect. The next theorem, known as the λ-*Lemma* due to Palis [7] is a tool of capital importance when both trying to detect chaos in our dynamical system and for linearization results, which are used extensively as we have already seen and we will also revisit later on.

Theorem 2.25. *(λ-Lemma) Let f be a C^1 diffeomorphism of $\mathbb{R}^n$ with a hyperbolic fixed of periodic point p having s and u dimensional stable and unstable manifolds ($s+u=n$) respectively, and let D be a u-disk in $W^u(p)$. Let Δ be a u-disk meeting $W^s(p)$ transversely at some point q. Then,*

$$\bigcup_{n\geq 0} f^n(\Delta) \tag{9}$$

contains u-disks arbitrarily C^1 close to D.

Remark 2.26. Note that, if there is a transversal homoclinic point $q \in W^u(p) \cap W^s(p)$, then Δ of Theorem 2.25 can be chosen to be a u-disc in $W^u(p)$. In this case the Lambda Lemma implies that $W^u(p)$ accumulates on itself, and, similarly when $s = u = 1$ ($n = 2$), this leads to the homoclinic tangle as shown in Figure 10.

The detection of hyperbolic invariant sets is a common denominator in the analyses of chaotic behaviour in any specific dynamical system. The following Theorem provides us with a criterion for the existence of hyperbolic invariant sets for a diffeomorphism.

Theorem 2.27. *(The Smale-Birkhoff Homoclinic Theorem) Let $f : \mathbb{R}^n \to \mathbb{R}^n$ be a diffeomorphism such that p is a hyperbolic fixed point and there exists a point $q \neq p$ of transversal intersection between $W^s(p)$ and $W^u(p)$. Then f has an invariant set where there exists chaos.*

Remark 2.28. In Theorem 2.27 we make reference to an invariant set where there exists chaos. We will see in the next section, Section 3, that the chaos we refer to is induced by an extremely rich discrete dynamical system called Smale horseshoe.

3. Smale Horseshoe

A fundamental part in the study of dynamical systems is the detection of chaos. In this section, following the explanations in Guckenheimer and Holmes [7], we present a kind of map known as the Smale Horseshoe.

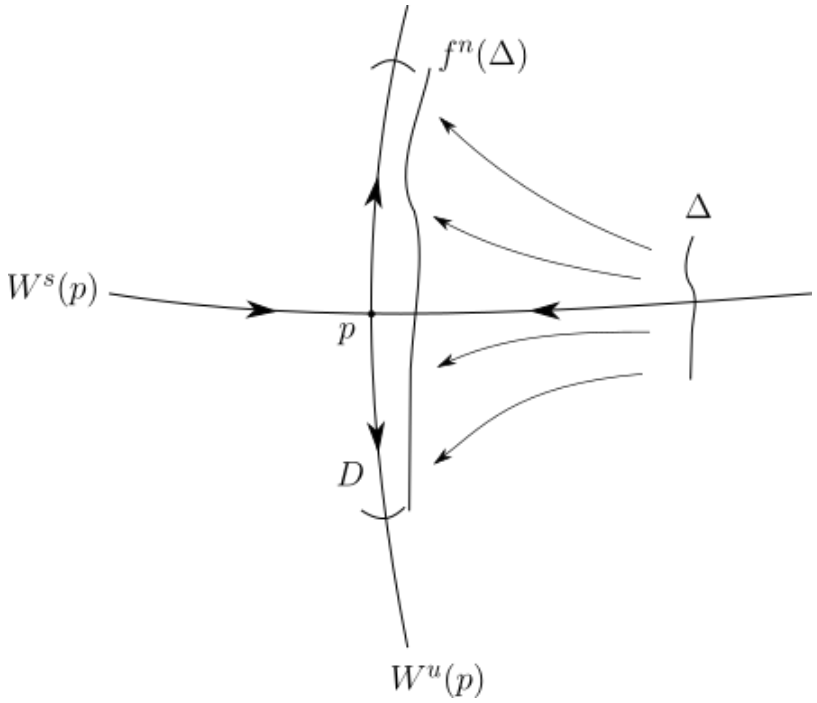

Figure 9: The transversal disk Δ approximates the disk $D \subset W^u(p)$ after n iterations of f.

We will see that when a dynamical system has a horseshoe map acting on a set of points we can codify the dynamics of these points with symbols. As we have seen in Section 2 we will establish an homeomorphism between the set of points that can be codified and the set of symbol sequences. This will enable us to prove the existence of chaos in the set where the horseshoe map acts.

3.1 Construction of the Smale Horseshoe

We begin with the unit square $S = [0,1] \times [0,1]$ in the plane and define a mapping $f : S \to \mathbb{R}^2$ so that $f(S) \cap S$ consists of two components which are mapped rectilinearly by f.

We can think of the map as performing a linear vertical expansion and a horizontal contraction of S, by factors μ and λ, respectively. This action is followed by a folding. This folding is done so that the folded portion falls outside S. Therefore, the map restricted to $S \cap f^{-1}(S)$, is linear. See Figure 11.

Reversing the folding and stretching, we can see that the inverse image $f^{-1}(S \cap f(S)) = S \cap f^{-1}(S \cap f(S)) = S \cap f^{-1}(S)$ is two horizontal bands $H_1 = [0,1] \times [a, a + \mu^{-1}]$ and $H_2 = [0,1] \times [b, b + \mu^{-1}]$, on each of which f will have a constant Jacobian

$$\begin{pmatrix} \pm\lambda & 0 \\ 0 & \pm\mu \end{pmatrix}, \qquad (+ \text{ on } H_1, - \text{ on } H_2), \tag{10}$$

with $0 < \lambda < \frac{1}{2}$ and $\mu > 2$. On each H_i, the map f compresses horizontal segments by a factor of λ and stretches vertical segments by a factor of μ.

As f is iterated, most points either leave S or are contained in an image $f^i(S)$. Those points which do remain in S for all time form a set $\Lambda = \{x | f^i(x) \in S, -\infty < i < \infty\}$. This set Λ has quite a complicated

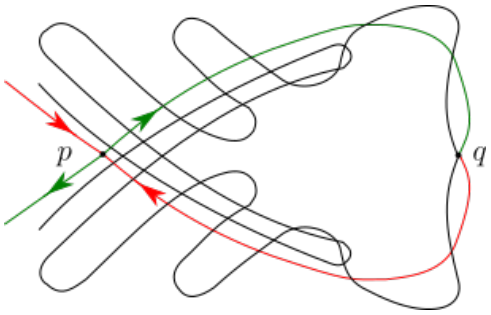

Figure 10: The Lambda Lemma implies homoclinic tangles.

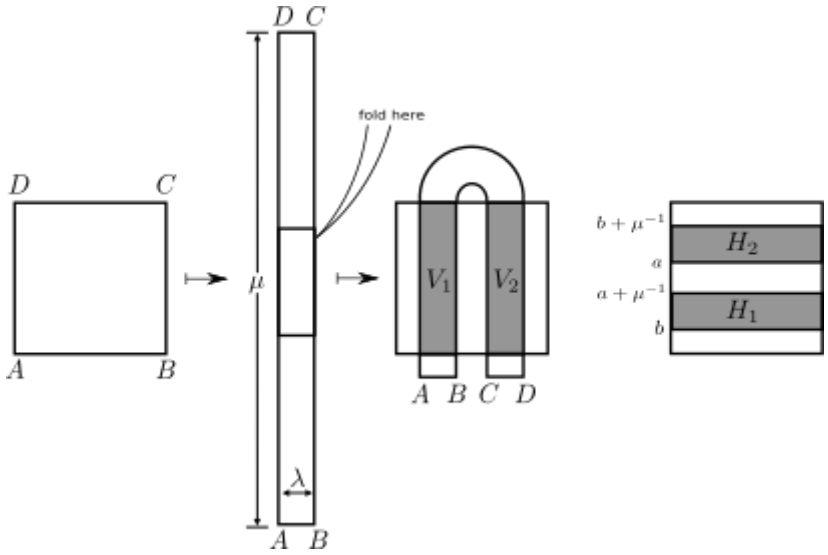

Figure 11: The Smale Horseshoe.

topological structure as we will now see. Each horizontal band H_i is stretched by f to a rectangle $V_i = f(H_i)$ which intersects both H_1 and H_2. Since f is rectilinear on H_i, those points that end up in H_i after applying f come from thinner horizontal strips in H_i. See Figure 12.

The union of the two horizontal strips can be written as $H_1 \cup H_2 = f^{-1}(S \cap f(S))$, so the four thinner strips that arise from the second iteration constitute $f^{-2}(S \cap f(S) \cap f^2(S))$. If we continue this argument inductively, we find that $f^{-n}(S \cap f(S) \cap \cdots \cap f^n(S))$ is the union of 2^n horizontal strips. The thickness of each of these is μ^{-n} since $|\partial f/\partial y| = \mu$ at all points of $H_1 \cup H_2$ and the first $(n-1)$ iterates of the horizontal strips remain inside $H_1 \cup H_2$. The intersection of all these horizontal strips (as $n \to \infty$) forms a Cantor set of horizontal segments. We will now discuss this structure.

Consider now the image under f^n of one of the 2^n horizontal strips in $f^{-n}(S \cap f(S) \cap \cdots \cap f^n(S))$. Using the chain rule, we have

$$Df^n = \begin{pmatrix} \pm\lambda^n & 0 \\ 0 & \pm\mu^n \end{pmatrix} \tag{11}$$

at these points, so the image is a rectangle of horizontal width λ^n which extends vertically from the top to the bottom of the square. The map f^n is 1-1, so the images of the horizontal strips are distinct. We conclude that $S \cap f(S) \cap \cdots \cap f^n(S)$ is the union of 2^n vertical strips, each of width λ^n. The intersection

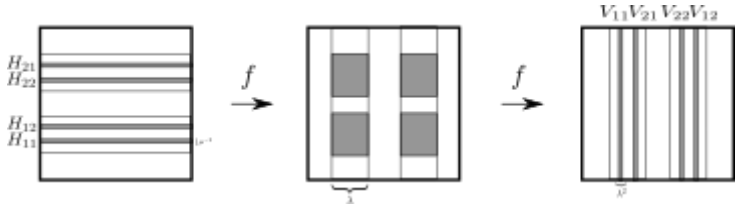

Figure 12: Iteration of f; $V_{ij} = f^2(H_{ij})$

of these sets over all $n \geq 0$ is a Cantor set of vertical segments composed of those points which are in the images of all the f^n. To be in Λ, a point x must be in both a vertical segment and a horizontal segment from the collection described above. Therefore, topologically, Λ is itself a Cantor set; its components are each points and each point of Λ is an accumulation point for Λ. In Figure 13 we show the sixteen components of $f^{-2}(S) \cap f^{-1}(S) \cap S \cap f(S) \cap f^2(S)$, to give an idea of the structure of Λ.

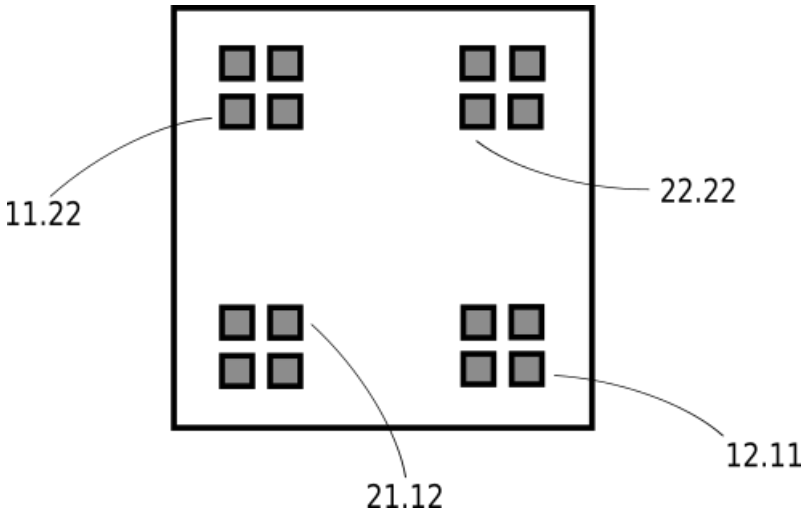

Figure 13: The small grey rectangles have width λ^2 and height μ^{-2}. They are the components of $\cap_{n=-2}^{2} f^n(S)$. The symbol sequences are as mentioned in Theorem 3.3.

So far, we have seen a description of the Smale Horseshoe which enables us to see how the iteration of f generates a 2-dimensional Cantor set. We can, however achieve a more complete description which contains information about the dynamics of each point. This is achieved by noting which horizontal band H_1 or H_2 each iterate of a point $x \in \Lambda$ visits, and use this information as a characterization of the point. Each point $x \in \Lambda$ will be characterized by a bi-infinite sequence of two symbols. The bi-infinite sequence associated to each $x \in \Lambda$ is a sequence $\mathbf{a} = \{a_i\}_{i \in \mathbb{Z}}$ of two symbols, 1 and 2 defined by $a_i = j$ if $f^i(x) \in H_j$. Let Σ be the set of all bi-infinite sequences of two symbols, we can define a function $d : \Sigma \times \Sigma \to \mathbb{R}$ as

$$d(\mathbf{a}, \mathbf{b}) = \sum_{i=-\infty}^{\infty} \delta_i 2^{-|i|}, \qquad \delta_i = \begin{cases} 0 & \text{if } a_i = b_i \\ 1 & \text{if } a_i \neq b_i \end{cases}. \tag{12}$$

As we claim in the following proposition, this function d can act as a distance in Σ.

Proposition 3.1. *The set Σ together with d is a metric space. Moreover, if $d(\mathbf{a}, \mathbf{b}) < 1/2^k$ for some $k \in \mathbb{N}$, $a_i = b_i$ for $|i| \leq k$ and if $a_i = b_i$ for $|i| \leq k$, then $d(\mathbf{a}, \mathbf{b}) \leq 1/2^{k-1}$.*

Proof. The series used in d are absolutely convergent;

$$\sum_{i=-\infty}^{\infty} \delta_i 2^{-|i|} = \sum_{i=-\infty}^{-1} \delta_i 2^{-|i|} + \sum_{i=0}^{\infty} \delta_i 2^{i} \leq 1 + 2 = 3. \tag{13}$$

Hence, d is well defined.

Clearly, $d(\mathbf{a}, \mathbf{b}) \geq 0$ and if $d(\mathbf{a}, \mathbf{b}) = 0$, then $\delta_i = 0$ for all $i \in \mathbb{Z}$. Therefore, $a_i = b_i$ for all $i \in \mathbb{Z}$ and so $\mathbf{a} = \mathbf{b}$. We can also plainly see that $d(\mathbf{a}, \mathbf{b}) = d(\mathbf{b}, \mathbf{a})$. As for the triangular inequality, if $\mathbf{c} \in \Sigma$, $d(\mathbf{a}, \mathbf{c}) + d(\mathbf{c}, \mathbf{b}) \geq d(\mathbf{a}, \mathbf{b})$. The inequality is satisfied because the disagreeing positions between $\mathbf{a}$ and $\mathbf{b}$ are counted once but we are also counting the positions in which $\mathbf{a}$ and $\mathbf{b}$ agree but at the same time disagree with $\mathbf{c}$.

Assume that $d(\mathbf{a}, \mathbf{b}) < 1/2^k$ and that $a_{k_1} \neq b_{k_1}$ for some $|k_1| \leq k$. Since $\delta_i = 1$,

$$\frac{1}{2^k} \leq \frac{1}{2^{k_1}} \leq \sum_{i=-\infty}^{\infty} \delta_i 2^{-|i|} < \frac{1}{2^k} \tag{14}$$

which is a contradiction.

Conversely, if $a_i = b_i$ for $|i| \leq k$,

$$d(\mathbf{a}, \mathbf{b}) = \sum_{|i| \geq k+1} \delta_i 2^{-|i|} \leq 1/2^{k-1} \tag{15}$$

□

Now that we have Σ defined as a metric space we want to describe a dynamical system over it. We will therefore define a map $\sigma : \Sigma \to \Sigma$ such that given $\mathbf{a} \in \Sigma$, $\sigma(\mathbf{a})_i = a_{i+1}$. This is known as the *shift* map. This map is a bijection with inverse $\sigma^{-1}(\mathbf{a})_i = a_{i-1}$ we claim the following properties for σ

Proposition 3.2. *The map σ is a homeomorphism. Moreover, as a dynamical system, $(\Sigma, \sigma, \mathbb{Z})$ satisfies the following properties*

(a) σ has periodic orbits of any period.

(b) The periodic orbits for σ are dense in Σ.

(c) It has a dense orbit which is not periodic.

Proof. To prove that σ is a homeomorphism we only need to see that it is continuous. Take $\varepsilon > 0$ and $\mathbf{a}, \mathbf{b} \in \Sigma$. Let $k \in \mathbb{N}$ be such that $1/2^{k-1} \leq \varepsilon$ and $\delta = 1/2^k$. Then if $d(\mathbf{a}, \mathbf{b}) < \delta$ we have that $a_i = b_i$ for $|i| \leq k$ which is equivalent to $a_{i+1} = b_{i+1}$ for $|i| \leq k - 1$. Therefore, $d(\sigma(\mathbf{a}), \sigma(\mathbf{b})) \leq 1/2^{k-1} \leq \varepsilon$ and σ is continuous. Note that σ^{-1} satisfies the exact same property.

(a) For a fixed $q \in \mathbb{N}$, a point $\mathbf{a} \in \Sigma$ will be q-periodic if $a_i = a_{i+q}$. We can obtain such a point by repeating the sequence of length q $00 \ldots 01$.

(b) Take $\mathbf{a} \in \Sigma$ and $\varepsilon > 0$. Let q be such that $1/2^{q-1} \leq \varepsilon$ and consider $\mathbf{a}^q \in \Sigma$ such that $a_i = a_i^q$ for $|i| \leq q$ and $\mathbf{a}^q$ having period $2q+1$. We have that $\mathbf{a}^q$ is of the form $\mathbf{a}^q = \{\cdots \overline{\sigma_{-q}\sigma_{-q+1}\cdots\sigma_{-1}\cdot\sigma_0\sigma_1\cdots\sigma_q}\cdots\}$. Then, $d(\mathbf{a}, \mathbf{a}^q) \leq 1/2^{q-1} \leq \varepsilon$.

(c) Lastly, the dense orbit is $\mathbf{x} \in \Sigma$ formed by all the finite length sequences

$$\mathbf{x} = \{\cdots \sigma_{-2}\sigma_{-1} \cdot 01|00\ 01\,10\,11|000\,001\,011\cdots\}. \tag{16}$$

The value of $\mathbf{x}_i$ for $i \leq -1$ does not matter. This is because for a given $\varepsilon > 0$ and $\mathbf{a} \in \Sigma$ there is m such that $\sigma^m(\mathbf{x})_i = x_{i+m} = a_i$ for $|i| \leq q$ with $1/2^q < \varepsilon$. □

The above proposition is telling us that the shift map is in fact a chaotic map because it is sensitive to initial conditions, it is topologically transitive (due to the dense orbit) and the periodic orbits are dense.

Earlier in this section we have given a glimpse of the idea behind the bi-infinite sequences. Once we understand the dynamics in Σ, we want to relate it to the dynamics in Λ. The following theorem establishes this relationship in the form of a homeomorphism between Σ and Λ.

Theorem 3.3. *There is an homeomorphism ϕ between Λ and Σ, such that the sequence $\mathbf{b} = \phi(f(x))$ is obtained from the sequence $\mathbf{a} = \phi(x)$ by shifting indices one place: $\mathbf{b} = \sigma(\mathbf{a})$.*

Proof. The proof of this theorem is a very useful tool to understand how symbolic dynamics works. Therefore, we will give a brief sketch of the proof, depicting the important ideas.

Take the two symbols of the theorem to be 1 and 2. The map is defined by the recipe

$$\phi(x) = \{a_i\}_{i=-\infty}^{\infty}, \qquad \text{with } f^i(x) \in H_{a_i}. \tag{17}$$

In words, x is in Λ if and only if $f^i(x)$ is in $H_1 \cup H_2$ for each i, and we associate to x the sequence of indices that tells us which of H_1 and H_2 contains each $f^i(x)$. This description of ϕ leads directly to the shift property described in the theorem. Since $f^{i+1}(x) = f^i(f(x))$, it follows that $\phi(f(x))$ is obtained from $\phi(x)$ by shifting indices. To see that ϕ is both 1-1 and continuous, we look at the set of x's which each possess a given central string of symbols. Specifying $b_{-m}, b_{-m+1}, \dots \cdot b_0, \dots, b_n$ we denote as $R(b_{-m}, b_{-m+1}, \dots \cdot b_0, \dots, b_n)$ the set of x's for which $f^i(x) \in H_{b_i}$ for $-m \leq i \leq n$. We observe inductively that $R(b_{-m}, \dots, b_n)$ is a rectangle of height $\mu^{-(n+1)}$ and width λ^m, obtained from the intersection of a horizontal and a vertical strip. As one lets m, $n \to \infty$, the diameter of the sets $R(b_{-m}, b_{-m+1}, \dots \cdot b_0, \dots, b_n) \to 0$. Consequently, ϕ is both 1-1 and continuous.

The final point is that ϕ is onto. This is crucial for the applications of symbolic dynamics. The reason that ϕ is onto is that for each choice of $b_{-m}, b_{-m+1}, \dots \cdot b_0, \dots, b_n$, the set $R(b_{-m}, b_{-m+1}, \dots \cdot b_0, \dots, b_n)$ is nonempty. Note that $R(b_0, \dots, b_n, b_{n+1})$ is a horizontal strip mapped vertically from top to bottom of the square S by f^{n+1}. Therefore $f^{n+1}(R(b_0, \dots, b_n, b_{n+1}))$ intersects each H_i and $R(b_0, \dots, b_n, b_{n+1})$ is a nonempty horizontal strip extending across S. Similarly, we have already observed that $S \cap f(S) \cap \cdots \cap f^m(S)$ consists of 2^m vertical strips. Each of these is a set of the form $R(b_{-m}, \dots, b_{-1})$ and all sequences $b_{-m}, \dots, b_{-1}$ occur. Finally, $R(b_{-m}, \dots, b_n)$ is nonempty because every vertical strip $R(b_{-m}, \dots, b_{-1})$ intersects every horizontal strip $R(b_0, \dots, b_n)$ and $R(b_{-m}, \dots, b_n) = R(b_{-m}, \dots, b_{-1}) \cap R(b_0, \dots, b_n)$. □

The correspondence ϕ between Λ and Σ imparts to Λ a symbolic description. In fact, the basic property of Theorem 3.3 can be restated as the following equation

$$\phi(f|_\Lambda) = \sigma \circ \phi. \tag{18}$$

This equation expresses the topological conjugacy of $f|_\Lambda$ and σ. Written as $f|_\Lambda = \phi^{-1} \circ \sigma \circ \phi$, it has the immediate consequence that

$$f^n|_\Lambda = \phi^{-1} \circ \sigma^n \circ \phi, \tag{19}$$

so that ϕ maps orbits of f in Λ to orbits of σ in Σ. The description of σ is explicit enough that many dynamical properties are readily determined.

Corollary 3.4. *The horseshoe map f has an invariant Cantor set Λ such that:*

a) Λ *contains a countable set of periodic orbits of arbitrarily long periods.*

b) Λ *contains an uncountable set of bounded nonperiodic motions.*

c) Λ *contains a dense orbit.*

The above description of the horseshoe just given is robust with respect to small changes in the map f. The assumption that f is a linear map on $H_1 \cup H_2$ can be dropped in the sense that, if $\tilde{f}$ is a perturbation of f small enough, the Jacobian derivative of $\tilde{f}$ can be nonconstant but is still close to that of f. Qualitatively, nothing changes. The sets $S \cap \tilde{f}(S) \cap \cdots \cap \tilde{f}^n(S)$ will still consist of 2^n sort of vertical strips. Similarly, $\tilde{f}^{-n}(S) \cap \cdots \cap S$ will consist of 2^n sort of horizontal strips. Both of them will no longer be exactly rectangles but the set of points whose $\tilde{f}$-iterates remain in S form a set $\tilde{\Lambda}$ which is topologically conjugate to the shift in Σ.

This can be summarised by saying that any sufficiently C^1 close map $\tilde{f}$ has an invariant Cantor set $\tilde{\Lambda}$ with $\tilde{f}|_{\tilde{\Lambda}}$ topologically equivalent to f_Λ.

3.2 Hyperbolic Invariant Sets

In chaotic dynamical behaviour it is important to understand how an invariant set Λ attracts or repels trajectories. In this case, we will study what is known as a *hyperbolic structure* for Λ in a discrete dynamical system, which is a way to classify the tangent space of its points. In first place, we will give a definition of invariant set.

Definition 3.5. A set of points $\Lambda \subset \mathbb{R}^n$, is said to be invariant for the the discrete dynamical system defined by $f : \mathbb{R}^n \to \mathbb{R}^n$ if for each $x \in \Lambda$, $f^m(x) \in \Lambda$ for all $m \in \mathbb{Z}$.

Now, we proceed to give a definition of hyperbolic structure for Λ.

Definition 3.6. Let Λ be an invariant set for f, a hyperbolic structure for Λ is a continuous invariant direct sum decomposition $T_\Lambda \mathbb{R}^n = E^u_\Lambda \oplus E^s_\Lambda$ with the property that there are constants $C > 0$, $0 < \lambda < 1$ such that:

(1) if $v \in E^u_x$, then $|Df^{-n}(x)v| \leq C\lambda^n |v|$,

(2) if $v \in E^s_x$, then $|Df^n(x)v| \leq C\lambda^n |v|$

Remark 3.7. (i) In this definition, $T_\Lambda \mathbb{R}^n$ consists of all the tangent vectors to $\mathbb{R}^n$ at all points of Λ. For each $x \in \Lambda$, $T_x\mathbb{R}^n$ is the tangent space at x and $T_x\mathbb{R}^n = E^u_x \oplus E^s_x$ is a direct sum splitting of this vector space into subspaces of dimensions u and s ($u + s = n$).

(ii) The derivative Df of f maps $T_x\mathbb{R}^n$ to $T_{f(x)}\mathbb{R}^n$. The invariance of the definition requires that $Df(E^s_x) = E^s_{f(x)}$ and $Df(E^u_x) = E^u_{f(x)}$. The continuity of the splitting means that as x varies in Λ, one can find continuously varying bases for E^u_x and E^s_x. In general, the splitting cannot be chosen to be smooth with respect to x, but can be chosen to be Hölder continuous.

(iii) The hyperbolicity conditions (1) and (2) state that, infinitesimally, vectors in E^s (respectively E^u) are contracted exponentially in forward (respectively backwards) time at an exponential rate λ which is uniform for all points of Λ and all choices of vectors in the invariant subspaces.

3.3 Generalised Smale Horseshoe

As said on the previous subsection, the Smale Horseshoe is robust with respect to small changes. We are concerned now in finding out how to extend our methods to nonlinear maps. In first place, we need a looser definition of horizontal and vertical strips $\{H_i\}$ and $\{V_i\}$ of the square S.

Definition 3.8. A vertical curve $x = v(y)$ is a curve for which

$$0 \leq v(y) \leq 1, \qquad |v(y_1) - v(y_2)| \leq \mu |y_1 - y_2| \qquad \text{for } 0 \leq y_1 \leq y_2 \leq 1 \tag{20}$$

for some $0 < \mu < 1$. Similarly a horizontal curve $y = h(x)$ is curve for which

$$0 \leq h(x) \leq 1, \qquad |h(x_1) - h(x_2)| \leq \mu |x_1 - x_2| \qquad \text{for } 0 \leq x_1 \leq x_2 \leq 1. \tag{21}$$

Given two nonintersecting vertical curves $v_1(y) < v_2(y)$, $y \in [0,1]$, we can define a vertical strip

$$V = \{(x,y) \mid x \in [v_1(y), v_2(y)],\ y \in [0,1]\}. \tag{22}$$

Given two nonintersecting horizontal curves $h_1(x) < h_2(x)$, $x \in [0,1]$, we can define a horizontal strip

$$H = \{(x,y) \mid y \in [h_1(x), h_2(x)],\ x \in [0,1]\}. \tag{23}$$

Finally, the width of vertical and horizontal strips is defined as

$$d(V) = \max_{y \in [0,1]} |v_2(y) - v_1(y)|, \qquad d(H) = \max_{x \in [0,1]} |h_2(x) - h_1(x)|. \tag{24}$$

We can now see that the following statements hold.

Lemma 3.9. *If $V^1 \supset V^2 \supset V^3 \ldots$ is a sequence of nested vertical (or horizontal) strips and if $d(V^k) \to 0$ as $k \to \infty$ then $\cap_{k=1}^{\infty} V^k$ is a vertical (or horizontal curve).*

Proof. Given a sequence of nested vertical strips, every vertical strip in the sequence is of the form

$$V_k = \{(x,y) \mid x \in [v_1^k, v_2^k],\ y \in [0,1]\} \quad k = 1, \ldots, n. \tag{25}$$

Now, if we fix $y' \in [0,1]$, since the strips are nested, for every k we have a sequence of nested closed intervals

$$I_k = [v_1^k(y'), v_2^k(y')]. \tag{26}$$

As it is well known, the intersection of all these intervals is a unique point,

$$\lim_{n \to \infty} \bigcap_{k=1}^{n} I_k = v'. \tag{27}$$

Hence, the point (v', y') is a point in $\cap_{k=1}^{\infty} V_k$. Let $0 \leq y' \leq y'' \leq 1$, consider two points $(v', y'), (v'', y'') \in \cap_{k=1}^{\infty} V_k$, since $d(V^k) \to 0$ as $k \to \infty$, we have that

$$|(v', y') - (v'', y'')| \leq \mu |y' - y''| \quad 0 < \mu < 1. \tag{28}$$

Hence the limit of nested vertical strips is a vertical curve. The proof works exactly the same in the case of horizontal strips. □

Lemma 3.10. *A vertical curve $v(y)$ and a horizontal curve $h(x)$ intersect in precisely one point.*

Proof. Observe, that the intersection between a vertical band and a horizontal band is a closed compact region that can be fitted into a closed rectangle. Fitting the successive rectangles from the intersection of the nested bands and following the nested intervals idea, we have a unique limiting point. □

In particular, to each pair of curves (and hence to each pair of sequences of nested strips) there corresponds exactly one point $x \in S$. We can now state our hypotheses on the map $f : S : \mathbb{R}^2$.

H1 Let $\mathcal{I}$ be the set $\{1, 2, \dots, N\}$ and let H_i, V_i for $i \in \mathcal{I}$ be disjoint horizontal and vertical strips and let $f(H_i) = V_i$, $i \in \mathcal{I}$.

H2 f contracts vertical strips and f^{-1} contracts horizontal strips uniformly in the following sense. Let v_1, $v_2 \in V_i$ be any two vertical curves bounding a vertical substrip $V_i' \subseteq V_i$, then $f(V_i') \cap V_j$ is a vertical strip and

$$d(f(V_i') \cap V_j) \leq \nu d(V_i') d(V_j)/d(V_i), \tag{29}$$

for some $\nu \in (0, 1)$ and $i, j \in \mathcal{I}$. Similarly, letting h_1, $h_2 \in H_i$ be any two horizontal curves bounding a horizontal substrip $H_i' \subseteq H_i$, then $f^{-1}(H_i') \cap H_j$ is a horizontal strip and $d(f^{-1}(H_i') \cap H_j) \leq \nu d(H_j)$.

As an alternative to H2, if we have a C^1 map $f = (f_1, f_2)$ with linearization Df or

$$\begin{pmatrix} \xi \\ \eta \end{pmatrix} \mapsto \begin{bmatrix} \frac{\partial f_1}{\partial x} & \frac{\partial f_1}{\partial y} \\ \frac{\partial f_2}{\partial x} & \frac{\partial f_2}{\partial y} \end{bmatrix} \begin{pmatrix} \xi \\ \eta \end{pmatrix} \tag{30}$$

then H2 can be replaced by

H3 There exist sets (sector-bundles) $F^u = \{(\xi, \eta) || \xi | < \mu |\eta|\}$ defined over $\bigcup_{i \in \mathcal{I}} V_i$ and $F^s = \{(\xi, \eta) || \eta | < \mu |\xi|\}$ defined over $\bigcup_{i \in \mathcal{I}} U_i$ with $0 < \mu < 1$ such that $Df(S^u) \subset F^u$ and $Df^{-1}(F^s) \subset S^s$. Moreover, if $Df(\xi_0, \eta_0) = (\xi_1, \eta_1)$ and $Df^{-1}(\xi_0, \eta_0) = (\xi_{-1}, \eta_{-1})$ then $|\eta_1| \geq (1/\mu)|\eta_0|$ and $|\xi_{-1}| \geq (1/\mu)|\xi_0|$. See Figure 14.

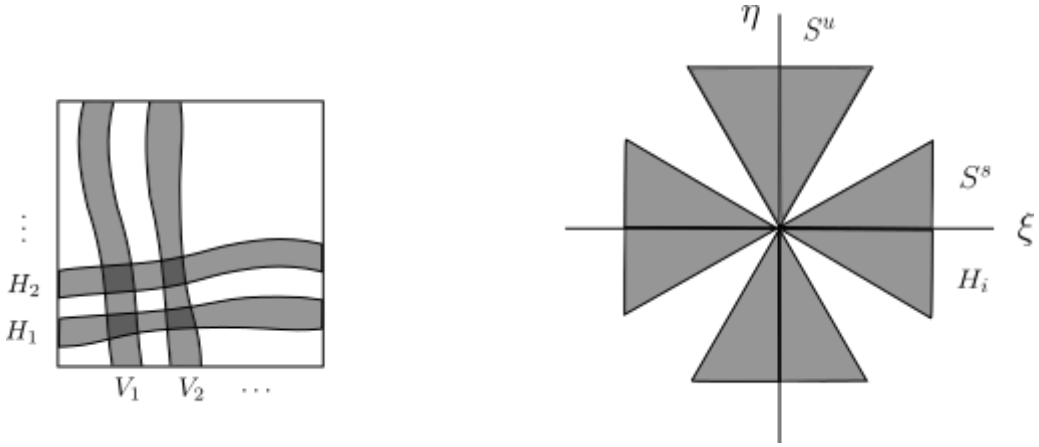

Figure 14: Nonlinear strips (left) and sectors (right).

H3 can only be used when f is differentiable, in which case it is usually easier to check than H2. It is also important to note that we can link these hypotheses in the following way.

Proposition 3.11. *H1 and H3, with* $0 < \mu < \frac{1}{2}$*, imply H2 with* $\nu = \mu/(1-\mu)$.

To prove this result, in first place we show that the preimage under f of any horizontal strip H_i is a set of thinner horizontal strips H_{ji} and the image of any vertical strip V_k is a set of thinner vertical strips V_{kl}. We then verify the contraction estimates that $d(H_{ji}) \leq \nu d(H_j)$ and $d(V_{kl}) \leq \nu d(V_k)$, with $\nu = \mu/(1-\mu)$.

We can now proceed to expose the result for the generalized Smale Horseshoe.

Theorem 3.12. *If f is a two-dimensional homeomorphism satisfying H1 and H2 then f possesses an invariant set Λ, topologically equivalent to a shift σ on Σ: the set of bi-infinite sequences of elements $\mathcal{I}$. That is, there exists a homeomorphism h of Σ onto Λ such that $f|_\Lambda = h \circ \sigma \circ h^{-1}$. Furthermore, if f is a C^r diffeomorphism ($r \geq 1$) satisfying H1 and H3 with $0 < \mu < \frac{1}{2}$, and $|\det(Df)|, |\det(Df)|^{-1} \leq \frac{1}{2}\mu^{-2}$, then Λ is hyperbolic.*

4. The Sil'nikov Bifurcation

One of the main objectives of this work is to study the existence of Smale horseshoes near homoclinic orbits of three dimensional dynamical systems in order to prove the existence of chaos in such systems. The case we are concerned with is the homoclinic bifurcation of a saddle-focus. In this section we will introduce the notion of structural stability of a system and we will see how homoclinic orbits of different types behave under perturbation. We will end up announcing the Sil'nikov Theorem, that we will later prove in Section 5. This section follows the development by Yuri A. Kuznetsov in [8]

4.1 Hyperbolic Equilibrium Persistence

In order to introduce the notion of structural stability, we will first take a look at how hyperbolic equilibrium points persist under small perturbations. This will give us some insight on how to treat perturbations and what to expect from them when applied to other objects such as homoclinic orbits, which will be our case.

$$\dot{x} = f(x), \qquad x \in \mathbb{R}^n, \tag{31}$$

where f is smooth. Assume that $f(x_0) = 0$ and it is therefore an equilibrium point of the system. From Equation (31) we can derive a one-parameter perturbed system

$$\dot{x} = f(x) + \varepsilon g(x), \qquad x \in \mathbb{R}^n, \tag{32}$$

where g is also smooth and ε is a small parameter. Note that if we set $\varepsilon = 0$ in (32) we retrieve system (31). System (32) has an equilibrium point $x(\varepsilon)$ for any small enough $|\varepsilon|$ such that $x(0) = x_0$. Indeed, the equilibrium points of (32) are obtained by solving the equation

$$F(x, \varepsilon) = f(x) + \varepsilon g(x) = 0, \tag{33}$$

with $F(x_0, 0) = 0$. We also have that $A_0 = DF(x_0, 0) = Df(x_0)$, the Jacobian matrix of (31) at x_0, which has nonzero determinant as it is an hyperbolic equilibrium point. Now, the Implicit Function Theorem guarantees the existence of a smooth function $x = x(\varepsilon)$, $x(0) = x_0$ satisfying

$$F(x(\varepsilon), \varepsilon) = 0 \tag{34}$$

for small values of $|\varepsilon|$. The Jacobian matrix of $x(\varepsilon)$ in (32)

$$A_\varepsilon = \left(\frac{df(x)}{dx} + \varepsilon \frac{dg(x)}{dx} \right) |_{x=x(\varepsilon)}, \tag{35}$$

depends smoothly on ε and coincides with A_0 in (31) at $\varepsilon = 0$. As the eigenvalues of a matrix that depends smoothly on a parameter change continuously with the variation of this parameter, we have that A_ε will have no eigenvalues on the imaginary axis for sufficiently small values of $|\varepsilon|$ since it has no such eigenvalues at $\varepsilon = 0$. We can say that $x(\varepsilon)$ is a hyperbolic equilibrium for any $|\varepsilon|$ small enough, the number of stable and unstable eigenvalues will remain fixed and systems (31) and (32) are locally topologically equivalent near the equilibrium point. This is what is known as local structural stability.

Definition 4.1. We start with the definition of a homoclinic orbit. Consider a continuous-time dynamical system defined by the flux ϕ_t which is the solution of the system of ordinary differential equations

$$\dot{x} = f(x), \qquad x = (x_1, \dots, x_n)^T \in \mathbb{R}^n \tag{36}$$

where f is smooth. Let $x_0 \in \mathbb{R}^n$ be an equilibrium point of the system (36) (this is, $f(x_0) = \mathbf{0}$).

An orbit Γ_0 starting at a point $x \in \mathbb{R}^n$ is called homoclinic to the equilibrium point x_0 of system (36) if $\phi_t(x) \to x_0$ as $t \to \pm\infty$.

Definition 4.2. An orbit Γ_0 starting at a point $x \in \mathbb{R}^n$ is called heteroclinic to the equilibrium points x_1 and x_2 of system (36) if $\phi_t(x) \to x_1$ as $t \to -\infty$ and $\phi_t(x) \to x_2$ as $t \to +\infty$.

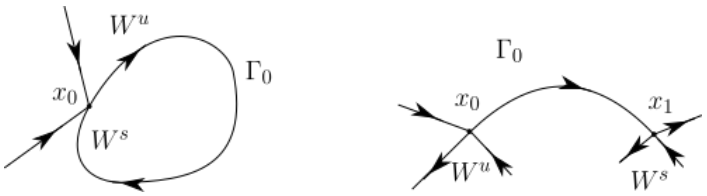

Figure 15: Two-dimensional homoclinic orbit (left) and a heteroclinic (right).

Note that a homoclinic orbit Γ_0 to the equilibrium point x_0 belongs to the intersection of its unstable and stable sets; $\Gamma_0 \subset W^u(x_0) \cap W^s(x_0)$. Similarly, a heteroclinic orbit Γ_0 to the equilibria x_1 and x_2 satisfies $\Gamma_0 \subset W^u(x_1) \cap W^s(x_2)$. Also, in Definitions 4.1 and 4.2 we do not require the equilibria to be hyperbolic. Figure 16 shows for example, a homoclinic orbit to a saddle-node point with an eigenvalue $\lambda_1 = 0$. In fact, orbits homoclinic to hyperbolic equilibria are of particular interest since their presence results in structural instability, which means that the structure is preserved under perturbation, while the equilibria themselves are structurally stable, that is, if a dynamical system having a hyperbolic fixed point is perturbed, the perturbed system will also have a hyperbolic fixed point.

Lemma 4.3. *A homoclinic orbit to a hyperbolic equilibrium of Equation* (36) *is structurally unstable.*

This Lemma assures that we can perturb a system with an orbit Γ_0 homoclinic to x_0 such that the phase portrait in a neighbourhood of $\Gamma_0 \cup x_0$ becomes topologically nonequivalent to the original one. In fact, the homoclinic orbit simply disappears for generic C^1 perturbations of the system. This is a bifurcation of the phase portrait. To prove the Lemma, we shall recall some notions of transversality theory. For instance, a surface and a curve intersecting with a nonzero angle at some point in $\mathbb{R}^3$ are

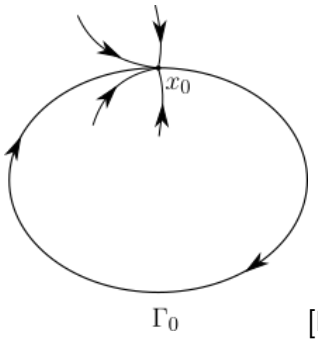

[h]

Figure 16: Homoclinic orbit Γ_0 to a saddle-node.

transversal. The main property of transversal intersection is that it persists under small C^1 perturbations of the manifolds. In other words, if manifolds M and N intersect transversally, so will sufficiently C^1-close manifolds. Conversely, if the manifolds intersect nontransversally, generic perturbations make them either nonintersecting or transversally intersecting.

Throughout this discussion, as we will only deal with saddle-focus hyperbolic equilibria, we will assume the sets W^u and W^s to be smooth invariant manifolds that intersect transversally at the equilibrium point. Any sufficiently C^1-close system has a nearby saddle-focus point and its invariant manifolds are C^1-close to the corresponding original ones in a neighbourhood of the saddle-focus point.

Proof. of Lemma 4.3.

Suppose that system (36) has a hyperbolic equilibrium x_0 with n_+ eigenvalues with positive real parts and n_- eigenvalues with negative real parts, $n_\pm > 0$, $n_+ + n_- = n$. Assume that the corresponding stable and unstable manifolds $W^u(x_0)$ and $W^s(x_0)$ intersect along a homoclinic orbit. To prove the Lemma, we shall see that the intersection cannot be transversal. Indeed, at any point x of this orbit, the vector $f(x)$ is tangent to both manifolds $W^u(x_0)$ and $W^s(x_0)$. Therefore, we can find no more than $n_+ + n_- - 1 = n - 1$ independent tangent vectors to these manifolds, since $\dim W^u(x_0) = n_+$ and $W^s(x_0) = n_-$. Moreover, any generic perturbation of (36) splits the manifolds in that remaining direction and they fail to intersect any more near Γ_0. □

We now can proceed to characterize the behaviour of the stable and unstable manifolds near homoclinic bifurcations. We will start by discussing saddles in dimension two systems followed by saddle-nodes in dimension three systems. Lastly, we will see the Sil'nikov bifurcation Theorem for saddle-focus.

Homoclinic bifurcation in planar systems Consider a planar system with a homoclinic orbit to a saddle x_0 as shown in the central part of Figure 17. Introduce a one-dimensional local cross-section Σ to the stable manifold $W^s(x_0)$ near the saddle, as shown in the figure. Choose a coordinate ξ along Σ such that the point of intersection with the stable manifold corresponds to $\xi = 0$. This construction is possible for any sufficiently close systems. However, for such systems the unstable manifold W^u generically does not return to the saddle. Figure 17 illustrates the two possibilities. The manifolds either split up or down. Denote by ξ^u the ξ-value of the intersection of W^u with Σ.

Definition 4.4. The scalar $\beta = \xi^u$ is called a split function.

In fact, the split function is a function defined on the original and perturbed systems. It becomes a

smooth function of parameters for a parameter dependent system. The equation

$$\beta = 0$$

is a bifurcation condition for the homoclinic bifurcation in $\mathbb{R}^2$. Thus, the homoclinic bifurcation in this case has codimension one.

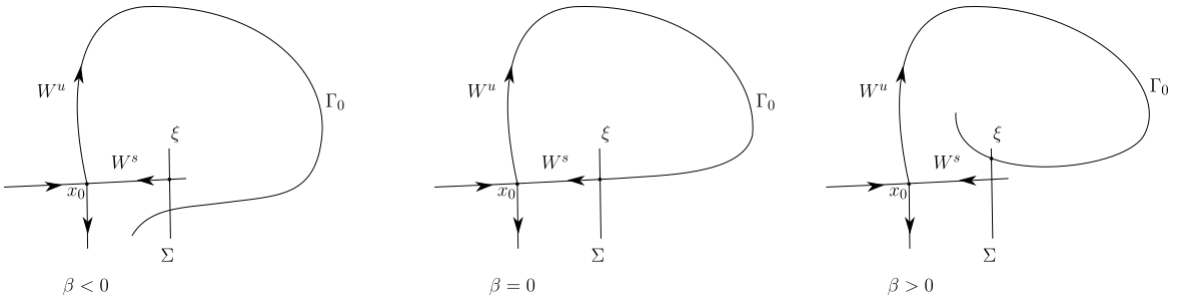

Figure 17: Split function in the planar case.

Example 4.5. Lemma 4.3 in the planar case has a constructive proof due to Andronov. Consider a system

$$A = \begin{cases} \dot{x_1} = f_1(x_1, x_2) \\ \dot{x_2} = f_2(x_1, x_2). \end{cases} \tag{37}$$

Assume that this system has an homoclinic orbit at an equilibrium point x_0. Take $\alpha \in \mathbb{R}$ small. We can perturbate the system with the rotation matrix

$$\begin{pmatrix} 1 & -\alpha \\ \alpha & 1 \end{pmatrix} \tag{38}$$

in order to obtain the rotated system

$$\begin{cases} \dot{x_1} = f_1(x_1, x_2) - \alpha f_2(x_1, x_2) \\ \dot{x_2} = \alpha f_1(x_1, x_2) + f_2(x_1, x_2). \end{cases} \tag{39}$$

Observe that if $\alpha \neq 0$ is a small perturbation, the tangent vector at any point of the homoclinic orbit ceases to be tangent to one of the manifolds. This means that the intersection of the two manifolds is empty and therefore, the homoclinic orbit no longer exists.

Homoclinic bifurcation to a saddle in $\mathbb{R}^3$ It is also possible to define a split function in this case. Consider a system in $\mathbb{R}^3$ with a homoclinic orbit Γ_0 to a saddle x_0. Assume that $\dim W^u = 1$ (if not, reverse the time direction) and introduce a two dimensional cross-section Σ with coordinates (ξ, η). Suppose that $\xi = 0$ corresponds to the intersection of Σ with the stable manifold W^s of x_0. As before, this can be done for all sufficiently close systems. Let (ξ^u, η^u) be the point of intersection of W^u with Σ. Then, the split function can be defined as in the planar case before; $\beta = \xi^u$. Its zero, $\beta = 0$ gives a condition for the homoclinic bifurcation in $\mathbb{R}^3$. In addition, it also of codimension one.

Homoclinic bifurcation to a saddle-focus in $\mathbb{R}^3$ We now have the tools to study the case of the saddle-focus, that is eigenvalues $\lambda_1 > 0$, $\lambda_2 = \overline{\lambda}_3$ and $\operatorname{Re} \lambda_2 < 0$.

Definition 4.6. The eigenvalues with negative real part that are closest to the imaginary axis are called leading or principal eigenvalues, while the corresponding eigenspace is called leading or principal eigenspace.

Thus, almost all orbits on W^s approach a generic saddle along the one-dimensional leading eigenspace. In the saddle-focus case, there are two leading eigenvalues $\lambda_2 = \overline{\lambda}_3$, and the leading eigenspace is two-dimensional.

Definition 4.7. A saddle quantity σ of a saddle of saddle-focus is the sum of the positive eigenvalue and the real part of a leading eigenvalue.Therefore, $\sigma = \lambda_1 + \lambda_2$ for a saddle, and $\sigma = \lambda_1 + \mathrm{Re}\lambda_{2,3}$ for a saddle-focus.

The following theorem characterises the saddle-focus bifurcation in 3 dimensions. In the next section we will see that in the situation of this particular bifurcation we can prove the existence of a countable set of Smale horseshoes.

Theorem 4.8. *(Saddle-focus, $\sigma_0 > 0$) Suppose that a three-dimensional system*

$$\dot{x} = f(x, \alpha), \qquad x \in \mathbb{R}^3, \qquad \alpha \in \mathbb{R} \tag{40}$$

with a smooth f, has at $\alpha = 0$ a saddle-focus equilibrium point $x_0 = 0$ with eigenvalues $\lambda_1(0) > 0 > Re\lambda_{2,3}(0)$ and a homoclinic orbit Γ_0. Assume that the following genericity conditions hold:

1. $\sigma_0 = \lambda_1(0) + Re\lambda_{2,3}(0) > 0$,
2. $\lambda_2(0) \neq \lambda_3(0)$.

Then, system (40) has an infinite number of saddle limit cycles in a neighbourhood U_0 of $\Gamma_0 \cup x_0$ for all sufficiently small $|\beta|$.

5. Sil'nikov Theorem

The focus of this work is to study the conditions under which horseshoes appear in three dimensional flows in sections near to a homoclinic trajectory to a fixed point. The following result by Sil'nikov [1965], shows how horseshoes appear in return maps defined on a transversal section to a homoclinic orbit to a hyperbolic fixed point with two conjugate complex eigenvalues with negative real part and a real positive eigenvalue. It is important to stress that in the proof of this result that we present below can be found in [7]. At the very start, we assume that the flow can be perturbed into a linear system. Of course this kind of assumption overlooks that by no means this is true in general. Later on, we will see that it can be justified but for the time being, we will stick to it.

Consider a flow ϕ_t in $\mathbb{R}^3$ for which the associated vector field has an equilibrium point at the origin with a real positive eigenvalue λ and a pair of complex eigenvalues ω, $\overline{\omega}$ which have negative real parts (the case where λ is negative and $\mathrm{Re}(\omega)$ positive is dealt with similarly). The stable manifold theorem allows us to introduce coordinates so that the local unstable manifold is contained in the z-axis and the local stable manifold is contained in the (x, y) plane. We assume further that the trajectory γ in the unstable manifold which points upward near 0 is a homoclinic orbit which enters the (x, y) coordinate plane and spirals toward the origin as $t \to \infty$, see Figure 18.

In this situation it is possible to find a section in which the return map is well defined for orbits near γ in order to prove the following theorem.

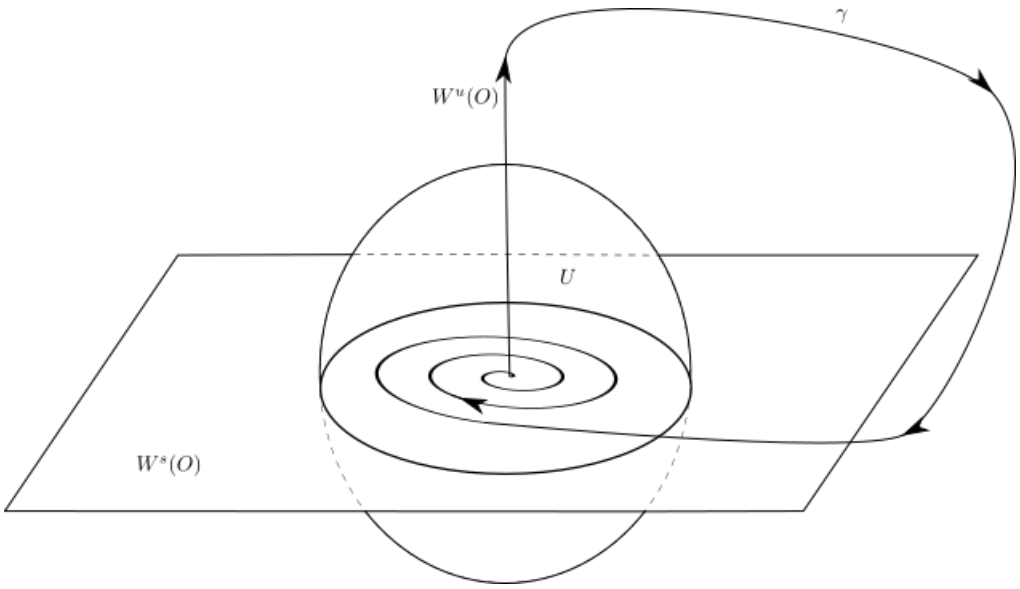

Figure 18: A homoclinic orbit that enters the (x, y) plane and spirals toward the origin.

Theorem 5.1. *If $0 < -Re\ \omega < \lambda$, then the flow ϕ_t can be perturbed to ϕ'_t which has a homoclinic orbit γ' near γ and the return map of γ' for ϕ'_t has a countable set of horseshoes.*

Remark 5.2. Theorem 5.1 claims the existence of a a countable set of horseshoes in a perturbed flow of ϕ'_t. Note that if this happens, then as a consequence to the symbolic description of the horseshoe there must be infinitely many periodic orbits and we can therefore deduce Theorem 4.8.

Proof. The proof of this theorem requires a thorough analysis of the flow of trajectories passing near the origin. However, if the flow ϕ_t is perturbed so that its vector field is linear in a neighbourhood U of the origin, the analysis needed is significantly simplified. We therefore assume throughout the rest of the proof that our original vector field has this property. The system of equations we are working with is the following,

$$\begin{bmatrix} \dot{x} \\ \dot{y} \\ \dot{z} \end{bmatrix} = \begin{bmatrix} \alpha & -\beta & 0 \\ \beta & \alpha & 0 \\ 0 & 0 & \lambda \end{bmatrix} \begin{pmatrix} x \\ y \\ z \end{pmatrix} \quad \text{where } \omega = \alpha + \beta i. \tag{41}$$

Note that the set of points with $z = 0$ is an invariant set in which solutions spiral towards the origin. The line of points with $x = y = 0$ is also an invariant set. In this case, trajectories within the line move away from the origin.

The above system of equations can be explicitly solved. For $(x, y, z) \in U$, the solution to (41) is;

$$\phi_t(x, y, z) = \begin{pmatrix} e^{\alpha t}\cos\beta t & -e^{\alpha t}\sin\beta t & 0 \\ e^{\alpha t}\cos\beta t & e^{\alpha t}\sin\beta t & 0 \\ 0 & 0 & e^{\lambda t} \end{pmatrix} \begin{pmatrix} x \\ y \\ z \end{pmatrix} \tag{42}$$

Observe that as trajectories flow close to the origin, the radial coordinate $r = \sqrt{x^2 + y^2} = e^{\alpha t}$ decreases $(\alpha < 0)$ while $|z|$ increases $(\lambda > 0)$.

We define the surfaces Σ_0 and Σ_1 by

$$\Sigma_0 = \{(x, y, z) | x^2 + y^2 = r_0^2 \text{ and } 0 < z < z_1\},$$
$$\Sigma_1 = \{(x, y, z) | x^2 + y^2 < r_0^2 \text{ and } z = z_1 > 0\}$$

By choosing r_0 and z_1 small enough, we can assume that Σ_0 and Σ_1 are in the neighbourhood U where the flow is linear. Trajectories flow from Σ_0 to Σ_1. Our goal is to compute the mapping $\psi : \Sigma_0 \to \Sigma_1$ which associates to each point $a \in \Sigma_0$, the first intersection with Σ_1 of the trajectory starting at a (see Figure 19).

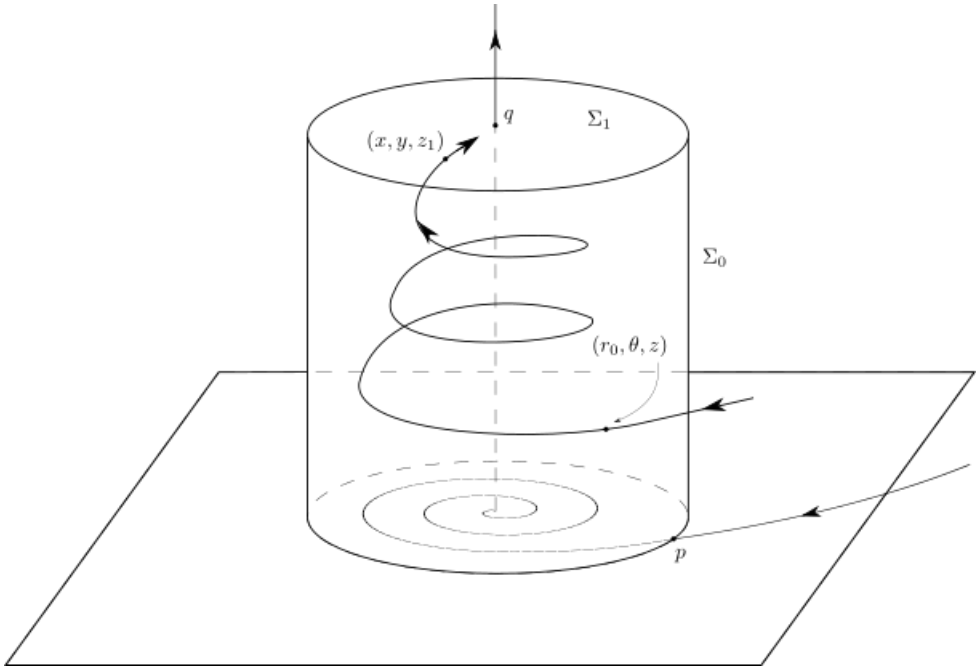

Figure 19: Sections Σ_0 and Σ_1.

The expression for ψ is given by solving $z_1 = e^{\lambda t} z$ for t to obtain the time of flight $t = \lambda^{-1} \ln(z_1/z)$, and substituting the result into (42). We obtain

$$\phi_t(x, y, z) = \left(\left(\frac{z_1}{z}\right)^{\alpha/\lambda} [(\cos\gamma)x - (\sin\gamma)y], \left(\frac{z_1}{z}\right)^{\alpha/\lambda} [(\sin\gamma)x + (\cos\gamma)y], z_1 \right) \tag{43}$$

where $\gamma = \beta\lambda^{-1} \ln(z_1/z)$. Setting $x = r_0 \cos\theta$, $y = r_0 \sin\theta$, we may then express $\psi : \Sigma_0 \to \Sigma_1$ as a two-dimensional diffeomorphism whose domain has coordinates $\theta = \arctan(y/x)$ and z, and whose range has coordinates x, y:

$$\psi(\theta, z) = \left(r_0 \left(\frac{z_1}{z}\right)^{\alpha/\lambda} \cos(\theta + \gamma), r_0 \left(\frac{z_1}{z}\right)^{\alpha/\lambda} \sin(\theta + \gamma) \right) = (\psi_1(\theta, z), \psi_2(\theta, z)). \tag{44}$$

Note that every vertical segment $\theta = \text{const.}$ in Σ_0 is mapped into a logarithmic spiral which encircles the z-axis and lies in Σ_1. These spirals can be obtained by introducing polar coordinates R and Θ over the

range of ψ

$$R = \sqrt{(\psi_1(\theta,z))^2 + (\psi_2(\theta,z))^2} = r_0(z_1/z)^{\alpha/\lambda},$$
$$\Theta = \arctan(\psi_2(\theta,z)/\psi_1(\theta,z)) = \theta + \gamma = \theta + \beta\lambda^{-1}\ln(z_1/z).$$

Isolating z_1/z in the expression for Θ and substituting it in the expression for R, we obtain the equation of a logarithmic spiral

$$R = r_0 e^{\alpha\beta^{-1}(\Theta-\theta)}. \tag{45}$$

In particular, we want to see that vertical segments are stretched as they wrap around the spiral. In order to do so, we compute the Jacobian derivative of ψ;

$$D\psi(\theta,z) = \begin{bmatrix} \frac{\partial\psi_1}{\partial\theta} & \frac{\partial\psi_1}{\partial z} \\ \\ \frac{\partial\psi_2}{\partial\theta} & \frac{\partial\psi_2}{\partial z} \end{bmatrix}. \tag{46}$$

This derivative can be conveniently written for later purposes, as the product of two matrices

$$D\psi(\theta,z) = r_0\left(\frac{z_1}{z}\right)^{\alpha/\lambda}\begin{bmatrix}\cos\gamma & -\sin\gamma \\ \sin\gamma & \cos\gamma\end{bmatrix}\begin{bmatrix} -\sin\theta & \frac{-\alpha\cos\theta+\beta\sin\theta}{\lambda z} \\ \\ \cos\theta & \frac{-\alpha\sin\theta-\beta\cos\theta}{\lambda z}\end{bmatrix}. \tag{47}$$

Thus we find that

$$\det(D\psi) = \left(\frac{\alpha r_0^2 z_1^{2\alpha/\lambda}}{\lambda}\right) z^{-(1+2\alpha/\lambda)}. \tag{48}$$

Therefore, for z sufficiently small, ψ contracts areas if $2\alpha < -\lambda$. This is consistent with the fact that the vector field has divergence $2\alpha+\lambda$ at the saddle point. However, since $-1 < \alpha/\lambda < 0$, even when ψ contracts areas, vertical segments $\{\theta = \text{const.}\ ;\ z \in (z, z_0)\}$ in Σ_0 are mapped into logarithmic spirals of radius $r_0(z_1/z)^{\alpha/\lambda}$ as we have seen before (45), and thus their lengths are stretched by an amount which becomes unbounded as $z \to 0$.

Denote now by p the intersection of $W^u(0)$ with Σ_0 and by q the point $(0,0,z_1) = W^u(0) \cap \Sigma_1$. The flow from q to p along $W^u(0)$ is nonsingular, so there is a diffeomorphism ϕ from a neighbourhood of q in Σ_1 to a neighbourhood of p in the surface $\tilde{\Sigma}_0 = \{(x,y,z) | x^2+y^2 = r_0, |z| < z_0\}$ which sends a point to the first intersection of its trajectory with $\tilde{\Sigma}_0$. The return map of Σ_0 near p is given by $\phi\circ\psi$ for those points r with $\phi(\psi(r)) \in \Sigma_0$. Changing coordinates by a rotation around the z-axis, we may assume that p lies on the x-axis ($\theta = 0$). Pick a small domain V in Σ_0 defined by

$$V = \{(r,\theta,z) \mid r = r_0, |\theta| < \delta, 0 < z < \varepsilon\}, \tag{49}$$

where ε is chosen such that $\psi(V)$ is contained in the domain of ϕ and δ will be specified later.

Each vertical segment of V is mapped to a spiral around q in Σ_1, and ϕ maps this spiral diffeomorphically into $\tilde{\Sigma}_0$ with $\phi(q) = p$. If δ is chosen sufficiently large, relative to ε, then each spiral in $\phi\circ\psi(V)$ cuts through V vertically many times until one reaches a portion of the spiral which does not cut through the top of V.

We want to locate subsets of V in which $\phi\circ\psi$ has a horseshoe. Note that (44) implies that if z varies along a vertical segment $J \subset V$ with $z \in (z', z'')$, where $(\beta/\lambda)(\log(z_1/z') - \log(z_1/z'')) = 2\pi$ or equivalently $z''/z' = \exp(2\pi\lambda\beta)$, then $\psi(J)$ makes one full turn of a logarithmic spiral. The distance of $\psi(J)$ from q is of the order of $(z_1/z)^{\alpha/\lambda}$, $z \in J$. The ratio $(z_1/z)^{\alpha/\lambda}/z \to \infty$ as $z \to 0$. Fix $\delta > 0$ small in the definition of V and pick (z', z'') with the properties

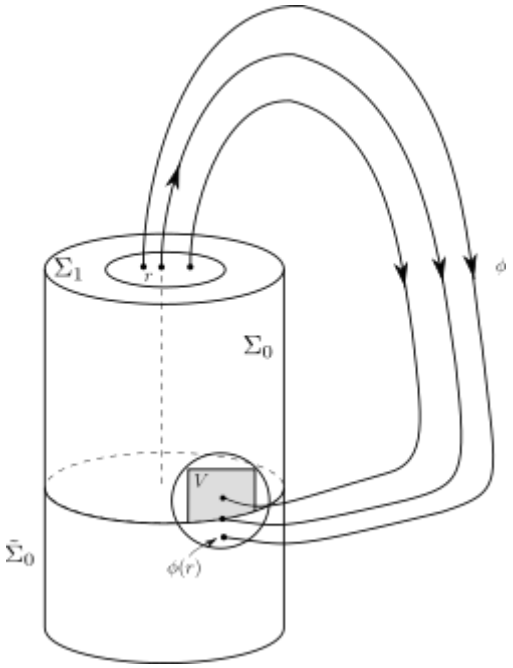

Figure 20: The return map ϕ.

1. $z''/z' = \exp(2\pi\lambda/\beta)$,
2. z', z'' are sufficiently small that $(z_1/z)^{\alpha/\lambda} < \delta$ for all $z \in (z', z'')$.
3. if $|\theta| < \delta$, then the images $\phi \circ \psi(r_0, \theta, z')$ and $\phi \circ \psi(r_0, \theta, z'')$ do not lie in Σ_0.

Define $W = \{(r_0, \theta, z) \in V | z \in (z', z'')\}$ and observe that (5.1) implies that the image $\phi \circ \psi(W)$ looks like a horseshoe mapping.

To demonstrate that $W \cap \phi \circ \psi(W)$ contains a horseshoe, we need to show that $D(\phi \circ \psi)$ satisfies the conditions of Theorem 3.12;

H1 Let $\mathcal{J}$ be the set $\{1, 2, ..., N\}$ and let H_i, V_i for $i \in \mathcal{J}$ be disjoint horizontal and vertical strips and let $f(H_i) = V_i$, $i \in \mathcal{J}$.

H3 There exist sets (sector-bundles) $S^u = \{(\xi, \eta) || \xi | < \mu |\eta|\}$ defined over $\bigcup_{i \in \mathcal{J}} V_i$ and $S^s = \{(\xi, \eta) || \eta | < \mu |\xi|\}$ defined over $\bigcup_{i \in \mathcal{J}} H_i$ with $0 < \mu < 1$ such that $Df(S^u) \subset S^u$ and $Df^{-1}(S^s) \subset S^s$. Moreover, if $Df(\xi_0, \eta_0) = (\xi_1, \eta_1)$ and $Df^{-1}(\xi_0, \eta_0) = (\xi_{-1}, \eta_{-1})$ then $|\eta_1| \geq (1/\mu)|\eta_0|$ and $|\xi_{-1}| \geq (1/\mu)|\xi_0|$.

Satisfaction of H1 is immediate. Moreover, since ϕ is a diffeomorphism on Σ_1 from (47) we have

$$D(\phi \circ \psi)(r_0, \theta, z) = r_0 \left(\frac{z_1}{z}\right)^{\alpha/\lambda} A \begin{bmatrix} \cos\gamma & -\sin\gamma \\ \sin\gamma & \cos\gamma \end{bmatrix} \begin{bmatrix} -\sin\theta & \frac{-\alpha\cos\theta + \beta\sin\theta}{\lambda z} \\ \cos\theta & \frac{-\alpha\sin\theta - \beta\cos\theta}{\lambda z} \end{bmatrix}, \tag{50}$$

Where $A = D\phi(\psi(r_0, \theta, z))$. We can rewrite (50) in the form

$$z^{-(\alpha/\lambda+1)} BC \begin{bmatrix} z & 0 \\ 0 & 1 \end{bmatrix} \tag{51}$$

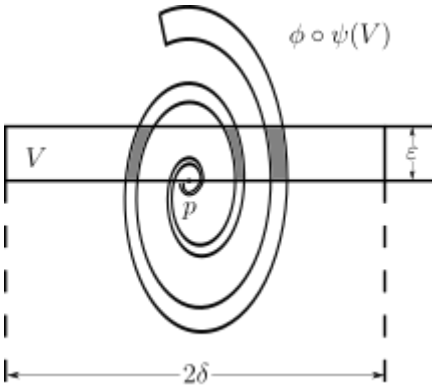

Figure 21: V and $\phi \circ \psi(V)$.

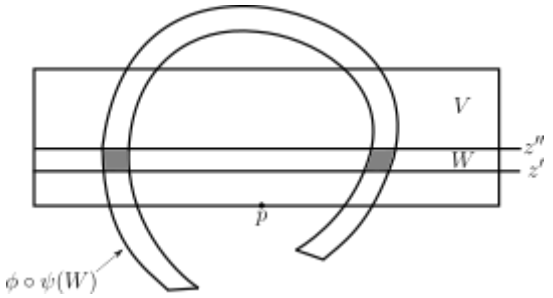

Figure 22: $\phi \circ \psi|_W$ has a horseshoe : $W \cap \phi \circ \psi(W)$ shown shaded.

where

$$B = r_0 z_1^{\alpha/\lambda} A \begin{bmatrix} \cos\gamma & -\sin\gamma \\ \sin\gamma & \cos\gamma \end{bmatrix}, \tag{52}$$

and the matrix

$$C = \begin{bmatrix} -\sin\theta & \frac{-\alpha\cos\theta+\beta\sin\theta}{\lambda z} \\ \\ \cos\theta & \frac{-\alpha\sin\theta-\beta\cos\theta}{\lambda z} \end{bmatrix} \tag{53}$$

is nonsingular and approximately constant in each component of $W \cap \phi \circ \psi(W)$, since $|\theta| < \delta$. Moreover, since the points in $W \cap \phi \circ \psi(W)$ have images under ψ whose arguments in Σ_1 differ by approximately π, the values of B in the two components of $W \cap \phi \circ \psi(W)$ differ approximately by multiplication by

$$-I = \begin{bmatrix} -1 & 0 \\ 0 & -1 \end{bmatrix}$$

When z is small, $z^{-(\alpha/\lambda+1)}$ is large and $z^{-\alpha/\lambda}$ is small. We observe that the eigenvalues of the product

$$\mu \begin{bmatrix} b_{11} & b_{12} \\ b_{21} & b_{22} \end{bmatrix} \begin{bmatrix} c_{11} & c_{12} \\ c_{21} & c_{22} \end{bmatrix} \begin{bmatrix} 0 & 0 \\ 0 & 1 \end{bmatrix} = \mu \begin{bmatrix} 0 & b_{11}c_{12} + b_{12}c_{22} \\ 0 & b_{21}c_{12} + b_{22}c_{22} \end{bmatrix} \tag{54}$$

are 0 and $\mu(b_{21}c_{12} + b_{22}c_{22})$, with eigenvectors

$$v_1 = (1, 0) \qquad \text{and} \qquad ((b_{11}c_{12} + b_{12}c_{22}), (b_{21}c_{12} + b_{22}c_{22})), \tag{55}$$

respectively. Since $\mu = z^{-(\alpha/\lambda+1)}$, as $z \to 0$ the second eigenvalue becomes large as we choose strips with z', $z'' \to 0$ and, provided the ratio

$$|(b_{21}c_{12} + b_{22}c_{22})/(b_{11}c_{12} + b_{12}c_{22})| \tag{56}$$

remains bounded away from zero, then the eigenvectors of 0 and $\mu(b_{21}c_{12} + b_{22}c_{22})$ remain in disjoint cones. Moreover, the eigenvectors and eigenvalues of (50) are close to those of the singular matrix (54) for, being distinct, they vary smoothly with the matrix coefficients. If $(b_{21}c_{12} + b_{22}c_{22})$ is not bounded away from 0 for points of $V \cap \phi \circ \psi(V)$ as $z \to 0$, then we must perturb the flow ϕ_t to accomplish this. A perturbation which has the effect of rotating trajectories around γ so that the perturbed return map is the composition (on the left) with a rigid rotation will work.

The sectorial structure for (53) is now obtained from the limiting values of the eigenvectors of this product as z', $z'' \to 0$. (The limit values exist, because $\theta \to 0$ and $\gamma \pmod{\pi}$ approaches the value which determines the line in Σ_1 which $D\phi(q)$ maps to the horizontal line in the tangent space to Σ_0 at p.) Any small sectors around these limiting values satisfy (H3) when z' and z'' are sufficiently small. Choosing a sequence of rectangles W in V whose heights decrease geometrically, we obtain a sequence of horseshoes for our perturbed flow, which still has a homoclinic orbit for the equilibrium at the origin. □

6. The Sil'nikov Problem

In Section 5 we considered a three dimensional dynamical system with a hyperbolic fixed point with two conjugate complex eigenvalues with negative real part and a positive real eigenvalue. We took notice that in order to prove the existence of Horseshoes on a transversal section to the homoclinic orbit we had to assume that in a neighbourhood of the origin our flow could be perturbed into a linear flow. This is not a general assumption and we therefore must think of the problem in a slightly different, but also natural, way.

We will describe the orbits of our system in a more suitable way to the problem we are treating. Roughly speaking, we will consider adequate transversal sections and the time of flight between them as a new variable.

Also note that in this section we are not going to constrain ourselves to a three-dimensional space. All the results work in arbitrary dimension. This development of the Sil'nikov problem is due to Bo Deng [3]. We have followed the notation introduced in this work by Deng. It is also important to mention that some of the proofs in this paper have been omitted. The proof of the most important one (proof of Theorem 6.5 below) is provided.

In Section 6.2 we will carefully define the concept of Sil'nikov data which is as we mentioned above, a way of considering the time of flight as a new variable. In Section 6.3 we prove the existence and uniqueness of a solution (solution of the Sil'nikov problem) that satisfies the Sil'nikov data. Subsection 6.4 introduces a series of bounds that the solution to the Sil'nikov problem and its derivatives satisfy. We will use these bounds of the Sil'nikov solution to prove an important result, the λ-Lemma. Altogether, these results will allow us in Subsection 6.5 to develop an (exponential) expansion for the solution of the Sil'nikov problem. Then, in Subsection 6.6 we expose the relevance of the exponential expansion by proving the C^1 linearization of two-dimensional systems near a hyperbolic equilibrium point with an homoclinic orbit.

6.1 A Toy Example

Before diving deep into the concepts of Sil'nikov data and Sil'nikov solution, we may want to look at a simple example in order to gain some insight. We will do so by considering a simple two-dimensional system,

$$\begin{cases} \dot{x} = \lambda x \\ \dot{y} = \mu y \end{cases} \quad \text{with} \quad \lambda < 0 \quad \text{and} \quad \mu > 0. \tag{57}$$

Clearly enough, the solution to this system is

$$x(t) = e^{\lambda t} x_0 \quad \text{and} \quad y(t) = e^{\mu t} y_0. \tag{58}$$

These solutions induce the following phase portrait in the first quadrant as shown in Figure 23.

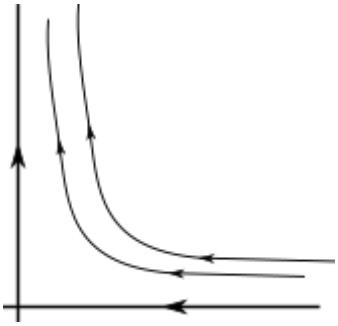

Figure 23: Phase portrait of $(x, y)(t) = (e^{\lambda t} x_0, e^{\mu t} y_0)$

Note that in this phase portrait the origin is a fixed point and the x-axis is the stable variety and the y-axis is the unstable variety.

The idea behind the Sil'nikov data is that instead of having a solution $(x, y)(t)$ such that $(x, y)(0) = (x_0, y_0)$ we want to have a solution depending essentially on the starting and ending points and the time it takes for the solution to go from one to the other. To do this, we set up two sections on the plane; $y = y_1$ and $x = x_0$ as in Figure 24.

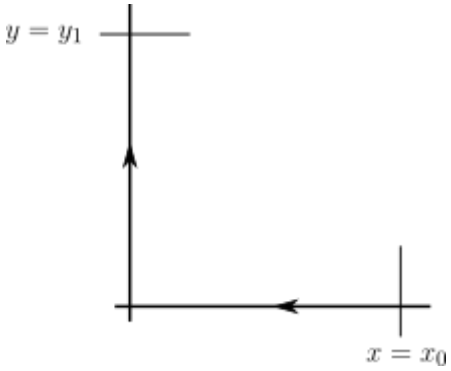

Figure 24: The two sections $x = x_0$ and $y = y_0$.

Now, this is where one of the key ideas comes to play. Instead of considering a solution that satisfies the system of differential equations and the property $(x, y)(0) = (x_0, y_0)$ we look for solutions that also satisfy the set of differential equations but we now choose a slightly different conditions. Namely we want solutions such that

$$x(0) = x_0 \quad \text{and} \quad y(\tau) = y_1 \quad \text{for some} \quad \tau > 0. \tag{59}$$

In other words, we want solutions of the system of equations such that at time 0 the x component is x_0 and such that at time τ, the y component is y_1 (see Figure 25)

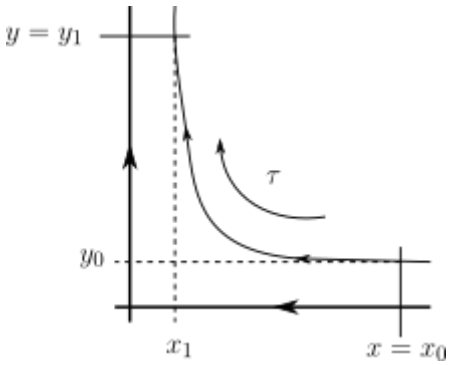

Figure 25: We look for solutions that go from section $x = x_0$ to section $y = y_1$ with time τ.

Note that in this case we can explicitly compute τ by solving $y_1 = y(t)$, which yields $\tau = \mu^{-1} \log \frac{y_1}{y_0}$.

Furthermore, for the example we are working, we can easily modify the initial solution to fit the new conditions,

$$x(t) = e^{\lambda t} x_0 \quad \text{and} \quad y(t) = e^{\mu(t-\tau)} y_1. \tag{60}$$

In conclusion, we have gone from considering the initial value problem to a modified version of it where we will depend on the triplet (τ, x_0, y_1) which will be known as the Sil'nikov data. A solution of the system of equations together with its Sil'nikov data is called a solution to the Sil'nikov problem.

As already mentioned, we will show that under mild conditions a solution to the Sil'nikov data is unique. We will also see a series of interesting results which will allow us to understand much better the behaviour of these solutions.

6.2 Sil'nikov Data

Throughout, $m > 0$ and $n > 0$ are two integers and $d = m + n$. The variables $x = (x^{(1)}, ..., x^{(m)}) \in \mathbb{R}^m$ and $y = (y^{(1)}, ..., y^{(n)}) \in \mathbb{R}^n$. $A \in \mathbb{R}^{m \times m}$ and $B \in \mathbb{R}^{n \times n}$ are two matrices. We will denote the sup norm for vectors in any Euclidean space as $|\cdot|$. $U \subset \mathbb{R}^d$ is a neighbourhood of the origin and $f \in C^{k+1}[U, \mathbb{R}^m]$ and $g \in C^{k+1}[U, \mathbb{R}^n]$ with $k \geq 1$. $\| \cdot \|_k$ is the usual sup norm in the Banach space $C^k[U, \mathbb{R}^i]$ with $i = m, n$ or d.

Consider the following two hypotheses:

(H1) There exists constants $\lambda < 0 < \mu$ and $C_1 > 1$ satisfying

$$|e^{At}| \leq C_1 e^{\lambda t}, \qquad \text{for all } t \geq 0$$

and

$$|e^{Bt}| \leq C_1 e^{\mu t}, \qquad \text{for all } t \leq 0$$

(H2) Assume that $f \in C^{k+2}[U, \mathbb{R}^m]$, $g \in C^{k+2}[U, \mathbb{R}^n]$ with $k \geq 1$ and

$$\begin{aligned} f(0, y) &= 0 \qquad \text{for all } (0, y) \in U, \\ g(x, 0) &= 0 \qquad \text{for all } (x, 0) \in U, \\ Df(0, 0) &= 0 \qquad \text{and} \qquad Dg(0, 0) = 0. \end{aligned}$$

Consider a system of autonomous ordinary differential equations

$$\begin{aligned} \dot{x} &= Ax + f(x, y) \\ \dot{y} &= By + g(x, y) \end{aligned} \qquad (x, y) \in U \tag{61}$$

with A, B, f and g satisfying (H1) and (H2), respectively. Note that every autonomous ordinary differential equation $\dot{z} = F(z)$ with $z \in \mathbb{R}^d$ and $F \in C^{k+1}$ is C^{k+1} locally conjugate to equation (61) in a neighbourhood of its hyperbolic equilibrium. We will consider solutions to (61) in the following way.

Definition 6.1 (Sil'nikov data)**.** Let $(x, y) : I \to U$ be a solution of equation (61) with I being the maximum existence interval with respect to U. Since equation (61) is autonomous, we may always assume $0 \in I$.

For given $\tau \geq 0$, $x_0 \in \mathbb{R}^m$ and $y_1 \in \mathbb{R}^n$, (x, y) is the solution to the Sil'nikov problem for equation (61) if $[0, \tau] \subseteq I$, and the following conditions are satisfied:

$$x(0) = x_0 \qquad \text{and} \qquad y(\tau) = y_1. \tag{62}$$

The values (τ, x_0, y_1) are called the Sil'nikov data.

Denote by $(x, y)(t) = (x, y)(t; \tau, x_0, y_1)$ the solution to equations (61) and (62) if it is uniquely determined by its Sil'nikov data (τ, x_0, y_1). It is important to emphasise that the solution $(x, y)(t; \tau, x_0, y_1)$ is not the flux as we commonly know it. It is the solution that at time 0 $x(0) = x_0$ and at time τ $y(\tau) = y_1$.

Remark 6.2. It is very important to note that the Sil'nikov problem is reduced to the initial value problem when $\tau = 0$. But it is neither the initial value nor a boundary value problem in general, namely when $\tau > 0$.

6.3 Existence, Uniqueness and Continuous Dependence of the Sil'nikov Data

In this subsection we will prove the existence and uniqueness and continuous dependence on the Sil'nikov data of the solutions of the Sil'nikov problem. This is done by using a result from functional analysis, the Banach Fixed Point Theorem. We start with the definition of contraction map. Roughly speaking it is a map that for any two points in a vector space, the images of these points are always closer than the points themselves.

Definition 6.3. Let X be a vector space and $\| \cdot \|$ a norm over X. Assume that the couple $(X, \| \cdot \|)$ is a complete metric space. Then, a map $F : X \to X$ is called a contraction mapping on X if there exists $K \in [0, 1)$ such that for all $x, y \in X$

$$\| F(x) - F(y) \| \leq K \| x - y \| . \tag{63}$$

The constant K is known as the Lipschitz constant.

Theorem 6.4 (Banach Fixed Point Theorem)**.** *Let $(X, \| \cdot \|)$ be a non-empty complete metric space with a contraction mapping $F : X \to X$. Then F has a unique fixed point x^*. This means that $F(x^*) = x^*$. Furthermore, x^* can be found by taking a sequence starting at an arbitrary element $x_0 \in X$ and recurrently computing $x_n = F(x_{n-1})$ for $n \geq 1$. Then $x_n \to x^*$.*

Proof. Let $x_0 \in X$ be arbitrary and define a sequence $\{x_n\}$ by setting $x_n = F(x_{n-1})$. In first place we note that we have the inequality

$$\begin{aligned} \| x_{n+1} - x_n \| = \| F(x_n) - F(x_{n-1}) \| \leq K \| x_n - x_{n-1} \| = K \| F(x_{n-1}) - F(x_{n-2}) \| \leq \\ \leq K^2 \| x_{n-1} - x_{n-2} \| = K^2 \| F(x_{n-2}) - F(x_{n-3}) \| \leq \ldots \leq K^n \| x_1 - x_0 \| . \end{aligned} \tag{64}$$

It follows by induction on n that this inequality is satisfied for all natural n.

We can now show that $\{x_n\}$ is a Cauchy sequence. Let m and n be natural numbers such that $n < m$.

$$\begin{aligned} \| x_m - x_n \| &\leq \| x_m - x_{m-1} \| + \| x_{m-1} - x_{m-2} \| + \cdots + \| x_{n+1} - x_n \| \\ &\leq K^{m-1} \| x_1 - x_0 \| + K^{m-2} \| x_1 - x_0 \| + \cdots + K^n \| x_1 - x_0 \| \\ &\leq K^n \| x_1 - x_0 \| \sum_{i=0}^{m-n-1} K^i \\ &\leq K^n \| x_1 - x_0 \| \sum_{i=0}^{\infty} K^i \\ &= K^n \| x_1 - x_0 \| \left(\frac{1}{1-K} \right). \end{aligned} \tag{65}$$

Since $K < 1$, for every $\varepsilon > 0$ we can find natural N large enough so that

$$K^N < \frac{\varepsilon(1-K)}{\| x_1 - x_0 \| + 1}. \tag{66}$$

Now, choosing m and n greater than N we can write

$$\| x_m - x_n \| \leq K^n \| x_1 - x_0 \| \left(\frac{1}{1-K} \right) < \left(\frac{\varepsilon(1-K)}{\| x_1 - x_0 \|} \right) \| x_1 - x_0 \| \left(\frac{1}{1-K} \right) = \varepsilon. \tag{67}$$

This proves that the sequence $\{x_n\}$ is Cauchy. The completeness of $(X, \| \cdot \|)$ assures that the sequence has a limit $x^* \in X$. Also, x^* must be a fixed point of F:

$$x^* = \lim_{n \to \infty} x_n = \lim_{n \to \infty} F(x_{n-1}) = F\left(\lim_{n \to \infty} x_{n-1} \right) = F(x^*). \tag{68}$$

As a contraction mapping, F is continuous so it is justified to bring the limit inside F. Lastly, F cannot have more than one fixed point $(X, \| \cdot \|)$ since any pair of distinct fixed points x_1* and x_2^* would contradict the contraction of F

$$\| F(x_1^*) - F(x_2^*) \| = \| x_1^* - x_2^* \| < K \| x_1^* - x_2^* \| . \tag{69}$$

□

This is a very important result which will allow us to prove several results throughout this work. We will now use it to prove the uniqueness of the solution to the Sil'nikov problem. The procedure will be to derive from the system of equations a contractive mapping on to a function space. From the Banach Fixed Point Theorem, there will be a unique fixed point which will be our solution to the Sil'nikov problem.

Theorem 6.5. *Suppose that equation (61) satisfies (H1), (H2) and $f, g : U \to \mathbb{R}^{n+m}$ are C^{k+1}, $k \geq 1$. There exists a neighbourhood $V \subset U$ of the origin in $\mathbb{R}^m \times \mathbb{R}^n$ such that*

(a) For every $(\tau, \xi, \eta) \in \mathbb{R}_+ \times V$, there exist a constant $t_0 > \tau$ depending on (τ, ξ, η) and a unique solution $(x, y) : [0, t_0] \to U$ satisfying $x(0) = \xi$ and $y(\tau) = \eta$. That is the Sil'nikov problem in Definition 6.1 can be solved.

(b) Let $x := x(t; \tau, \xi, \eta)$ and $y := (t; \tau, \xi, \eta)$ be the solution to the Sil'nikov problem, then (x, y) is C^{k+1} in (t, τ, ξ, η).

Proof. Althoug an outline of the proof of this result can be found in [3], we have taken the time to fill in every detail of this proof. This will provide the reader with a valuable insight on the techniques used to work with Sil'nikov data and the solutions to the Sil'nikov Problem, such as the use of the Banach Fixed Point Theorem.

To prove this theorem we first note that the existence and uniqueness of solutions to the Sil'nikov problem of equations (61) and (62) are equivalent to the existence and uniqueness of a fixed point for a functional operator. Indeed, we define this operator by applying variation of constants to equation (61) with the constraint (62). Let $(x(t), y(t)) = (e^{At}u(t), e^{Bt}v(t))$ be a solution of (61) for some functions $u(t), v(t)$. Notice that since e^{At} and e^{Bt} are invertible matrices this is not a restriction. Differentiation with respect to t yields the following expression:

$$(\dot{x}(t), \dot{y}(t)) = (Ae^{At}u(t) + e^{At}\dot{u}(t), Be^{Bt}v(t) + e^{Bt}\dot{v}(t)). \tag{70}$$

We now substitute the above expressions for $x(t)$, $\dot{x}(t)$, $y(t)$ and $\dot{y}(t)$ into (61) and we obtain

$$Ae^{At}u(t) + f(x(t), y(t)) = Ae^{At}u(t) + e^{At}\dot{u}(t) \tag{71}$$
$$Be^{Bt}v(t) + g(x(t), y(t)) = Be^{Bt}v(t) + e^{Bt}\dot{v}(t). \tag{72}$$

We now simplify the equations and isolate $\dot{u}(t)$ and $\dot{v}(t)$ respectively,

$$\dot{u}(t) = e^{-At}f(x(t), y(t))$$
$$\dot{v}(t) = e^{-Bt}g(x(t), y(t)).$$

Integrating the first equation between 0 and t and the second one between τ and t,

$$\int_0^t e^{-As}f(x(s), y(s))ds = u(t) - u(0)$$
$$\int_\tau^t e^{-Bs}g(x(s), y(s))ds = v(t) - v(\tau).$$

Recall that we want to find $(x(t), y(t))$ satisfying $x(0) = \xi$ and $y(\tau) = \eta$. Then, taking into account that $u(0) = x(0) = \xi$ and that $v(\tau) = e^{-B\tau}y(\tau) = e^{-B\tau}\eta$ and manipulating the expressions, we transform our

equations into

$$\begin{aligned} x(t) &= e^{At}\xi + \int_0^t e^{A(t-s)} f(x(s), y(s))ds \\ y(t) &= e^{B(t-\tau)}\eta + \int_\tau^t e^{B(t-s)} g(x(s), y(s))ds. \end{aligned} \tag{73}$$

We therefore conclude that a pair of solutions of (61) must also satisfy (73). The advantage of this new formulation of (61) is twofold: it is a fixed point equation and the derivatives of x and y are not involved in the equation.

We are going to use the fixed point theorem to prove that the operator defined by equation (73) is a contractive operator defined in a suitable Banach space. In other words, fix $V \subset U$ and $(\tau, \xi, \eta) \in \mathbb{R}_+ \times V$. Then, for every $t_0 > \tau$ we take W such that $V \subset W \subset U$. We consider the function space

$$\mathcal{X} = \{(x, y) \in C([0, t_0], W) \quad | \quad x(0) = \xi, y(\tau) = \eta\}. \tag{74}$$

We define for every $(x, y) \in \mathcal{X}$ the operator $F : \mathcal{X} \to \mathcal{X}$, $F(x, y)(t) = (F_1(x, y)(t), F_2(x, y)(t))$ as

$$F_1(x, y)(t) = e^{At}\xi + \int_0^t e^{A(t-s)} f(x(s), y(s))ds \tag{75}$$

$$F_2(x, y)(t) = e^{B(t-\tau)}\eta + \int_\tau^t e^{B(t-s)} g(x(s), y(s))ds. \tag{76}$$

We can clearly see that if $(x, y) \in \mathcal{X}$, then $F(x, y)$ is continuous and

$$F(x, y)(0) = \xi \quad \text{and} \quad F(x, y)(\tau) = \eta. \tag{77}$$

We take $|\cdot|$ to be any norm in $\mathbb{R}^{n+m}$ and we define the norm $\|\cdot\|$ for $z = (x, y) \in \mathcal{X}$ as $\| z \| = \sup_{t\in[0,t_0]} (|z(t)|)$. Let $B_\rho \subset \mathcal{X}$ be the radius ρ ball in $\mathcal{X}$, namely $B_\rho = \{(x, y) \in \mathcal{X}; \| (x, y) \| \leq \rho\}$. Now, we are going to check that $F : B_\rho \to B_\rho$ is contractive when $\rho \ll 1$.

We start with F_1. From (H1), we have that

$$|F_1(x, y)(t)| \leq C_1 e^{\lambda t}|\xi| + \int_0^t C_1 e^{\lambda(t-s)} |f(x(s), y(s))| \, ds. \tag{78}$$

(H2) assures that f is of order 2 at $(0, 0)$. Hence, for some constant K, $|f(x, y)| \leq K(|x|^2 + |y|^2)$ and so we obtain that,

$$\begin{aligned} C_1 e^{\lambda t}|\xi| + \int_0^t C_1 e^{\lambda(t-s)} |f(x(s), y(s))|ds &\leq C_1 \left(e^{\lambda t}|\xi| + K \int_0^t e^{\lambda(t-s)} (\| x \|^2 + \| y \|^2)ds \right) \\ &\leq C_1 \left(e^{\lambda t}|\xi| + K\rho^2 \int_0^t e^{\lambda(t-s)} ds \right) = C_1 \left(e^{\lambda t}|\xi| + K\rho^2 \left(\frac{-1}{\lambda} \right) (1 - e^{\lambda t}) \right). \end{aligned} \tag{79}$$

Since $\lambda < 0$,

$$C_1 \left(e^{\lambda t}|\xi| + K\rho^2 \left(\frac{-1}{\lambda} \right) (1 - e^{\lambda t}) \right) \leq C_1 \left(|\xi| + \frac{K\rho^2}{|\lambda|} \right). \tag{80}$$

By choosing $|\xi| < \frac{\rho}{2C_1}$ and $\rho < \frac{|\lambda|}{2KC_1}$, we have that

$$C_1\left(|\xi| + \frac{K\rho^2}{|\lambda|}\right) < \frac{\rho}{2} + \frac{\rho}{2} = \rho \tag{81}$$

Similarly, we can bind F_2. From (H1) if $0 \leq t \leq \tau$,

$$|F_2(x,y)(t)| \leq C_1 e^{\mu(t-\tau)}|\eta| + \int_t^\tau C_1 e^{\mu(t-s)}\,|g(x(s),y(s))|\,ds. \tag{82}$$

From (H2) we can say that g is also of order 2 at $(0,0)$. Namely, for some constant K, $|g(x,y)| \leq K(|x|^2+|y|^2)$ and so we obtain that

$$\begin{aligned} C_1 e^{\mu(t-\tau)}|\eta| + \int_t^\tau C_1 e^{\mu(t-s)}|g(x(s),y(s))|ds &\leq C_1\left(e^{\mu(t-\tau)}|\eta| + K\int_t^\tau e^{\mu(t-s)}(\parallel x \parallel^2 + \parallel y \parallel^2)ds\right) \\ &\leq C_1\left(e^{\mu(t-\tau)}\eta + K\rho^2\int_t^\tau e^{\mu(t-s)}ds\right) = C_1 e^{\mu(t-\tau)}\left(|\eta| + \frac{K\rho^2}{\mu}\right). \end{aligned} \tag{83}$$

Since $t-\tau < 0$,

$$C_1\left(e^{\mu(t-\tau)}|\eta| + \frac{K\rho^2}{\mu}\right) \leq C_1\left(|\eta| + \frac{K\rho^2}{\mu}\right). \tag{84}$$

By choosing $|\eta| < \frac{\rho}{2C_1}$ and $\rho < \frac{\mu}{2KC_1}$ we have that

$$C_1\left(|\eta| - \frac{K\rho^2}{\mu}\right) < \frac{\rho}{2} + \frac{\rho}{2} = \rho. \tag{85}$$

We are now left to see how can we bind $F_2(x,y)(t)$ for $\tau < t \leq t_0$. We can not apply (H1) in this case.

$$|F_2(x,y)(t)| \leq |e^{B(t-\tau)}||\eta| + \int_\tau^t |e^{B(t-s)}g(x(s),y(s))|ds. \tag{86}$$

However,

$$|e^{Bt}| = |e^{Bt_0}e^{B(t-t_0)}| \leq |e^{Bt_0}|C_1 e^{\mu(t-t_0)} = \bar{C}_1 e^{\mu(t-t_0)} \tag{87}$$

and we can proceed analogously as before provided that t_0 is a fixed constant. In this case the radius ρ will depend on t_0. Indeed, we can apply (H2) now and (87),

$$\begin{aligned} |F_2(x,y)(t)| &\leq \bar{C}_1 e^{\mu(t-\tau-t_0)}|\eta| + \bar{C}_1 K\int_\tau^t e^{\mu(t-s-t_0)}\left(\parallel x \parallel^2 + \parallel y \parallel^2\right)ds \\ &\leq \bar{C}_1 e^{-\mu\tau}|\eta| + \bar{C}_1 K\rho e^{-\mu\tau} \\ &\leq \bar{C}_1|\eta| + \bar{C}_1 K\rho^2. \end{aligned} \tag{88}$$

Now, by taking $|\eta| < \frac{\rho}{2\bar{C}_1}$ and $\rho < \frac{1}{2K\bar{C}_1}$ we have that

$$\bar{C}_1|\eta| + K\rho^2\bar{C}_1 < \frac{\rho}{2} + \frac{\rho}{2} < \rho. \tag{89}$$

Hence, $|F(x,y)(t)| < \rho$ for all $(x(t), y(t)) \in B_\rho$. We can therefore assure that F maps B_ρ to B_ρ. Take

$$\rho < \min\{\frac{|\lambda|}{2KC_1}, \frac{\mu}{2KC_1}, \frac{1}{2K\bar{C}_1}\}. \tag{90}$$

Notice that the neighbourhood V has been chosen as $V = \{|(\xi,\eta) < \frac{\rho}{2\bar{C}_1}\}$ and $W = \{|(x,y)| < \rho\}$.

We are left to check that F is Lipschitz with Lipschitz constant smaller than 1. Namely, F is contractive. This is, for $(x,y), (\tilde{x},\tilde{y}) \in B_\rho$ we must check that there exists $L < 1$ such that

$$\| F(x,y) - F(\tilde{x},\tilde{y}) \| \leq L \| (x,y) - (\tilde{x},\tilde{y}) \| \tag{91}$$

As before, we will start by bounding F_1.

$$|F_1(x,y)(t) - F_1(\tilde{x},\tilde{y})(t)| = \left| e^{At}\xi + \int_0^t e^{A(t-s)} f(x(s),y(s))ds - e^{At}\xi - \int_0^t e^{A(t-s)} f(\tilde{x}(s),\tilde{y}(s))ds \right|. \tag{92}$$

Using (H1), we have that

$$\begin{aligned} |F_1(x,y)(t) - F_1(\tilde{x},\tilde{y})(t)| &\leq \left| \int_0^t e^{A(t-s)} f(x(s),y(s))ds - \int_0^t e^{A(t-s)} f(\tilde{x}(s),\tilde{y}(s))ds \right| \\ &= \left| \int_0^t e^{A(t-s)} [f(x(s),y(s)) - f(\tilde{x}(s),\tilde{y}(s))]ds \right| \\ &\leq \int_0^t \left| e^{A(t-s)} \right| |f(x(s),y(s)) - f(\tilde{x}(s),\tilde{y}(s))| \, ds \\ &\leq \int_0^t C_1 e^{\lambda(t-s)} |f(x(s),y(s)) - f(\tilde{x}(s),\tilde{y}(s))| ds. \end{aligned} \tag{93}$$

We now use a well-known result, the Mean Value Theorem. It is known that for $z, \tilde{z} \in U$,

$$|f(z) - f(\tilde{z})| \leq \max_{w \in \overline{z\tilde{z}}} |Df(w)||z - \tilde{z}|. \tag{94}$$

If $|z|$, $|\tilde{z}| < \rho$, then since Df is continuous by (H2),

$$|Df(w)| \leq K|w| \leq K\rho. \tag{95}$$

Therefore, if $|z|$, $|\tilde{z}| < \rho$,

$$|f(z) - f(\tilde{z})| \leq K\rho|z - \tilde{z}|. \tag{96}$$

Notice that, when $(x,y), (\tilde{x},\tilde{y}) \in B_\rho$ we have that $\forall s \in [0,t]$, $|x(s)|, |y(s)|, |\tilde{x}(s)|, |\tilde{y}(s)| < \rho$. Therefore,

$$|f(x(s),y(s)) - f(\tilde{x}(s),\tilde{y}(s))| < K\rho|(x(s),y(s)) - (\tilde{x}(s),\tilde{y}(s))| < K\rho \| (x,y) - (\tilde{x},\tilde{y}) \|. \tag{97}$$

Then from (93),

$$\begin{aligned} |F_1(x,y)(t) - F_1(\tilde{x},\tilde{y})(t)| &\leq K\rho \| (x,y) - (\tilde{x},\tilde{y}) \| \, C_1 \int_0^t e^{\lambda(t-s)} ds \\ &\leq C_1 K\rho \| (x,y) - (\tilde{x},\tilde{y}) \|. \end{aligned} \tag{98}$$

Then

$$\| F_1(x,y) - F_1(\tilde{x},\tilde{y}) \| \leq C_1 K \rho \| (x,y) - (\tilde{x},\tilde{y}) \| \tag{99}$$

and we conclude that F_1 is contractive if $\rho < \frac{1}{KC_1}$.

We now check that F_2 is also contractive. Take $(x,y),(\tilde{x},\tilde{y}) \in B_\rho$,

$$\begin{aligned} &|F_2(x,y)(t) - F_2(\tilde{x},\tilde{y})(t)| \\ &= \left| e^{B(t-\tau)}\eta + \int_\tau^t e^{B(t-s)} g(x(s),y(s))ds - e^{B(t-\tau)}\eta - \int_\tau^t e^{B(t-s)} g(\tilde{x}(s),\tilde{y}(s))ds \right| \\ &\leq \left| \int_\tau^t e^{B(t-s)} [g(x(s),y(s)) - g(\tilde{x}(s),\tilde{y}(s))]ds \right| \\ &\leq \left| \int_\tau^t \left| e^{B(t-s)} \right| |g(x(s),y(s)) - g(\tilde{x}(s),\tilde{y}(s))| \right| ds. \end{aligned} \tag{100}$$

Now, using (H1) and (87),

$$\left| \int_\tau^t \left| e^{B(t-s)} \right| |g(x(s),y(s)) - g(\tilde{x}(s),\tilde{y}(s))ds| \right| \leq \left| \int_\tau^t \bar{C}_1 e^{\mu(t-s)} |g(x(s),y(s)) - g(\tilde{x}(s),\tilde{y}(s))| ds \right|. \tag{101}$$

Again, we use the Mean Value Theorem. For $z,\tilde{z} \in U$,

$$|g(z) - g(\tilde{z})| \leq \max_{w \in \overline{z\tilde{z}}} |Dg(w)||z - \tilde{z}|. \tag{102}$$

If $|z|, |\tilde{z}| < \rho$, by (H2)

$$|Dg(w)| \leq K|w| \leq K\rho. \tag{103}$$

Therefore, when $|z|, |\tilde{z}| < \rho$,

$$|g(z) - g(\tilde{z})| \leq K\rho |z - \tilde{z}|. \tag{104}$$

Notice that, when $(x,y),(\tilde{x},\tilde{y}) \in B_\rho$ we have that $\forall s \in [\tau,t]$, $|x(s)|, |y(s)|, |\tilde{x}(s)|, |\tilde{y}(s)| < \rho$. Therefore,

$$\begin{aligned} |g(x(s),y(s)) - g(\tilde{x}(s),\tilde{y}(s))| &\leq K\rho |(x(s),y(s)) - (\tilde{x}(s),\tilde{y}(s))| \\ &\leq K\rho \| (x,y) - (\tilde{x},\tilde{y}) \|. \end{aligned} \tag{105}$$

Then from (101),

$$\begin{aligned} |F_2(x,y)(t) - F_2(\tilde{x},\tilde{y})(t)| &\leq K\rho \| (x,y) - (\tilde{x},\tilde{y}) \| C_1 \int_\tau^t e^{\mu(t-s)} ds \\ &\leq C_1 K \rho \| (x,y) - (\tilde{x},\tilde{y}) \|. \end{aligned} \tag{106}$$

Thus, F_2 is also contractive. We can conclude that F is a contractive operator from B_ρ to itself. Due to the Banach Fixed Point Theorem, we have a unique fixed point z^* that satisfies $F(z^*) = z^*$. This means that z^* is also a solution to the Sil'nikov problem.

We do not prove here continuity and derivability with respect to initial conditions. The proof can be found in [3]. □

6.4 Exponential Bounds and λ-Lemma for D^n

This subsection will present in first place an important result on the solutions of the Sil'nikov problem. This is, essentialy, a set of bounds that will allow us to observe a phenomenon already described in Section 2.5, the λ-Lemma which is an important result when trying to detect chaos. The proofs that appear in this subsection are due to Bo Deng and can be found in [3].

Throughout, we denote $\overline{B^d(\delta)}$ to be the radius δ closed ball in $\mathbb{R}^d$ with its center at the origin:

$$\overline{B^d(\delta)} = \{z \in \mathbb{R}^d \quad ; \quad |z| \leq \delta\}. \tag{107}$$

Theorem 6.6. *Let A, B, f, g be as in (H1) and consider Equation (61). Let U, $V \subset \mathbb{R}^d$ and $(x, y)(t) = (x(t;\tau,\xi,\eta), y(t;\tau,\xi,\eta))$ with $\tau \geq 0$, $(\xi,\eta) \in V$, and $t \in [0, t_0]$ satisfy the conclusion of Theorem 6.5. Suppose that equation (61) satisfies hypotheses (H1), (H2) and f, g are C^{k+1} with $k \geq 1$.*

Then there exist constants C_2 and $\gamma_0 > 0$ independent of t, τ, ξ and η with $\overline{B^d(\gamma_0)} \subset U$ and $\overline{B^d(\gamma_0/2C_1)} \subset V$ such that for all $0 < \gamma \leq \gamma_0$ and $(\xi,\eta) \in \overline{B^d(\gamma/2C_1)}$, then the following estimates hold true for $0 \leq t \leq \tau$:

(a) $|x(t)| \leq \gamma e^{\lambda t}$ *and* $|y(t)| \leq \gamma e^{\mu(t-\tau)}$;

(b) $|D^\alpha x(t)| \leq C_2 e^{\lambda t}$ *and* $|D^\alpha y(t)| \leq C_2 e^{\mu(t-\tau)}$

(c) $|(\partial x/\partial\tau)(t)| \leq C_2\gamma e^{\lambda t+\mu(t-\tau)}$ *and* $|(\partial y/\partial\tau)(t)| \leq C_2\gamma e^{\mu(t-\tau)}$

(d) $|D^\beta(\partial x/\partial\tau)(t)| \leq C_2 e^{\lambda t+\mu(t-\tau)}$ *and* $|D^\beta(\partial y/\partial\tau)(t)| \leq C_2 e^{\mu(t-\tau)}$,

where D^α and D^β are the usual multi-indexed differentiation operators with respect to the spatial variables ξ and η up to the order $|\alpha| \leq k$ and $|\beta| \leq k-1$, respectively.

As we mentioned at the start of this subsection the proof of Theorem 6.6 is not included in this work. The proof uses deep functional analysis concepts. The reader can find it in Bo Deng's article [3]. We do not reproduce it in this work in order not to lose the focus from the main objective which is to study the solutions of the Sil'nikov problem.

Definition 6.7. We denote $\mathcal{D}^n$ as the graph of a smooth function h of $y \in \overline{B^n(\gamma_0/2C_1)}$ taking values in $\overline{B^m(\gamma_0/2C_1)}$; namely

$$h : \overline{B^n(\gamma_0/2C_1)} \to \overline{B^m(\gamma_0/2C_1)}. \tag{108}$$

We will say that D^n is C^k if h is C^k and we will refer to it as an n-dimensional disc. Denote $u_t(z_0)$ with $u_0(z_0) = z_0$ as the solution to equation (61) with the initial data z_0. Let

$$\mathcal{D}^n_\tau = u_\tau(\mathcal{D}^n) \cap \overline{B^d(\gamma_0/2C_1)}. \tag{109}$$

We will say $\mathcal{D}^n_\tau$ is C^k close to W^u_{loc} by ε if $\mathcal{D}^n_\tau$ is the graph of a C^k function h_τ of $y \in \overline{B^n(\gamma_0/2C_1)}$ such that all the derivatives of h_τ in y up to the order k are bounded by ε for all $y \in \overline{B^n(\gamma_0/2C_1)}$.

We can now extract from Theorem 6.6 (a) and (b) the following corollary.

Corollary 6.8. *(λ-Lemma for $\mathcal{D}^n$). Suppose that hypotheses (H1) and (H2) are satisfied and f and g are C^{k+1} with $k \geq 1$. Let γ_0 be as in Theorem 6.6.*

Then for every given n-dimensional disc $\mathcal{D}^n$ of class C^k there exist constants $\tau_0 > 0$ and $C_3 > 0$ such that $\mathcal{D}^n_\tau$ is C^k exponentially close to W^u_{loc} by $C_3 e^{\lambda\tau}$ for all $\tau \geq \tau_0$.

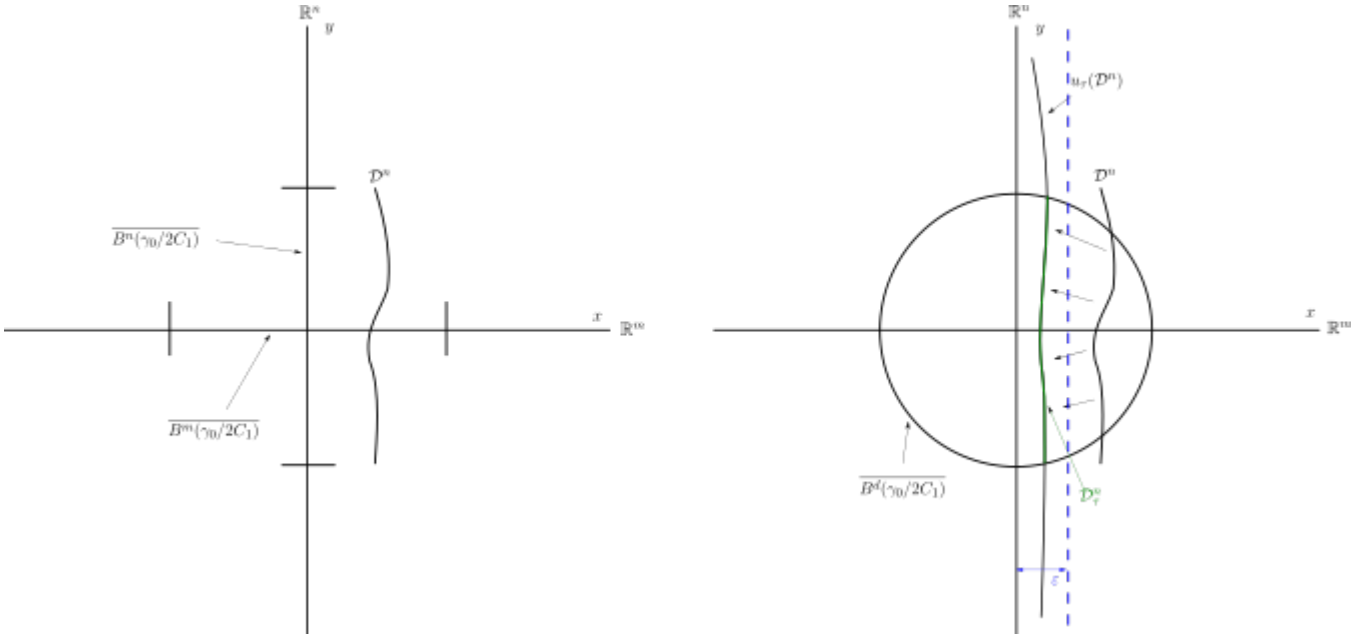

Figure 26: $\mathcal{D}^n$ depicted as the graph of a funtion $h : \overline{B^n(\gamma_0/2C_1)} \to \overline{B^m(\gamma_0/2C_1)}$ (left). $\mathcal{D}^n_\tau$ C^k close to the y-axis, which is the local unstable manifold W^u_{loc} in this case (right).

Proof. We want to see that $\mathcal{D}^n_\tau$ is C^k close to W^u_{loc}. Therefore, we will build a C^k function

$$\phi : \overline{B^n(\gamma_0/2C_1)} \to \overline{B^m(\gamma_0/2C_1)} \tag{110}$$

such that $\mathcal{D}^n_\tau$ will be the graph of this function defined in some neighbourhood of the origin. This function ϕ will be constructed in such a way that its norm is controlled by the bounds of the x component of the solution to the Sil'nikov problem seen in Theorem 6.6.

By definition of n-dimensional disk, we have that

$$\begin{aligned}\mathcal{D}^n_\tau =&\{(x_1, y_1) | x_1 = x(\tau; 0, h(y_0), y_0), y_1 = y(\tau; 0, h(y_0), y_0),\\ &\text{for those } |y_0| < \gamma_0/2C_1 \text{ such that } |x_1|, |y_1| < \gamma_0/2C_1\}.\end{aligned} \tag{111}$$

Note that in this description of $\mathcal{D}^n_\tau$ we have use the notation for the flux of a differential equation for x and y. That is, $(x(t; 0, x_0, y_0), y(t; 0, x_0, y_0))$ is now the flow of (61). From (a) in Theorem 6.6, if

$$e^{\lambda\tau}, e^{-\mu\tau} \leq 1/2C_1 \tag{112}$$

then we have

$$\mathcal{D}^n_\tau = \{(x_1, y_1) | x_1 = x(\tau; \tau, h(y_0), y_1), y_1 = y(\tau; 0, h(y_0), y_0), |y_0| < \gamma_0/2C_1, \text{ and } |y_1| < \gamma_0/2C_1\}. \tag{113}$$

Where we have again used the flux notation for y. We now fix any $\tau \geq 0$ and define the mapping $\nu_0(\cdot) = y(\tau; 0, h(\cdot), \cdot)$ from an open subset of $\overline{B^n(\gamma_0/2C_1)}$ onto $\overline{B^n(\gamma_0/2C_1)}$. This mapping is in fact a C^k diffeomorphism and the inverse ν_0^{-1} together with all of its derivatives up to order k are uniformly bounded in τ and y in $\overline{B^n(\gamma_0/2C_1)}$. Then the disc is described by

$$x_1 = x(\tau; \tau, h \circ \nu_0^{-1}(y_1), y_1) \tag{114}$$

□

6.5 Exponential Expansion and the Local Strong Unstable Manifold

In this subsection we introduce a key tool for the study of the solutions to the Sil'nikov problem, the exponential expansion. The construction of such an expansion for solutions will allow us to prove the C^1 linearisation of equation (61). We will also use it strongly in Section 7 to prove the Sil'nikov phenomenon in arbitrary dimension and in Section 8 to give a new proof of the Sil'nikov phenomenon in 3 dimensions.

Throughout this section, we assume that the matrix B in equation (61) takes the form

$$B = \begin{bmatrix} \mu & 0 \\ 0 & B_1 \end{bmatrix} \tag{115}$$

satisfying $\min\{\text{Re spec}(B_1)\} = \mu_1 > \mu > 0$, where $\text{spec}(B_1)$ is the set of all eigenvalues of the $(n-1) \times (n-1)$ matrix B_1. Note that in this case, (H1) is satisfied for the exact same μ, the principal positive eigenvalue of B. We call μ the principal positive eigenvalue because as it is the one with smallest real part, the eigenspace associated to it is the less repellent one (see Figure 27). Notice that by H2, the sets $\{x = 0\}$ and $\{y = 0\}$ are invariant and they correspond to W^u_{loc} and W^s_{loc}. Indeed on $\{x = 0\}$ the restricted dynamics is

$$\dot{y} = By + g(0, y) \tag{116}$$

and since $\text{spec}(B_1) \subset \{\lambda \in \mathbb{C};\ \text{Re}\lambda > 0\}$, the set $\{x = 0\}$ describes W^u_{loc}. This works analogously for $\{y = 0\}$.

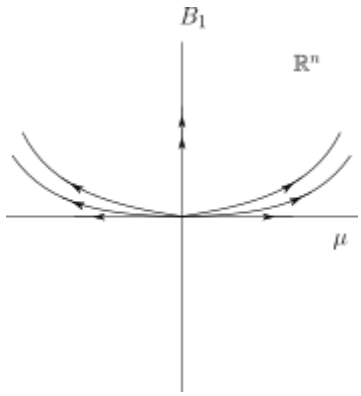

Figure 27: The horizontal axis shows the principal eigenspace, associated to μ.

From Theorem 6.6 (a), we can observe that the function Z defined as

$$Z(t; \tau, \xi, \eta) = y(t; \tau, \xi, \eta)e^{-\mu(t-\tau)} \tag{117}$$

is bounded in the C^k norm for $0 \leq t \leq \tau$, $\tau \geq 0$, $|\xi| \leq \gamma/2C_1$, $|\eta| \leq \gamma/2C_1$, and $\gamma \leq \gamma_0$, where γ_0 is as in Theorem 6.6. It will be of special interest to study the asymptotic behaviour of the function $Z(t; \tau, \xi, \eta)$ as $\tau \to +\infty$ for the sake of homoclinic and heteroclinic bifurcation problems. We therefore have the following result collecting the properties of Z.

Theorem 6.9. *Suppose the Hypotheses (H1), (H2) are satisfied and f and g are C^{k+1} with $k \geq 1$. If the matrix B takes the form (115) then for every arbitrary but fixed constant σ satisfying*

$$0 < \sigma < \min\{-\lambda, \mu, \mu_1 - \mu\}, \tag{118}$$

then there exist constants $0 < \gamma_1 < \gamma_0$ and C_4 independent of t, τ, ξ, and η such that function Z in (117) satisfies

(a) Z *and its derivatives in* t, τ, ξ *and* η *up to order* $k-1$ *converge exponentially at the order of* $C_4 e^{\sigma(t-\tau)}$ *as* $\tau \to \infty$.

(b) Let $\hat{Z} = (Z^{(2)}, \dots, Z^{(n)})$ *where* $Z = (Z^{(1)}, \dots, Z^{(n)})$. *Then* $\hat{Z}(t;\tau,0,\eta)$ *converges to zero as* $\tau \to \infty$.

The proof of this theorem will not be discussed in this work but can be found in Deng [3]. The above theorem assures that Z converges as $\tau \to \infty$. We can now extract the following conclusions.

Corollary 6.10. *Assume the conditions of Theorem 6.9 are satisfied. Let* $\phi(t,\xi,\eta) = \lim_{\tau\to\infty} Z(t;\tau,\xi,\eta)$ *for* $t \geq 0$, $|\xi| \leq \gamma_1$ *and* $|\eta| \leq \gamma_1$. *If* $k \geq 2$ *then* ϕ *is* C^{k-1} *and the following properties hold:*

(a) $\frac{\partial \phi}{\partial \xi}(t,0,0) = 0$ *and*

$$\frac{\partial \phi}{\partial \eta}(t,0,0) = \begin{bmatrix} 1 & 0 & \cdots & 0 \\ 0 & 0 & \cdots & 0 \\ \cdot & \cdot & \cdots & 0 \\ 0 & 0 & \cdots & 0 \end{bmatrix}, \qquad t \geq 0;$$

(b) $\phi(t,\xi,0) = (\phi^{(1)}, \dots, \phi^{(n)})(t,\xi,0) = 0, \qquad t \geq 0$ *and* $|\xi| \leq \gamma_1$

(c) $\hat{\phi}(t,0,\eta) = 0, \qquad t \geq 0$ *and* $|\eta| \leq \gamma_1$, *where* $\hat{\phi} = (\phi^{(2)}, \dots, \phi^{(n)})$.

Proof. To prove this corollary, we first recall the integral formula for the Sil'nikov problem (73) and, bearing in mind how we have defined Z in (117), we have that

$$Z(t;\tau,\xi,\eta) = e^{(B-\mu I)(t-\tau)}\eta + \int_\tau^t e^{B(t-s)} g(x(s),y(s)) ds e^{-\mu(t-\tau)}. \tag{119}$$

Differentiating this formula, together with the fact that $x(t) := x(t;\tau,0,0) = 0$ and $y(t) := y(t;\tau,0,0) = 0$, we obtain

$$\frac{\partial Z}{\partial \xi}(t;\tau,0,0) = 0 \qquad \text{and} \qquad \frac{\partial Z}{\partial \eta}(t;\tau,0,0) = e^{(B-\mu I)(t-\tau)}$$

Hence, Theorem 6.9 tells us that Z is convergent when $\tau \to \infty$ and the form (115) yield (a). Item (b) follows from $y(t;\tau,\xi,0) = 0$ and (c) is clearly a consequence from Theorem 6.9 (b). □

Theorem 6.9 and Corollary 6.10 allow us to give a decomposition for the y-component of the solution to the Sil'nikov problem in the following way

Corollary 6.11. *Under the conditions of Theorem 6.9 and Corollary 6.10* y*-component of the solution of the Sil'nikov problem can be expressed as*

$$y(t;\tau,\xi,\eta) = [\phi(t,\xi,\eta) + R(t;\tau,\xi,\eta)]e^{\mu(t-\tau)} \tag{120}$$

for all $0 \leq t \leq \tau$, $|\xi| \leq \gamma_1$ *and* $|\eta| \leq \gamma_1$ *with the function* ϕ *satisfying (a) and (b) of Corollary 6.10 and the remainder function* R *together with its derivatives up to the order* $k-1$ *are bounded by* $C_4 e^{\sigma(t-\tau)}$ *for* $0 \leq t \leq \tau$, $|\xi|\gamma_1$ *and* $|\eta| \leq \gamma_1$.

Definition 6.12. We refer to the function $\phi = \phi(t,\xi,\eta)$ as the *exponential expansion*. We also define the local strong unstable manifold W^{uu}_{loc} which is the $(n-1)$-dimensional submanifold of the stable manifold W^{u}_{loc} given by

$$W^{uu}_{\text{loc}} = \{(0,\eta) \mid \phi^{(1)}(0,0,\eta) = 0, |\eta| \leq \gamma_1\} \tag{121}$$

which are the points that are tangent to $y^{(1)} = 0$ at 0. γ_1 is a constant.

We can now show that all the solutions in $W^u_{\text{loc}} \setminus W^{uu}_{loc}$ are asymptotically tangent to the one-dimensional subspace of the principal unstable eigenvectors for the principal positive eigenvalue backwards in time. Through Corollary 6.10 we will be able to understand better the geometry of this exponential expansion.

Corollary 6.13. *Suppose the conditions of Theorem 6.9 are satisfied. Let γ_1 and the function ϕ be as in Corollary 6.10. Then*

(a) the $(n-1)$-dimensional submanifold given by

$$W^{uu}_{loc} = \{(0,\eta) | \phi^{(1)}(0,0,\eta) = 0, |\eta| \leq \gamma_1\}$$

is invariant for Equation (61) and it is C^{k-1} for $k \geq 2$;

(b) all the solutions in $W^u_{loc} \setminus W^{uu}_{loc}$ converge to the origin asymptotically along the $y^{(1)}$-axis as $t \to -\infty$.

Proof. We will use $y(t;0,x_0,y_0)$ for the flow and $y(t;\tau,x_0,y_0)$ for the Sil'nikov data. Notice that by Corollary 6.10 $\partial_\eta \phi^{(1)} = 0$ which means that it is tangent to $y^{(1)} = 0$ at 0.

(a) Let $x_1 = x(\tau;0,x_0,y_0)$ and $y_1 = y(\tau;0,x_0,y_0)$. Then by the uniqueness of the solution to the Sil'nikov problem of Equations (61) and (62) we have that $y(t-\tau;0,x_1,y_1) = y(t;\tau,x_0,y_1)$ (note that for $t=0$ and $t=\tau$, both sides of the equality have the same value). If we set $t=0$ and replace τ with t, since $x_0 = 0$ if and only if $x_1 = 0$ we see that the function $\bar{y}(t) := y(-t;0,0,y_1) = y(0;t,0,y_1)$ with initial data $\bar{y}(0) = y_1$ is the unique solution to the time-reversed equation in the unstable manifold ($x_0 = 0$):

$$\dot{y}(t) = -By - g(0,y). \tag{122}$$

Indeed, we can easily check this claim by differentiating the integral expression (73) for $\bar{y}(t) = y(-t;0,0,y_1)$ with respect to t,

$$\begin{aligned}
\frac{d}{dt}\bar{y}(t) &= \frac{d}{dt} e^{-Bt} y_1 + \int_0^{-t} e^{B(-t-s)} g(0, y(-s)) \\
&= -B \underbrace{\left[e^{-Bt} y_1 + e^{-Bt} \int_0^{-t} e^{-Bs} g(0,y(s)) ds \right]}_{\bar{y}(t)} - g(0, y(-t)) \\
&= -By - g(0,y)
\end{aligned}$$

Now, replace y_1 with y_0 and let $\bar{y}(t) = \bar{y}(t;y_0)$. Then, the exponential expansion (120) yields $\bar{y}(t;y_0) = [\phi(0,0,y_0) + R(0;t,0,y_0)]\, e^{-\mu t}$ for $t \geq 0$. Note that the group property of the flow and the exponential expansion allows us to write $\bar{y}(t;y_0) = \bar{y}(t-s;\bar{y}(s;y_0)) = [\phi(0,0,\bar{y}(s;y_0)) + R(0;t-s,0,\bar{y}(s;y_0))]\, e^{-\mu(t-s)}$ for any fixed $s \leq t$ in the definition interval of $\bar{y}$. From these two expressions for $\bar{y}(t;y_0)$ we can conclude that

$$\begin{aligned}
e^{-\mu t}\phi(0,0,y_0) &= e^{-\mu(t-s)} \\
\phi(0,0,y_0) &= e^{\mu s}\phi(0,0,\bar{y}(s,y_0)).
\end{aligned}$$

In particular, $\phi^{(1)}(0,0,y_0) = 0$ if and only if $\phi^{(1)}(0,0,\bar{y}(s;y_0)) = 0$. This proves (a).

(b) By part (c) of Corollary 6.10 we conclude from the solution $\bar{y}(t;y_0)$ above that $\bar{y}(t;y_0) = e^{-\mu t} R(0;t,0,y_0)$ which is of order $e^{-(\mu+\sigma)}$. Hence we have that any solution in $W^u_{\text{loc}} \setminus W^{uu}_{\text{loc}}$ converge to the origin asymptotically along the $y^{(1)}$-axis as $t \to \infty$. $\mathbb{R}^2$ □

6.6 A New Proof on C^1-Linearization in $\mathbb{R}^2$

In Section 5 we introduced Theorem 5.1 which, under a set of conditions, claimed the existence of a countable set of horseshoes for the Poincaré map near the homoclinic orbit of the system. Recall that at the start of the Theorem's proof, one assumes that the system can be C^1-linearized. This assumption is under no circumstances trivial and is in fact the main goal to which the results we have seen in this section point to. We will use the exponential expansion presented in Definition 6.12 of a solution in order to prove C^1-linearization in a low-dimensional case, $\mathbb{R}^2$. We will assume that Equation (61) is given in $\mathbb{R}^2$, which means that $m = n = 1$ and also satisfies (H1) and (H2). Let $A = \lambda$ and $B = \mu$. Equation (61) takes the form

$$\begin{cases} \dot{x} = \lambda x + f(x, y) \\ \dot{y} = \mu y + g(x, y) \end{cases} \tag{123}$$

This subsection follows the work of Deng [3]. Both Theorem 6.16 and its proof are due to Deng [3].

Definition 6.14. Equation (123) is said to admit a C^1-linearization if there exists a C^1 diffeomorphism in a neighbourhood of the origin which transforms the orbits of Equation (123) into the orbits of its linearized equation

$$\begin{aligned} \dot{u} &= \lambda u \\ \dot{v} &= \mu v. \end{aligned} \tag{124}$$

and preserves their orientation. In other words, system (123) and (124) are differentiably equivalent.

Remark 6.15. Hartman's Theorem assures that a dynamical system with a hyperbolic equilibrium point is topologically conjugated to its linear part. Recall that two systems are conjugated if there exists a homeomorphism sending solutions to solutions. Namely, if $\varphi(t, x)$ (respectively $\psi(t, y)$) are the flows of $\dot{x} = f(x)$, $\dot{y} = g(y)$, they are conjugated if

$$h(\varphi(t, x)) = \psi(t, h(y)) \tag{125}$$

for some homeomorphism h. However the definition of C^1 linearization allows

$$h(\varphi(t, x)) = \psi(t', h(y)) \tag{126}$$

with $t' = \tau(t, x)$ with $\frac{d\tau}{dt} > 0$, being h a diffeomorphism.

We shall give a proof to the following theorem using the exponential expansion (120).

Theorem 6.16. *Suppose that f and g satisfy (H2) and belong to the class C^{k+1} with $k \geq 2$. Then Equation (61) admits a C^1-linearization.*

Before giving the proof of this result, we will first derive the corresponding exponential expansion for the x-component of the solution $x(t; \tau, \xi, \eta)$. Let $(\bar{x}, \bar{y})(t) = (\bar{x}(t; \tau, \xi, \eta), \bar{y}(t; \tau, \xi, \eta))$ be the solution of the time reversed equation of Equation (123)

$$\begin{aligned} \dot{x} &= -\lambda x - f(x, y) \\ \dot{y} &= -\mu y - g(x, y) \end{aligned} \tag{127}$$

satisfying

$$\bar{x}(\tau) = \xi \qquad \text{and} \qquad \bar{y}(0) = \eta. \tag{128}$$

This exists and is unique due to Theorem 6.5. Applying the exponential expansion form (120) to $\bar{x}(t)$ we have

$$\bar{x}(t) = [\phi(t, \xi, \eta) + R(t; \tau, \xi, \eta)]e^{-\lambda(t-\tau)} \tag{129}$$

for some ϕ and R satisfying the stated properties as in Corollary 6.11. The uniqueness of solutions of Equations (127) and (128) assures us that

$$x(t; \tau, \xi, \eta) = \bar{x}(\tau - t; \tau, \xi, \eta) = [\phi(\tau - t, \xi, \eta) + R(\tau - t; \tau, \xi, \eta)]e^{\lambda t}. \tag{130}$$

Also, we still have $y(t; \tau, \xi, \eta) = [\psi(t, \xi, \eta) + r(t; \tau, \xi, \eta)]e^{\mu(t-\tau)}$ by (120) with some appropriate ψ and r.

Proof. (Theorem 6.16) First we will specify the needed neighbourhoods of the origin for both nonlinear and linear equations, namely Equation (123) and Equation (124). Fix $0 < \gamma < \gamma_0/2$ with γ_0 as in Theorem 6.9. Define

$$\begin{aligned} u_r &= \phi(0, \gamma, 0) > 0, \quad u_l = \phi(0, -\gamma, 0) < 0 \\ v_t &= \psi(0, 0, \gamma) > 0 \quad \text{and} \quad v_b = \psi(0, 0, -\gamma) < 0. \end{aligned} \tag{131}$$

This is due to the property that $\partial_\xi \phi(0, 0, 0) = 1$ and $\partial_\eta \psi(0, 0, 0) = 1$ by Corollary 6.10. Take $B^2(2\gamma)$ for Equation (123) and the rectangular region

$$\Omega = \{(u, v) | u_l \leq u \leq u_r, v_b \leq v \leq v_t\} \tag{132}$$

for Equation (127). Next we will build a mapping π from a neighbourhood $U \subset B^2(2\gamma)$ of the origin into Ω which will map an orbit of Equation (61) in U into an orbit of Equation (127) in Ω.

Consider now the first quadrant in $B^2(2\gamma)$ only. We can choose $x_0 = \gamma$ and $y_1 = \gamma$ fixed, the solution $(x, y)(t; \tau, x_0, y_1)$ to the Sil'nikov problem of Equations (123) and (128) is uniquely determined by τ.

Similar for $u_0 = u_r$ and $v_1 = v_t$, the solution $(u, v)(t; \tau, u_0, v_1)$ to the Sil'nikov problem for the linear Equation (127) is also uniquely determined by τ. In fact, we can explicitly express it as

$$u(t; \tau, u_0, v_1) = u_0 e^{\lambda t} \qquad \text{and} \qquad v(t; \tau, u_0, v_1) = v_1 e^{t-\tau}. \tag{133}$$

This property defines a one-to-one correspondence which induces a map that takes (x, y) into (u, v). To be more precise, let (x, y) be a point from the former local orbit for the nonlinear equation. Then, there is a unique time τ_1 and τ_2 with $\tau_1 + \tau_2 = \tau$ such that on that orbit, (x, y) is time τ_1 away from the right face and time τ_2 away from the top face (see Figure 28), namely

$$x = x(\tau_1; \tau_1, \gamma, y) = [\phi(0, \gamma, y) + R(0; \tau_1, \gamma, y)]e^{\lambda \tau_1}. \tag{134}$$

Notice that from the definition of u_l and u_r in (131),

$$u_r = x(\tau_1; \tau, \gamma, 0). \tag{135}$$

We have also used that $R(0; \tau, \gamma, 0) = 0$. Take a point (u, v) from the corresponding local orbit for the linear Equation (127) satisfying the same property to Ω as (x, y) to $B^2(\gamma)$. In fact, this point can be explicitly expressed as

$$u = u_r e^{\lambda \tau_1}. \tag{136}$$

Define $\pi(x, y) = (u, v)$. Properties (134) and (136) are also valid for $y = 0$, so we can extend π into the x-axis and y-axis and carry out the same construction to the other quadrants in $B^2(2\gamma)$ and Ω. It is

clear that π is well defined in a neighbourhood of U of $B^2(2\gamma)$ and satisfies the desired property of taking orbits into orbits (see Figure 28). We are now left to prove that π is a diffeomorphism. π is clearly C^0 and C^1 everywhere except at the origin. We will therefore show that $D\pi(0,0) = I$, the identity in $\mathbb{R}^2$. Let $u = \pi_1(x,y)$ and $v = \pi_2(x,y)$. By (136) we have

$$D\pi_1(x,y) = \lambda u_r e^{\lambda\tau_1} D\tau_1 \tag{137}$$

To compute $D\tau_1$ we differentiate (134) and obtain

$$(1,0) = \lambda[\phi + R]e^{\lambda\tau_1} D\tau_1 + [D\phi + DR + R'_\tau D\tau_1]e^{\lambda\tau_1}, \tag{138}$$

where $\phi = \phi(0,\gamma,y)$, from Corollary 6.10 $D\phi = (0, \phi'_y(0,\gamma,y))$ and $DR = (R_x, R_y)$. Solving for $D\tau_1$ we obtain

$$D\tau_1 = \frac{1}{[\lambda\phi + \lambda R + R'_\tau]e^{\lambda\tau_1}}\{(1,0) - (D\phi + DR)e^{\lambda\tau_1}\}. \tag{139}$$

Substituting (139) into (137) and cancelling $e^{\lambda\tau_1}$ from both the numerator and denominator, we have

$$D\pi_1(x,y) = \frac{\lambda u_r}{[\lambda\phi + \lambda R + R'_\tau]}\{(1,0) - (D\phi + DR)e^{\lambda\tau_1}\}. \tag{140}$$

Now, as $(x,y) \to 0$ from (134) we can see that $\tau_1 \to 0$ because, as we pointed out in (135) we have that $x(\tau_1;\tau_1,\gamma,0) = u_r$ and τ_1 has to be 0. Therefore, passing to the limit $(x,y) \to 0$ in (140) above and using the definition of u_r and the property that R, $R'_\tau \to 0$ as $\tau_1 \to 0$ we have that $\lim_{(x,y)\to 0} D\pi_1(x,y) = (1,0)$ uniformly in x and y. In the same way we can show

$$\lim_{(x,y)\to 0} D\pi_2(x,y) = (0,1) \qquad \text{uniformly in } x \text{ and } y. \tag{141}$$

Hence, we obtain the desired result $D\pi(0,0) = I$. □

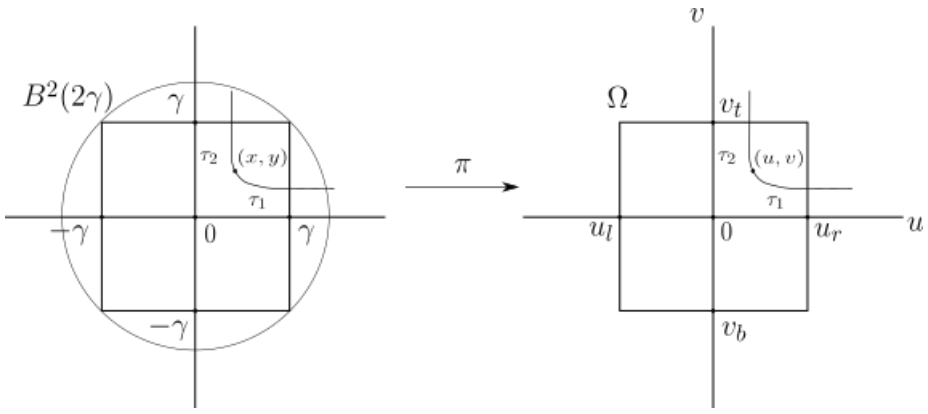

Figure 28: Regions $B^2(2\gamma)$ and Ω.

7. Bo Deng Approach to the Sil'nikov Homoclinic Saddle-Focus Theorem

In Section 5 we have seen a proof of the Sil'nikov Theorem which tells us when horseshoes appear in systems with a hyperbolic fixed point and a homoclinic orbit. In Section 6, we have seen results that have

helped us to develop new tools to understand better the solution to the Sil'nikov problem. Following the work from Bo Deng [4] we will review how he uses the exponential expansion in order to prove a result on the existence of horseshoes in systems of arbitrary dimension. We note that we will only write the initial steps of the proof in order not to excessively complicate the reading of this work. The results and proofs in this section are due to Bo Deng [4].

7.1 The Block Shift Automorphism

Let $\mathbb{N} = \{1, 2, 3, ...\}$ be the set of natural numbers with the discrete topology. This is, every subset in $\mathbb{N}$ is considered to be an open set. We compactify it by adding the symbol ∞ to $\mathbb{N}$ and denote by $\bar{\mathbb{N}} = \mathbb{N} \cup \{\infty\}$ the resulting one-point compactified space. Note that a typical open neighbourhood of ∞ consists of all the integers $k \geq M$ for a given integer $M > 0$, which is usually very large. We consider the bi-infinite product of copies of $\bar{\mathbb{N}}$, denoted by $S = \prod_{k\in\mathbb{Z}} P_k$ with $P_k \equiv \bar{\mathbb{N}}$. Since $\bar{\mathbb{N}}$ is Hausdorff (recall that a topological space $\mathcal{X}$ is Hausdorff if for any two distinct points in $\mathcal{X}$ there exist disjoint neighbourhoods that contain each of them) and compact, so is the product S. Furthermore, a point $s \in S$ is a bi-infinite sequence of the form $s = (\cdots s_{-1}.s_0 s_1 \cdots)$ with $s_i \in \bar{\mathbb{N}}$ for all $i \in \mathbb{Z}$.

Definition 7.1. We can define a typical topological basis element (recall that a basis of a topological space is a collection of open sets for which the union of all of them form the whole space) B for a given sequence $s \in S$. The basis element B must satisfy the following: there exist two integers $m \leq 0 \leq n$ and integers $M_{k_i} > 0$ which are associated only with those indexes $m \leq k_i \leq n$ such that $s_{k_i} = \infty$. A sequence $\bar{s} \in B$ if and only if $\bar{s}_{k_i} \geq M_{k_i}$ with $\bar{s}_{k_i} \in \bar{\mathbb{N}}$ for those $m \leq k_i \leq n$ such that $s_{k_i} = \infty$ and $\bar{s}_k = s_k$ for all the other indexes such that $s_k \neq \infty$, $m \leq k \leq n$.

Given an integer $s_i > 0$, denote by $\check{s}_i$ the segment of s_i symbols of the symbol s_i. This is,

$$\check{s}_i = \underbrace{s_i \cdots s_i}_{s_i \text{ times}}.$$

The objective now is to define with these symbols set Ω_ρ which will turn out to be a Cantor set. Let $\rho > 1$ be a constant and Ω_ρ denote the subspace of S consisting of sequences of the following forms:

(1) $(\cdots \check{s}_{-1}.\check{s}_0\check{s}_1 \cdots)$

(2) $(\cdots \infty \check{s}_m \cdots .\check{s}_0\check{s}_1 \cdots)$ for all $m < 0$

(3) $(\cdots \infty.\infty \cdots)$.

Where, $s_{i+1} \leq \rho s_i$ and $s_i, s_{i+1} \neq \infty$ for $i \in \mathbb{Z}$ as in (1) and $i \geq m$ as in (2), respectively. Also, $\cdots\infty$ and $(\cdots\infty.\infty\cdots)$ here stand for leftward and doubly infinite sequences of the symbol ∞, respectively. It is straightforward to check that if we extend the notation $\check{s}_i$ with $s_i = \infty$ to standing for $\check{s}_i = \cdots\infty$ if $i < 0$ and $\check{s}_i = \infty\cdots$, respectively a leftward and rightward infinite sequence of the symbol ∞. If $i \geq 0$, then all the sequences of Ω_ρ can be expressed by a single form $\check{s} = (\cdots \check{s}_{-1}.\check{s}_0\check{s}_1 \cdots)$ with $s_{i+1} \leq \rho s_i$, where s_i, $s_{i+1} \in \bar{\mathbb{N}}$ and $i \in \mathbb{Z}$. Denote by Ω_ρ^∞, Ω_ρ^u and Ω_ρ^h the subsets of sequences of types (1), (2) and (3) respectively. Then, $\Omega_\rho \cup \Omega_\rho^u \cup \Omega_\rho^h$. More importantly, since S is metrizable, it can be verified that Ω_ρ is compact because of the constraint $s_{i+1} \leq \rho s_i$. Moreover, Ω_ρ^∞ and Ω_ρ^u are dense subsets of Ω_ρ and Ω_ρ is a Cantor Set. It is compact, totally disconnected and perfect.

We define a map σ_b over the set D_ρ of all those sequences $\check{s} = (\cdots \check{s}_{-1}.\check{s}_0\check{s}_1 \cdots) \in \Omega_\rho$ such that $s_0 \neq \infty$ and $\sigma_b((\cdots \check{s}_{-1}.\check{s}_0\check{s}_1 \cdots)) = (\cdots \check{s}_{-1}\check{s}_0.\check{s}_1 \cdots)$. This means that the period is shifted over the entire initial segment $\check{s}_0$. Therefore, the domain of the map σ_b is

$$D_\rho = \{(\cdots \check{s}_{-1}.\check{s}_0\check{s}_1 \cdots) \in \Omega_\rho \quad | \quad s_0 \neq \infty\} \tag{142}$$

and the range

$$R_\rho = \{(\cdots \check{s}_{-1}.\check{s}_0\check{s}_1 \cdots) \in \Omega_\rho | s_1 \neq \infty\}. \tag{143}$$

It is direct to verify that the map $\sigma_b : D_\rho \subset \Omega_\rho \to R_\rho \subset \Omega_\rho$ is a homeomorphism in its domain of definition. The map σ_b is referred to as the block shift automorphism.

7.2 The Main Result

In this subsection we will present the main result from [4] that ensures the existence of countably many horseshoes in a system with a homoclinic saddle-focus orbit.

We consider a system of ordinary differential equations

$$\dot{z} = F(z), \qquad z \in \mathbb{R}^d, \tag{144}$$

where $f : \mathbb{R}^d \to \mathbb{R}^d$ is of class C^r with $r \geq 1$ and $d \geq 3$. Assume that the origin is a hyperbolic equilibrium point, $F(0) = 0$ and the linearization $DF(0)$ has no eigenvalues on the imaginary axis of the complex plane. As we have already defined in Section 4, a homoclinic point p_0, is a point that satisfies that $z(t, p_0) \to 0$ as $|t| \to \infty$, where $z(t, p_0)$ denotes the solution $z(t)$ of equation (144) that satisfies the initial condition $z(0) = p_0$. Denote by $\gamma(p_0) = \{z(t, p_0) | t \in \mathbb{R}\}$ the orbit of the system through p_0.

Let Σ be a codimension one cross section transverse to the vector field F at the homoclinic point p_0. In particular, Σ is a $(d-1)$-dimensional ball centered at p_0 such that the vector field F is transverse to Σ. The associated Poincaré map Π is defined on the set $\mathcal{D}$ of those points such that $p \in \mathcal{D}$ if and only if there exists the first return time $\kappa(p) > 0$. This is, $z(t, p) \in \Sigma$ for $0 < t \leq \kappa(p)$ if and only if $t = \kappa(p)$. Denote by $R = \Pi(\mathcal{D})$ the range of the Poincaré map.

Remark 7.2. Let $q = z(t_1, p_0)$ which is also a homoclinic point, then

$$\gamma(q) = \{z(t - t_1, p_0)\} = \gamma(p_0). \tag{145}$$

Once we have stated the above preliminary notions, for the main result we consider a system of ordinary differential equations (144) with a nondegenerate homoclinic-saddle-focus orbit satisfies the following conditions:

(a) The principal unstable eigenvalues, eigenvalues having the smallest positive real part, of the linearization $DF(0)$ at the equilibrium point $z = 0$ are a pair of complex conjugates $\mu \pm i\omega$ with $\omega \neq 0$. And, if $\lambda < 0$ denotes the largest real part of all the stable eigenvalues, we assume $0 < \mu < \lambda$.

(b) There is a homoclinic orbit $\gamma(p_0)$ to the saddle focus equilibrium point $z = 0$ that is in the generic position. That is,

$$\dim T_p W^s \cap T_p W^u = 1 \qquad \text{for every} \qquad p \in \gamma(p_0), \tag{146}$$

where T_pW means the tangent space of a given manifold W at a point $p \in W$ and W^s and W^u denote the stable manifold and the unstable manifold of the origin respectively.

(c) As $t \to -\infty$, the homoclinic trajectory $z(t, p_0)$ is asymptotically tangent to the principal unstable eigenvector subspace, the linear span of the eigenvectors of the eigenvalues $\mu \pm i\omega$.

(d) The system satisfies the strong inclination property. This means that there is a submanifold W_0 of the unstable manifold W^u that contains the homoclinic point p_0 and has the same dimension as the strong unstable manifold W^{uu} such that the limit

$$\lim_{t\to\infty} T_{p_t} W_t = T_q W^{uu}_{\text{loc}} \qquad \textit{with} \qquad q = 0 \tag{147}$$

exists, where $p_t = z(t, p_0)$ and $W_t = z(t, W_0)$.

We can now state the main result.

Theorem 7.3. *Suppose the vector field f of Equation (144) is of class C^5 and the conditions $(a) - (d)$ are satisfied. Given any constant ρ satisfying $1 < \rho < -\lambda/\mu$, there is a Cantor set $\Lambda_\rho \subset \Sigma$ such that the dynamics of the Poincaré map Π on Λ_ρ is topologically conjugate to the block shift automorphism σ_b on the symbolic subspace Ω_ρ (i.e. there exists an homeomorphism h such that $h \circ \Pi = \sigma_b \circ h$). More precisely, there is a homeomorphism $\phi : \Omega_\rho \to \Lambda_\rho$ such that $\Pi = \phi \circ \sigma_b \circ \phi^{-1}$ on $\Lambda_\rho - \{p_0\}$. Moreover, $\phi(\Omega^u_\rho) \cup \{p_0\} = \Lambda_\rho \cap W^u$, which is dense in Λ_ρ and $\phi(\cdots\infty.\infty\cdots) = p_0$, the homoclinic point.*

7.3 Proof of Theorem 7.3

Many topological conjugacy problems can be recast into a fixed-point problems to which the contraction mapping principle applies. This is also the case of the proof of this theorem. We divide the proof into three parts which are the set up steps for the contraction mapping principle.

To start with, we recall the Poincaré map Π described above and we modify it slightly so that it is more suitable for our purposes. Choose a sufficiently small neighbourhood U of the origin, the size of which will be specified later. Choose two codimension one cross sections Σ_0 and Σ_1 (see Figure 29) in U with the property that Σ_0 is transverse to the portion of the homoclinic orbit, $\gamma(p_0) \cap W^s_{\text{loc}}$, which lies in the local stable manifold while Σ_1 is transverse to $\gamma(p_0) \cap W^u_{\text{loc}}$. The cross section Σ is replaced by the new cross section Σ_0 from now on. The Poincaré map Π is defined as the composition of the local map $\Pi_0 : D \to \Sigma_1$ and the global map $\Pi_1 : \Sigma_1 \to \Sigma_0$. Here, D denotes the set of points of Σ_0 such that $p \in D$ if and only if there is a first time $\kappa_0(p) > 0$ such that $z(t, p) \in \Sigma_1$ for $0 < t \leq \kappa_0(p)$ if and only if $t = \kappa_0(p)$. The reason that the entire cross section Σ_1 can be assumed to be the domain of the map Π_1 is based on the property of continuous dependence of initial conditions for the solutions of Equation (144). In addition, it is also based on the fact that the connecting time from the homoclinic point $p_1 = \gamma(p_0) \cap \Sigma_1$ to p_0 via the homoclinic trajectory $z(t, p_1)$ is finite. Therefore, the set D is also the domain for the composition $\Pi_1 \circ \Pi_0$, which is defined as the Poincaré return map. Note that the intersection of the local stable manifold with Σ_0, which is the homoclinic point p_0, is not in the domain of the map Π while the image $\Pi_1(W^u_{\text{loc}} \cap \Sigma_1)$ is not in the range of the map Π.

The Local Poincaré Map In this part, we will discuss the local Poincaré map Π_0. We begin by fixing some normalized coordinate systems for the cross sections Σ_0 and Σ_1. We will then introduce the concept of Sil'nikov variables and we will end by introducing these variables to our systems.

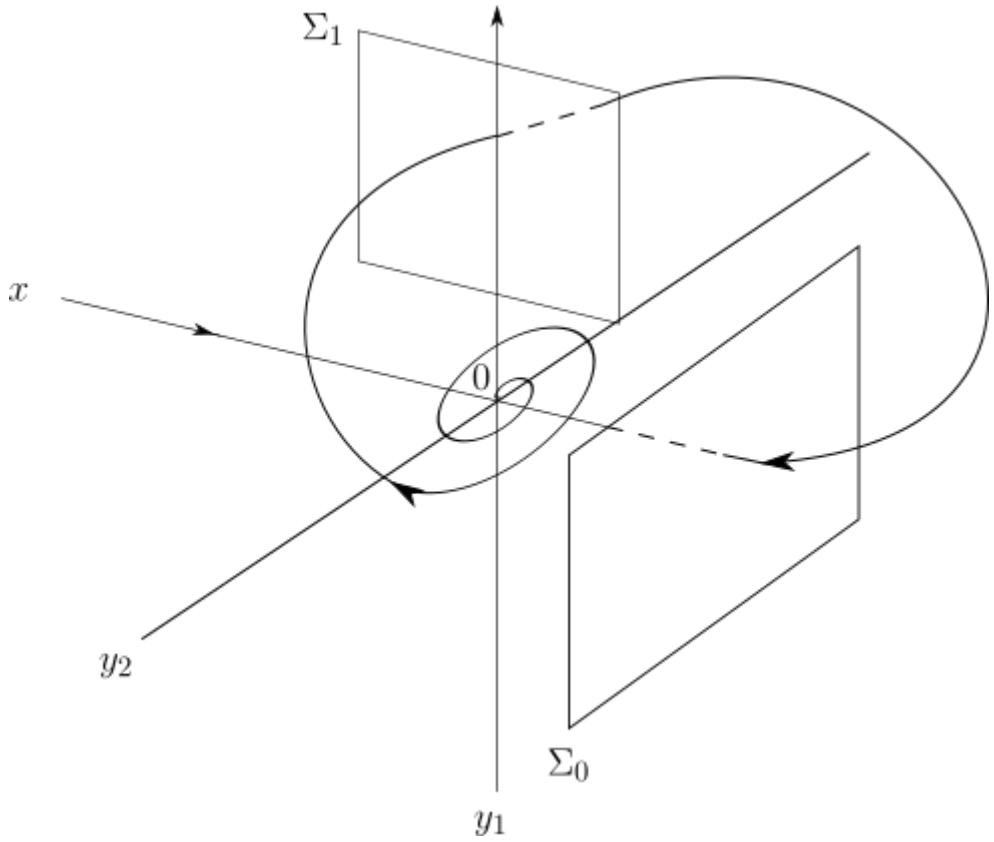

Figure 29: The sections Σ_0 and Σ_1.

We give to the neighbourhood U a local C^5 coordinate system (x, y) which is normalized in such a way that

$$W^u_{\text{loc}} = \{x = 0\} \qquad \text{and} \qquad W^s_{loc} = \{y = 0\} \tag{148}$$

locally. In addition, let the y-coordinate be chosen so that the strong unstable manifold is given by

$$W^{uu}_{\text{loc}} = \{y^{(1)} = y^{(2)} = 0, x = 0\} \tag{149}$$

locally, where $y^{(1)}$ and $y^{(2)}$ are the first two components of the vector y. Such coordinate system can be achieved by the invariant manifold theory. Note that under the C^5 assumption for the vector field F, this new coordinate system is C^4 instead.

The coordinates we have chosen give rise to the corresponding local coordinates on the cross sections Σ_0 and Σ_1. On Σ_0, x can be adjusted so that for the homoclinic point $p_0 = (\bar{x}_0, 0)$ all the components of the vector $\bar{x}_0$ except for the first, $\bar{x}_0^{(1)}$ are zero. Therefore, we can assume that $\Sigma_0 = \{x^{(1)} = \bar{x}_0^{(1)}\}$ locally and use (ξ, y) as the local coordinate system which is related to $(x, y) \in \Sigma_0$ by $x = (\bar{x}_0^{(1)}, \xi)$. A local coordinate system for Σ_1 can be chosen similarly. Indeed, since the homoclinic trajectory $z(t, p_0)$ is asimptotically tangent to the principal unstable eigenvector space, which is the $y^{(1)}, y^{(2)}$-plane under the above normalized coordinate (x, y), as $t \to -\infty$, we can choose $p_1 = (0, \bar{y}_1)$ so that all the components of the vector $\bar{y}_1$ except for the first, $\bar{y}_1^{(1)}$ are zeroes. $(x, y) \in \Sigma_1$ is obtained by relating $y = (\bar{y}_1^{(1)} + \eta^{(1)}, 0, \eta')$, where $\eta = (\eta^{(1)}, \eta')$.

We will end this sketch of the proof by presenting a crucial step which relates to what we have seen in Section 6. This is, we consider a change from the current variables to the Sil'nikov variables.

Sil'nikov Change of Variables: Let $p = (\xi, y) \in \mathcal{D} \subset \Sigma_0$ and $q = (x, \eta) = \Pi_0(p) \in \Sigma_1$ so that $z(\tau, p) = q$, where $\tau = \kappa_0(p)$. Define

$$\Delta = \{(\tau, \xi, \eta) \quad | \quad \tau \geq \tau_0, |\xi| \leq \delta, |\eta| \leq \delta\}, \tag{150}$$

where τ_0 is a large constant and δ a sufficiently small constant. In essence, we are taking points close to the stable manifold. We now claim the existence of functions that will allow us to introduce a change of variables.

Claim 7.4. *There exist C^1 functions X and Y of (τ, ξ, η) such that $z(\tau, p) = q$ is equivalent to*

$$x = X(\tau, \xi, \eta) \quad \textit{and} \quad y = Y(\tau, \xi, \eta). \tag{151}$$

Furthermore, the functions X and Y together with all the derivatives converge to zero uniformly in $|\xi| \leq \delta$ and $|\eta| \leq \delta$ as $\tau \to \infty$.

Note that this claim gives rise to a change of variables for the local map Π_0. Indeed, we can define a change

$$\begin{aligned} \rho_0 : \Delta &\to \mathcal{D} \\ (\tau, \xi, \eta) &\mapsto (\xi, Y(\tau, \xi, \eta)). \end{aligned} \tag{152}$$

The inverse is expressed explicitly as

$$\begin{aligned} \rho_0^{-1} : \mathcal{D} &\to \Delta \\ (\xi, y) &\mapsto (\tau, \xi, \eta), \end{aligned} \tag{153}$$

where τ and η are such that $(x, \eta) = q = z(\tau, p)$ with $p = (\xi, y)$. This is a crucial idea when proving this result. (τ, ξ, η) are called the Sil'nikov variables and Δ the Sil'nikov domain. Now, the local map Π_0, with the introduction of the Sil'nikov variables becomes

$$\begin{aligned} \tilde{\Pi}_0 = \Pi_0 \circ \rho_0 : \Delta &\to \Sigma_1 \\ (\tau, \xi, \eta) &\to (X(\tau, \xi, \eta), \eta) \end{aligned}. \tag{154}$$

This change of variables allows a partition of the Sil'nikov domain Δ which can be endowed with a symbolic description. This partition follows a horseshoe-like pattern.

8. A Different Proof for the Sil'nikov Theorem

Recall that in Section 5 we proved Theorem 5.1, which is Sil'nikov's result on the existence of Smale Horseshoes on a transversal section in a neighbourhood of a hyperbolic fixed point with a homoclinc orbit. We are well aware that the existence of Horseshoes implies chaotic behaviour and furthermore, in the case of Theorem 5.1 we encounter a set of countable horseshoes. An even *more* chaotic behaviour. However, in the proof of this result we assumed that there existed a neighbourhood of the fixed point in which the system was linear. Of course, this statement is not true in general. We have seen in Section 7 a proof for

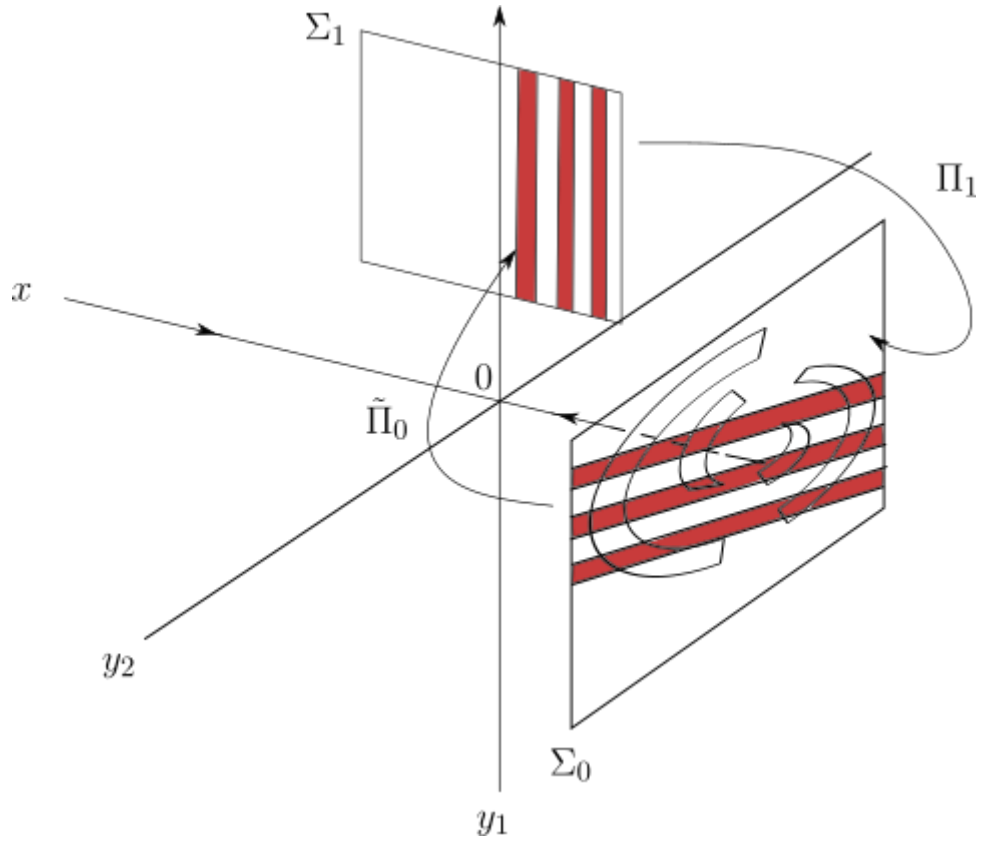

Figure 30: The decomposition of the domain Δ gives rise to a partition in $\mathcal{D}$ that presents self intersections with the iteration of the Poincaré map.

the existence of Horseshoes for arbitrary dimensional systems. The complexity of this proof may be found to be quite overwhelming at some points this is why we will restrict ourselves to dimension 3 where none of the arguments that appear in Bo Deng's approach [4] are needed in order to see a proof of Theorem 5.1 in which we will not assume that our system has a linearization property. We will mainly use ideas and results from Section 6 such as the Sil'nikov data and the exponential expansion of the solution to the Sil'nikov problem to prove it. This kind of approach can not be found in current bibliography and due to the intricacy of Bo Deng's work [4] we have taken the initiative to combine the results and ideas from Section 6 in order to remake the proof of Theorem 5.1. This will allow us to give both an understandable example of how to use the Sil'nikov data to solve a problem and a complete rigorous proof of Theorem 5.1.

We consider a flow in $\mathbb{R}^3$ induced by the system of differential equations

$$\begin{pmatrix} \dot{x} \\ \dot{y} \\ \dot{z} \end{pmatrix} = \begin{pmatrix} F_1(x,y,z) \\ F_2(x,y,z) \\ F_3(x,y,z) \end{pmatrix} \qquad \text{where } F \text{ is of class } C^{r+4}, r \geq 1. \tag{155}$$

We furthermore assume that the origin is an equilibrium point with an homoclinic orbit γ and that the

differential matrix at the equilibrium point has Jordan form

$$J = \begin{pmatrix} \alpha & \beta & 0 \\ -\beta & \alpha & 0 \\ 0 & 0 & \mu \end{pmatrix} \qquad \text{with } \alpha < 0 \text{ and } \mu > 0. \tag{156}$$

Proposition 8.1. *The system of equations* (155) *can be transformed into the system*

$$\begin{aligned} \begin{pmatrix} \dot{x} \\ \dot{y} \end{pmatrix} &= A \begin{pmatrix} x \\ y \end{pmatrix} + f(x, y, z) \\ \dot{z} &= \mu z + g(x, y, z) \end{aligned} \tag{157}$$

with $A = \begin{pmatrix} \alpha & \beta \\ -\beta & \alpha \end{pmatrix}$ *and, if* $U \subset \mathbb{R}^3$ *is a neighbourhood of the origin,* $f \in C^{k+1}(U, \mathbb{R}^2)$ *and* $g \in C^{k+1}(U, \mathbb{R})$ *with* $k \geq 1$. *Moreover,* f *and* g *satisfy*

$$f(0, 0, z) = 0 \qquad \text{for all} \quad (0, 0, z) \in U, \tag{158}$$
$$g(x, y, 0) = 0 \qquad \text{for all} \quad (x, y, 0) \in U, \tag{159}$$
$$Df(0, 0, 0) = 0 \qquad \text{and} \qquad Dg(0, 0, 0) = 0. \tag{160}$$

Proof. In first place, by doing a linear change of variables we can set the system so that the differential matrix is matrix (156). Now, we consider the parametrization of the stable manifold,

$$W^s = \{(x, y, z) \mid z = h_s(x, y)\} \quad \text{and} \quad W^u = \{(x, y, z) \mid (x, y) = (h_u^1(z), h_u^2(z))\}. \tag{161}$$

Notice that $h_s(x, y) = O_2(|(x, y)|^2)$ and $h_u^1(z), h_u^2(z) = O(|z|^2)$. The change of variables

$$\begin{aligned} u &= x - h_u^1(w), \\ v &= y - h_u^2(w), \\ w &= z - h_s(x, y), \end{aligned} \tag{162}$$

transforms (155) into

$$\begin{aligned} \begin{pmatrix} \dot{u} \\ \dot{v} \end{pmatrix} &= A \begin{pmatrix} u \\ v \end{pmatrix} + \tilde{f}(u, v, w) \\ \dot{w} &= w(\mu + \tilde{g}(u, v, w)). \end{aligned} \tag{163}$$

It is straightforward to check that (163) satisfies the conclusions of Proposition 8.1. We can henceforth assume that Equation (155) is in the form (157). □

We wish to define a return map near the origin and around γ. We will do this in two stages. We first define an inner map π_0 from a transversal section Σ_0 to another section Σ_1 defined as follows;

$$\begin{aligned} \Sigma_0 &= \{(x, y, z) \in \mathbb{R}^3 \mid x = c_0 \quad \text{and} \quad |y|, |z| \leq \delta\} \\ \Sigma_1 &= \{(x, y, z) \in \mathbb{R}^3 \mid z = c_1 \quad \text{and} \quad |x|, |y| \leq \delta\}, \end{aligned} \tag{164}$$

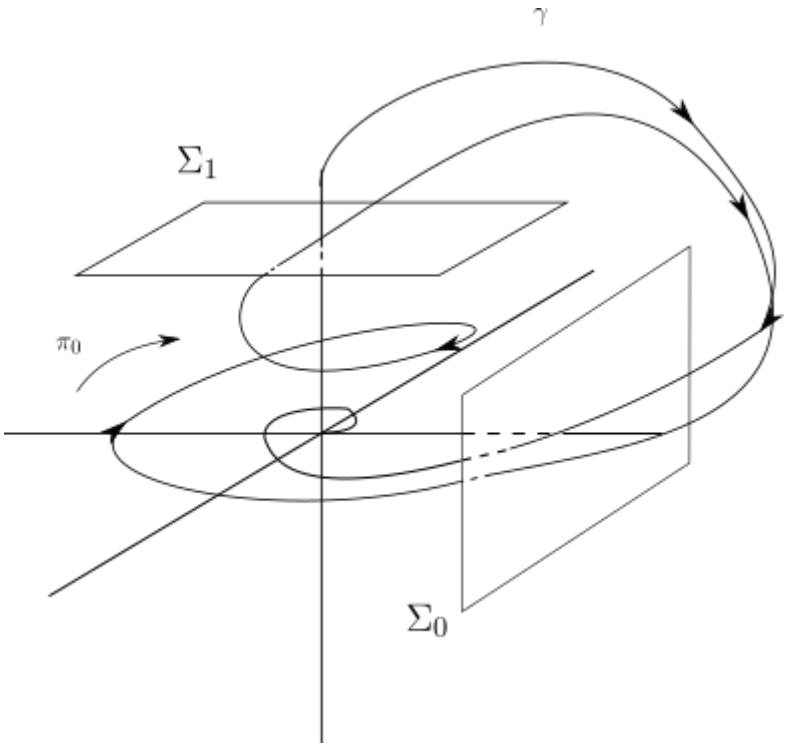

Figure 31: The figure shows the two chosen sections Σ_0 and Σ_1, the inner Poincaré map π_0 and the homoclinic orbit γ.

where c_0, c_1 and δ are small positive real fixed constants (see Figure 31).

Let $(x, y, z) : I \to U$ be a solution to Equation (157) where I is the maximum existence interval with respect to U. Since Equation (157) is autonomous we may assume that $0 \in I$. For a given $\tau \geq 0$, $(x_0, y_0) \in B_1 \subset \mathbb{R}^2$ and $z_1 \in B_2 \subset \mathbb{R}$, B_1 and B_2 open sets; (x, y, z) is the solution to the Sil'nikov problem for Equation (157) if $[0, \tau] \subseteq I$ and the following conditions are satisfied

$$(x, y)(0) = (x_0, y_0) \qquad \text{and} \qquad y(\tau) = y_1. \tag{165}$$

We note that $(\tau, (x_0, y_0), y_1)$ is the Sil'nikov data in this case. As we already know, in a neighbourhood of the origin, the Sil'nikov solution $(x, y, z)(t; \tau, (x_0, y_0), z_1)$ is unique.

In Σ_0 we can define a set D in the following way;

$$\begin{aligned} D = \{&(x_0, y_0, z_0) \in \Sigma_0 \quad | \quad \exists \tau (x_0, y_0, z_0) \quad \text{that satisfies} \\ &(x, y, z)(0) = (x_0, y_0, z_0) \notin \Sigma_1 \text{ for } 0 \leq t < \tau \text{ and } (x, y, z)(\tau) = (x_1, y_1, z_1) \in \Sigma_1\}. \end{aligned} \tag{166}$$

For a solution of the Sil'nikov problem $(x, y, z)(t; \tau, (c_0, y_0), c_1)$, $(x_0, y_0) \in D$, we can consider the exponential expansion of this solution. This is, there exists functions φ, ψ, R and r which are C^{k-1} for $k \geq 1$ such that

$$\begin{aligned} (x, y)(t; \tau, (x_0, y_0), z_1) &= e^{At}[\varphi(\tau - t, (x_0, y_0), z_1) + R(\tau - t; \tau, (x_0, y_0), z_1)] \\ z(t; \tau, (x_0, y_0), z_1) &= e^{\mu(t-\tau)}[\psi(t, (x_0, y_0), z_1) + r(t; \tau, (x_0, y_0), z_1)] \end{aligned} \tag{167}$$

and with the following properties,

a) $\frac{\partial\varphi}{\partial x_0}(t,(0,0),0) = \begin{pmatrix}0\\0\end{pmatrix}$ and $\frac{\partial\psi}{\partial x_0}(t,(0,0),0) = 0$.

b) $\frac{\partial\varphi}{\partial y_0}(t,(0,0),0) = \begin{pmatrix}0\\0\end{pmatrix}$ and $\frac{\partial\psi}{\partial y_0}(t,(0,0),0) = 0$.

c) $\frac{\partial\varphi}{\partial z_1}(t,(0,0),0) = \begin{pmatrix}1\\0\end{pmatrix}$ and $\frac{\partial\psi}{\partial z_1}(t,(0,0),0) = 1$.

d) For small enough $|(x_0,y_0)|$, $\varphi(t,(x_0,y_0),0) = 0$ and $\psi(t,(x_0,y_0),0) = 0$.

e) For small enough z_1, the second component of φ, $\varphi_2(t,(0,0),z_1) = 0$

f) R and r together with their derivatives up to order $k-1$ are bounded by $C_4e^{-\sigma t}$, $C_4e^{\sigma(t-\tau)}$ respectively and where $0 < \sigma < \min\{-\alpha,\mu\}$ and C_4 is a constant as in Subsection 6.5.

In our case, from the definition of the sections Σ_0 and Σ_1 we have $x_0 = c_0$ and $z_1 = c_1$. Therefore, we can rewrite the exponential expansion of the solution as

$$\begin{aligned}(x,y)(t;\tau,(c_0,y_0),c_1) &= e^{At}[\varphi(\tau-t,(c_0,y_0),c_1) + R(\tau-t;\tau,(c_0,y_0),c_1)]\\ z(t;\tau,(c_0,y_0),c_1) &= e^{\mu(t-\tau)}[\psi(t,(c_0,y_0),c_1) + r(t;\tau,(c_0,y_0),c_1)].\end{aligned} \tag{168}$$

Note that from the properties of φ and ψ, we can compute the Taylor expansion of these functions for a point $((c_0,y_0),c_1)$ near to $((0,0),0)$ at time τ;

$$\begin{pmatrix}\varphi_1(0,(c_0,y_0),c_1)\\ \varphi_2(0,(c_0,y_0),c_1)\\ \psi(\tau,(c_0,y_0),c_1)\end{pmatrix} = \begin{pmatrix}c_1 + O_2(c_0,y_0,c_1)\\ O_2(c_0,y_0,c_1)\\ c_1 + O_2(c_0,y_0,c_1)\end{pmatrix}. \tag{169}$$

We will use this sort of expansion many times later on.

In our case, the inner return map $\pi_0 : D \to \Sigma$ can be written as $\pi_0(y_0,\tau) = (x,y)(\tau;\tau,(c_0,y_0),c_1) = (x_1,y_1)$. Now, the formula for π_0 in terms of the exponential expansion is as in Subsection 6.5:

$$(x,y)(\tau;\tau,(c_0,y_0),c_1) = e^{\alpha\tau}\begin{pmatrix}\cos\beta\tau & -\sin\beta\tau\\ \sin\beta\tau & \cos\beta\tau\end{pmatrix}\begin{pmatrix}\varphi_1(0,(c_0,y_0),c_1) + R_1(0;\tau,(c_0,y_0),c_1)\\ \varphi_2(0,(c_0,y_0),c_1) + R_2(0;\tau,(c_0,y_0),c_1)\end{pmatrix} \tag{170}$$

We can find a more explicit expression for τ by isolating it from the exponential expansion of the z-component at $t = 0$;

$$\begin{aligned}\tau &= \mu^{-1}\log\left(\frac{\psi(0,(c_0,y_0),c_1) + r(0;\tau,(c_0,y_0),c_1)}{z_0}\right)\\ &= \mu^{-1}\left[\log\left(\frac{\psi(0,(c_0,y_0),c_1)}{z_0}\right)\left(1 + \frac{r(0;\tau,(c_0,y_0),c_1)}{\psi(0,(c_0,y_0),c_1)}\right)\right]\\ &= \underbrace{\mu^{-1}\log\left(\frac{\psi(0,(c_0,y_0),c_1)}{z_0}\right)}_{\tau_0} + \underbrace{\mu^{-1}\log\left(1 + \frac{r(0;\tau,(c_0,y_0),c_1)}{\psi(0,(c_0,y_0),c_1)}\right)}_{\tilde{\tau}}.\end{aligned} \tag{171}$$

Hence, we can write $\tau = \tau_0 + \tilde{\tau}$. In this expression for τ, we can verify that $\tilde{\tau}$ is small by considering the following space of continuous functions

$$B = \{\tilde{\tau} : [0,\delta)^2 \to [0,+\infty); \delta > 0 \quad \text{and} \quad \max_{(y_0,z_0)\in[0,\delta)^2} |\tilde{\tau}(z_0,y_0) z_0^{-\sigma/\mu}| < \infty\}, \tag{172}$$

where $|\cdot|$ refers to the absolute value. Furthermore, we also consider over B the norm

$$\begin{aligned} \|\cdot\|\colon B &\to [0,+\infty) \\ \tilde{\tau} &\mapsto \| \tilde{\tau} \| = \max_{(y_0,z_0)\in[0,\delta)^2} |\tilde{\tau}(y_0,z_0) z_0^{-\sigma/\mu}|. \end{aligned} \tag{173}$$

Now, $X = (B, \|\cdot\|)$ is a Banach space. The objective is to apply the Fixed Point Theorem to an operator $F : X \to X$ induced by the second term of τ, namely

$$F(\tilde{\tau}) = \mu^{-1} \log\left(1 + \frac{r(0;\tau_0+\tilde{\tau},(c_0,y_0),c_1)}{\psi(0,(c_0,y_0),c_1)}\right). \tag{174}$$

Lemma 8.2. *Let $R = 2 \| F(0) \|$ and denote by $B_R(0)$ the closed ball of radius R centered at the origin. The map $F : B_R(0) \to B_R(0)$ is contractive.*

Proof. Along this proof we will denote by K a generic constant which can change its value. We have that, for $|w| \ll 1$

$$|\log(1+w)| \le K|w| \tag{175}$$

and if $|w_1|, |w_2| \le 1/2$

$$|\log(1+w_1) - \log(1+w_2)| \le \sup_{|w|\le 1/2} \frac{|w_1 - w_2|}{1+w} \le K|w_1 - w_2|. \tag{176}$$

First, we prove that $\| F(0) \| < \infty$. Indeed, as $|\psi| \ge \frac{c_1}{2}$ if c_0, y_0, c_1 are small enough,

$$\left|\frac{r(0;\tau_0,(c_0,y_0),c_1)}{\psi(0,(c_0,y_0),c_1)}\right| \le \frac{e^{-\sigma\tau_0}}{c_1 + O_2} \le K e^{-\sigma\tau_0} \le K|z_0^{\sigma/\mu}| \le K\delta^{\sigma/\mu} \ll 1. \tag{177}$$

Then using (175)

$$|z_0^{-\sigma/\mu} F(0)| \le |z_0^{-\sigma/\mu}| K \left|\frac{r(0;\tau_0,(c_0,y_0),c_1)}{\psi(0,(c_0,y_0),c_1)}\right| \le K|z_0|^{-\sigma/\mu}|z_0|^{\sigma/\mu} \le K < \infty. \tag{178}$$

Now we check that the operator F is contractive. Let $\tilde{\tau}_1, \tilde{\tau}_2 \in B_R(0)$,

$$\begin{aligned} &\left|(F(\tilde{\tau}_1) - F(\tilde{\tau}_2))\, z_0^{-\sigma/\mu}\right| = \\ &\left|\mu^{-1}\left(\log\left(1 + \frac{r(0;\tau_0+\tilde{\tau}_1,(c_0,y_0),c_1)}{\psi(0,(c_0,y_0),c_1)}\right) - \log\left(1 + \frac{r(0;\tau_0+\tilde{\tau}_2,(c_0,y_0),c_1)}{\psi(0,(c_0,y_0),c_1)}\right)\right) z_0^{-\sigma/\mu}\right| \end{aligned} \tag{179}$$

By (176),

$$\left|(F(\tilde{\tau}_1) - F(\tilde{\tau}_2))\, z_0^{-\sigma/\mu}\right| \le K z_0^{-\sigma/\mu} \left|\frac{r(0;\tau_0+\tilde{\tau}_1,(c_0,y_0),c_1)}{\psi(0,(c_0,y_0),c_1)} - \frac{r(0;\tau_0+\tilde{\tau}_2,(c_0,y_0),c_1)}{\psi(0,(c_0,y_0),c_1)}\right|. \tag{180}$$

Here we have used that as in (177):

$$\left|\frac{r(0;\tau_0+\tilde{\tau}_j,(c_0,y_0),c_1)}{\psi(0,(c_0,y_0),c_1)}\right| < Ke^{-\sigma\tau_0}e^{-\sigma\tilde{\tau}_j} \leq K\delta^{-\sigma/\mu} < 1/2 \quad \text{for} \quad j=1,2. \tag{181}$$

By the Mean Value Theorem,

$$\begin{aligned} |r(0;\tau_0+\tilde{\tau}_1,(c_0,y_0),c_1) - r(0;\tau_0+\tilde{\tau}_2,(c_0,y_0),c_1)| &\leq \sup_{\tilde{\tau}\in\overline{\tilde{\tau}_1\tilde{\tau}_2}} |D_\tau r(0;\tau_0+\tilde{\tau},(c_0,y_0),c_1)||\tilde{\tau}_1-\tilde{\tau}_2| \\ &\leq K|\tilde{\tau}_1-\tilde{\tau}_2|e^{-\sigma\tau_0} \end{aligned} \tag{182}$$

where we have used that

$$|D_\tau r(0;\tau_0+\tilde{\tau},(c_0,y_0),c_1)| \leq e^{-\sigma\tau}. \tag{183}$$

Then

$$|\left(F(\tilde{\tau}_1)-F(\tilde{\tau}_2)\right)e^{-\sigma/\mu}| \leq Kz_0^{-\sigma/\mu}|\tilde{\tau}_1-\tilde{\tau}_2|e^{-\sigma\tau_0} = K \parallel \tilde{\tau}_1-\tilde{\tau}_2 \parallel \delta^{\sigma/\mu}. \tag{184}$$

For any δ small enough,

$$K\delta^{\sigma/\mu} < 1/2 \tag{185}$$

and then F is contractive. It remains to check that $F(B_R(0)) \subset B_R(0)$. Let $\tilde{\tau} \in B_R(0)$:

$$\begin{aligned} \parallel F(\tau) \parallel &\leq \parallel F(0) \parallel + \parallel F(0)-F(\tau) \parallel \\ &\leq \frac{R}{2} + \frac{1}{2} \parallel \tau - 0 \parallel \leq \frac{R}{2}+\frac{R}{2} = R \end{aligned} \tag{186}$$

and the proof is complete. □

Once we are aware of the form the time of flight τ takes, we can check that the image of a vertical segment in Σ_0, $y_0 =$ constant is mapped to a logarithmic spiral under π_0 for $z_0 \in [0,\delta)$ for some fixed $\delta > 0$ (Figure 32). Indeed, if we compute the radius R of a point $\pi_0(y_0,\tau)$;

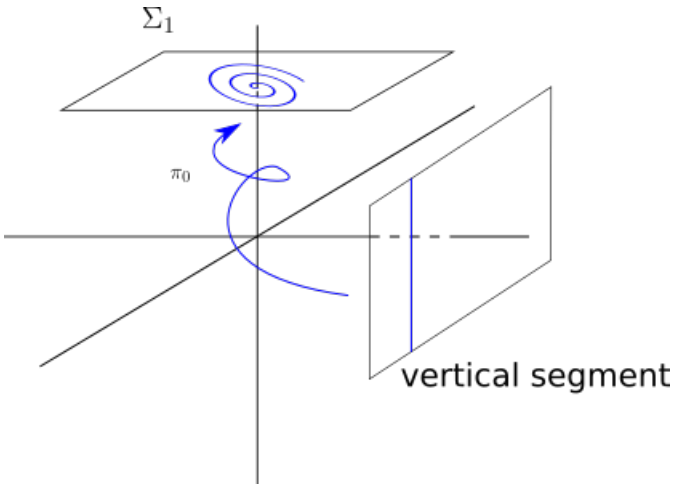

Figure 32: We must check that vertical segments in Σ_0 are mapped to spirals in Σ_1.

$$R = e^{\alpha\tau}\sqrt{(\varphi_1(0,(c_0,y_0),c_1)+R_1(0;\tau,(c_0,y_0),c_1))^2+(\varphi_2(0,(c_0,y_0),c_1)+R_2(0;\tau,(c_0,y_0),c_1))^2}. \tag{187}$$

From the properties of the exponential expansion and by operating the orders, from the above expression:

$$R = e^{\alpha\tau}\sqrt{\underbrace{\varphi_1(0,(c_0,y_0),c_1)^2+\varphi_2(0,(c_0,y_0),c_1)^2}_{c_1^2+O_2(c_0,y_0,c_1)}+O(e^{-\sigma\tau})}. \tag{188}$$

We denote $\rho_0 = \sqrt{\varphi_1(0,(c_0,y_0),c_1)^2+\varphi_1(0,(c_0,y_0),c_1)^2}$. Now, since $\tau = \tau_0+\tilde{\tau}$ from the expression for τ_0 we have

$$R = \left(\frac{z_0}{c_1+O_2(c_0,y_0,c_1)}\right)^{\frac{-\alpha}{\mu}} e^{\alpha\tilde{\tau}}\sqrt{\rho_0+\left(\frac{z_0}{c_1+O_2(c_0,y_0,c_1)}\right)^{\frac{\sigma}{\mu}} e^{-\sigma\tilde{\tau}}}. \tag{189}$$

We can observe that as $O(z_0^{\frac{\sigma}{\mu}}) \leq Kz_0^{\frac{\sigma}{\mu}}$ for some real K, (188) is in between,

$$\begin{aligned}\left(\frac{z_0}{c_1+O_2(c_0,y_0,c_1)}\right)^{\frac{-\alpha}{\mu}}\sqrt{\rho_0}\sqrt{1-Kz_0^{\frac{\sigma}{\mu}}} \leq R \leq \\ \left(\frac{z_0}{c_1+O_2(c_0,y_0,c_1)}\right)^{\frac{-\alpha}{\mu}}\sqrt{\rho_0}\sqrt{1+Kz_0^{\frac{\sigma}{\mu}}}.\end{aligned} \tag{190}$$

Bearing in mind that α is negative, we can clearly see that as z_0 tends to 0, the radius R of the images of π_0 also tends to 0. In order to emphasise the dependence on z_0 we will write $\pi_0 = \pi_0(y_0, z_0)$ although it will not always appear explicitly to avoid complicating the notation unnecessarily.

We have seen that for a vertical segment in Σ_0 the radius of the image under π_0 tends to 0 when z_0 tends to 0. This is not enough, we want to see that the image is a spiral. By looking at the expression for the exponential expansion in (170), we can see that not only does the modulus of a point in Σ_1 tend to 0 as z_0 tends to 0 but it also rotates due to the matrix exponential $e^{A\tau}$. Hence we obtain the spirals which by continuity of solutions with respect to initial conditions of differential equations, we have that these spirals are mapped diffeomorphically onto Σ_0. This means that if we take an horizontal band in Σ_0, this will be stretched into a spiral band in Σ_1 and then mapped again onto Σ_0, thus by considering the intersection of the horizontal bands in Σ_0 with the spiral bands also in Σ_0, we can see that the Poincaré map in Σ_0 maps horizontal bands to generalised vertical bands (Figure 33). This links with Theorem 3.12 which would yield the existence of a countable set of horseshoes. Note that in this way we achieve the same result as the one by Sil'nikov, Theorem 5.

9. A Look Into the Parabolic Case

Throughout this work, we have been mainly dedicated to the study of horseshoes appearing in systems with hyperbolic fixed points. As we have seen, there is an extensive bibliography that covers these cases. In this section we will concern ourselves with what happens if the fixed point of the system that we wish to study is a parabolic fixed point. In first place, we must define what parabolic fixed point means.

Definition 9.1. An equilibrium point x^* of a vector field F is parabolic if $DF(x^*)$ has some eigenvalues with real part equal to 0.

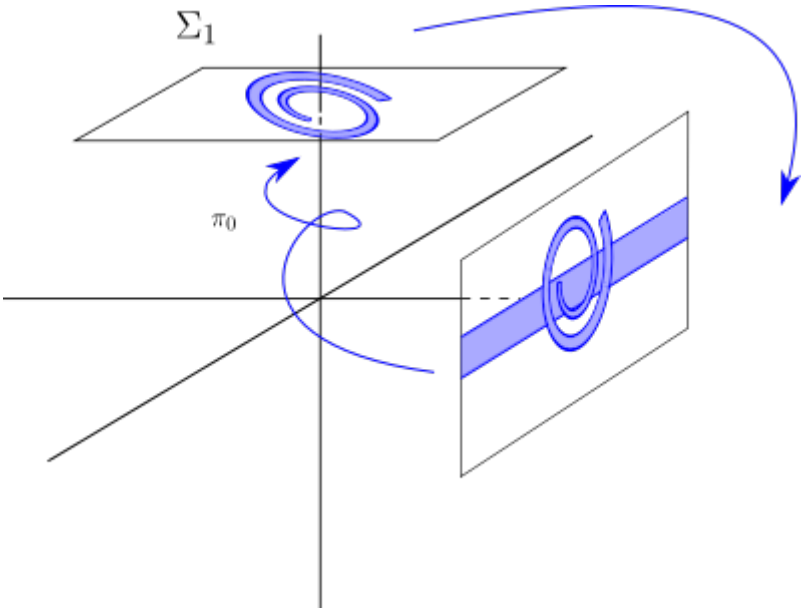

Figure 33: Due to the Poincaré map, in Σ_0, horizontal bands are mapped into spiral bands in Σ_0.

This definition may be better understood with an example. Consider the system

$$\begin{cases} \dot{x} = 3x \\ \dot{y} = y^2, \end{cases} \tag{191}$$

In this case, the origin is a fixed point and

$$DF(x, y) = \begin{pmatrix} 3 & 0 \\ 0 & 2y \end{pmatrix}. \tag{192}$$

This matrix, evaluated at the origin has eigenvalues 3 and 0 which means that it is a parabolic system.

The phenomenon we are studying, horseshoes in Sil'nikov-type flows, has not been studied as much when fixed points are parabolic (the lack of bibliography on the subject is a proof of it). This is what this section is about. We are going to present cases of parabolic systems which can be shown to contain or not horseshoes due to a Sil'nikov construction.

9.1 A First Case

We can obtain a first example of a three-dimensional system where instead of a hyperbolic equilibrium point we have a parabolic equilibrium by considering a system

$$\dot{u} = |u|^N F(u) \tag{193}$$

where $u = (x, y, z) \in \mathbb{R}^3$ and $|\cdot|$ is a norm over $\mathbb{R}^3$. Note that the result we are about to expose is also valid if instead of $|u|^N$ we have a positive function $\rho = \rho(x, y, z)$ which is 0 at the origin as a factor.

Claim 9.2. *If $\rho(u) > 0$ for all $u \in U\backslash\{0\}$ and $F(u)$ satisfies that the eigenvalues of $DF(0)$ are $\alpha \pm i\beta, \mu, \mu > 0$ and $-\alpha > \mu$, then the flow ϕ_t can be perturbed to ϕ'_t such that ϕ'_t has a homoclinic orbit γ' near γ and the return map of γ' for ϕ'_t has a countable set of horseshoes.*

We can find a change of time $t = t(s)$ such that if

$$\frac{du}{ds} = \frac{du}{dt} \cdot \frac{dt}{ds} = |u|^N F(u) \frac{dt}{ds} \tag{194}$$

then, by taking $\frac{dt}{ds} = \frac{1}{|u|^N}$ system (193) is transformed into

$$u' = F(u). \tag{195}$$

In this situation, as in Section 8, if F is such that

$$\begin{pmatrix} \dot{x} \\ \dot{y} \\ \dot{z} \end{pmatrix} = \begin{pmatrix} F_1(x,y,z) \\ F_2(x,y,z) \\ F_3(x,y,z) \end{pmatrix} \qquad \text{where } F \text{ is of class } C^{r+4},\ r \geq 1 \tag{196}$$

and we furthermore assume that the origin is an equilibrium point with an homoclinic orbit γ and that the differential matrix of F at the origin is

$$PDFP^{-1}(0) = \begin{pmatrix} \alpha & \beta & 0 \\ -\beta & \alpha & 0 \\ 0 & 0 & \mu \end{pmatrix} \qquad \text{with } \alpha < 0 \text{ and } \mu > 0. \tag{197}$$

Then performing the linear change $P^{-1}u = \tilde{u}$

$$\begin{aligned} \begin{pmatrix} \dot{\tilde{x}} \\ \dot{\tilde{y}} \end{pmatrix} &= A \begin{pmatrix} \tilde{x} \\ \tilde{y} \end{pmatrix} + O_2(\tilde{x}, \tilde{y}, \tilde{z}) \\ \dot{\tilde{z}} &= \mu \tilde{z} + O_2(\tilde{x}, \tilde{y}, \tilde{z}) \end{aligned} \tag{198}$$

with $A = \begin{pmatrix} \alpha & \beta \\ -\beta & \alpha \end{pmatrix}$. Hence, the Sil'nikov Theorem 5.1 assures that for system (195) there exists a set of countable Smale Horseshoes. As systems (195) and (193) have the same curves as orbits (they only differ in the amount of time needed to follow an orbit), we have that system (193) also has a Horseshoe.

9.2 Horseshoes in Parabolic Systems

We can look further into systems with parabolic fixed points. Consider a flow ϕ_t in $\mathbb{R}^3$ for which the associated vector field has a parabolic equilibrium point at the origin with a pair of complex eigenvalues ω, $\overline{\omega}$ which have negative real parts and a zero eigenvalue. As in all the other cases, we assume that there exists an homoclinic orbit at the origin. As in parabolic systems it is not possible to have an expansion in the way we did in Section 8, we will bypass this problem by assuming that in a neighbourhood of the origin our system is of a particular form.

Claim 9.3. *Consider a flow ϕ_t with an equilibrium point at the origin with an homoclinic orbit γ. Assume that in a neighbourhood of the origin, the flow is governed by the system of equations*

$$\begin{aligned} \begin{pmatrix} \dot{x} \\ \dot{y} \end{pmatrix} &= A \begin{pmatrix} x \\ y \end{pmatrix} \\ \dot{z} &= \mu z^N, \end{aligned} \tag{199}$$

where $\alpha + i\beta = \omega$, $A = \begin{pmatrix} \alpha & -\beta \\ \beta & \alpha \end{pmatrix}$, $\mu > 0$ *and* $N > 0$ *a natural number. Then, the Poincaré map around* γ *contains a countable set of horseshoes.*

We can explicitly integrate the system and find an expression for ϕ_t.

$$\begin{pmatrix} x \\ y \\ z \end{pmatrix}(t) = \begin{pmatrix} e^{\alpha t}\left(\cos(\beta t)x_0 - \sin(\beta t)y_0\right) \\ e^{\alpha t}\left(\sin(\beta t)x_0 + \cos(\beta t)y_0\right) \\ \left(z_0^{-(N-1)} - \mu(N-1)t\right)^{\frac{-1}{N-1}} \end{pmatrix}. \tag{200}$$

Note that as in the hyperbolic case, the radial coordinate $r = \sqrt{x^2 + y^2} = e^{\alpha t}\sqrt{x_0^2 + y_0^2}$ of trajectories that flow past near the origin decreases while the height z increases.

We now define two sections in the neighbourhood of the origin we are working in, Σ_0 and Σ_1. As in the proof of Theorem 5.1,

$$\begin{aligned} \Sigma_0 &= \{(x, y, z) | x^2 + y^2 = r_0^2 \quad \text{and} \quad 0 < z < z_1\} \\ \Sigma_1 &= \{(x, y, z) | x^2 + y^2 < r_0^2 \quad \text{and} \quad z = z_1 > 0\}. \end{aligned} \tag{201}$$

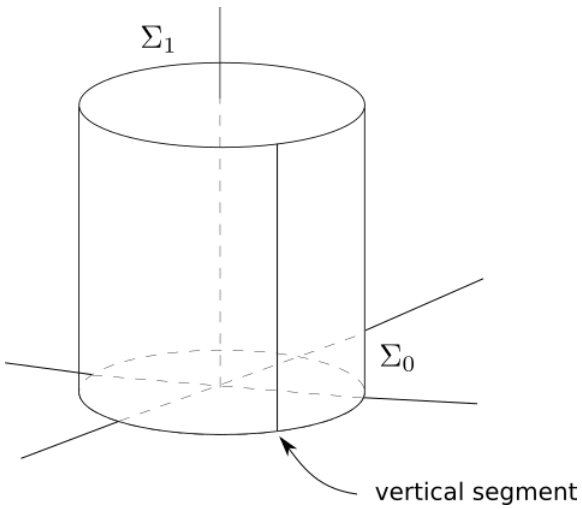

Figure 34: Sections Σ_0 and Σ_1.

We want to compute the mapping $\pi_0 : \Sigma_0 \to \Sigma_1$ which associates to every point in Σ_0 the first intersection with Σ_1 of the trajectory starting at that point.

The formula for π_0 is given by solving

$$z_1 = \left(z_0^{-(N-1)} - \mu(N-1)t\right)^{\frac{-1}{N-1}} \tag{202}$$

for t. This yields the time of flight

$$t_1 = \frac{-1}{\mu(N-1)}\left(z_1^{-(N-1)} - z_0^{-(N-1)}\right). \tag{203}$$

Substituting now the result into (200) we obtain

$$\phi_t(x,y,z) = \left(e^{\alpha t_1}[\cos(\beta t_1)x - \sin(\beta t_1)y], e^{\alpha t_1}[\sin(\beta t_1)x + \cos(\beta t_1)y], z_1\right). \tag{204}$$

We now endow Σ_0 with cylindrical coordinates by setting $x = r_0\cos\theta$ and $y = r_0\sin\theta$. Then, when $(x,y,z) \in \Sigma_0$

$$\phi_t(x,y,z) = e^{\alpha t_1} r_0(\cos(\beta t_1 + \theta), \sin(\beta t_1 + \theta)). \tag{205}$$

The domain of these coordinates is $\theta = \mathrm{Arg}(x+iy)$ and z. We can now express $\pi_0 : \Sigma_0 \to \Sigma_1$ as a two-dimensional diffeomorphism whose range has coordinates x, y:

$$\pi_0(\theta, z) = \left(e^{\alpha t_1} r_0 \cos(\beta t_1 + \theta), e^{\alpha t_1}\sin(\beta t_1 + \theta)\right). \tag{206}$$

It is now decisive to check that vertical segments in Σ_0; $\theta =$ constant are transformed into spirals parametrized by z. We start by checking that the radius R of points $\pi_0(\theta, z)$ decreases as z decreases;

$$R = r_0 e^{\alpha t_1} = e^{\alpha\left(\frac{-1}{\mu(N-1)}\left(z_1^{-(N-1)} - z^{-(N-1)}\right)\right)} r_0. \tag{207}$$

Since $\alpha < 0$ and z is fixed, the exponent is negative for every z and R tends to 0 as z tends to 0.

We also check that the angle spins. We compute Θ, the argument of $\pi_0(\theta, z)$ We trivially have that

$$\Theta = \beta t_1 + \theta = \frac{-\beta}{\mu(N-1)}(z_1^{-(N-1)} - z^{-(N-1)}) + \theta. \tag{208}$$

Hence, the angle continues to spin as in the hyperbolic case in Section 5. In fact it spins much faster. We could now follow an argument similar to the one in the proof of Theorem 5.1 in order to prove the existence of Smale Horseshoes in a small set in Σ_0 around the homoclinic orbit.

The parabolic system we have just seen allows us to justify the existence of Horseshoes if we multiply the (x,y) component by a power of z as follows

Claim 9.4. *Consider a flow ϕ_t with an equilibrium point at the origin with an homoclinic orbit γ. Assume that in a neighbourhood of the origin, the flow is governed by the system of equations*

$$\begin{aligned} \begin{pmatrix}\dot{x}\\ \dot{y}\end{pmatrix} &= z^M A \begin{pmatrix} x \\ y\end{pmatrix} \\ \dot{z} &= \mu z^N. \end{aligned} \tag{209}$$

where $\alpha + i\beta = \omega$, $A = \begin{pmatrix}\alpha & -\beta \\ \beta & \alpha\end{pmatrix}$, $\mu > 0$ and $N > 0$ a natural number. Then, the Poincaré map around γ contains a countable set of horseshoes.

In this case, as we did before in Subsection 9.1 we can do a change of time that satisfies that $\frac{dt}{ds} = \frac{1}{z^M}$. This way, we obtain that the original system is transformed into

$$\begin{aligned} \begin{pmatrix}\dot{x}\\ \dot{y}\end{pmatrix} &= A \begin{pmatrix} x \\ y\end{pmatrix} \\ \dot{z} &= \mu z^{N-M}. \end{aligned} \tag{210}$$

Now, if $N - M > 1$ we are clearly in the situation of Equation (199). And if $N - M = 1$, we are in the case of Theorem 5.1 where it is required that $|\alpha| < \mu$. In both cases we have the existence of Horseshoes. On the other hand, if $N - M = N' \leq 0$, if we follow the exact same set up as in (200), the expression for the time of flight is $t_1 = \frac{1}{\mu(|N'|+1)}\left(z_1^{|N'|+1} - z^{|N'|+1}\right)$. We can define π_0 in the same way as in (206). In this case, the polar coordinates of a point $\pi_0(\theta, z)$ are

$$R = e^{\frac{\alpha}{\mu(|N'|+1)}(z_1^{|N'|+1} - z^{|N'|+1})}. \tag{211}$$

Note that as z tends to 0, R decreases but does not tend to 0. We can also look a the angle,

$$\Theta = \frac{\beta}{\mu(|N'|+1)}(z_1^{|N'|+1} - z^{|N'|+1}) + \theta. \tag{212}$$

We can see that as z tends to 0, the angle Θ tends to a fixed value. Therefore, the image under π_0 of vertical segments in Σ_0 does not spiral enough. In this case, horseshoes will not appear in this way.

We continue to study parabolic systems that can be explicitly solved to see if Sil'nikov-like horseshoes appear. For instance, the system

$$\begin{aligned} \begin{pmatrix} \dot{x} \\ \dot{y} \end{pmatrix} &= A \begin{pmatrix} x \\ y \end{pmatrix} \\ \dot{z} &= \mu(x^2 + y^2)^N z \end{aligned} \tag{213}$$

can be explicitly solved,

$$\begin{pmatrix} x \\ y \\ z \end{pmatrix}(t) = \begin{pmatrix} e^{\alpha t}(x_0 \cos \beta t - y_0 \sin \beta t) \\ e^{\alpha t}(x_0 \sin \beta t + y_0 \cos \beta t) \\ e^{\frac{\mu}{2N\alpha}[e^{2N\alpha t} - 1]}|z_0| \end{pmatrix}. \tag{214}$$

We proceed exactly the same as before by defining two sections Σ_0 and Σ_1

$$\begin{aligned} \Sigma_0 &= \{(x, y, z) | x^2 + y^2 = r_0^2 \quad \text{and} \quad 0 < z < z_1\} \\ \Sigma_1 &= \{(x, y, z) | x^2 + y^2 < r_0^2 \quad \text{and} \quad z = z_1 > 0\}. \end{aligned} \tag{215}$$

Now, we compute the time it takes for a point in Σ_0 to reach Σ_1. In order to do so, we must solve $z_1 = z(t)$ for t. This is,

$$\begin{aligned} z_1 &= e^{\frac{\mu}{2N\alpha}[e^{2N\alpha t} - 1]}|z_0| \\ \frac{2N\alpha}{\mu} \log \frac{z_1}{|z_0|} + 1 &= e^{2N\alpha t} \end{aligned}. \tag{216}$$

Note that the left hand side of the above equation has to be positive in order to isolate t. This is if and only if

$$\frac{\alpha}{\mu} > \frac{-1}{2N \log\left(\frac{z_1}{z_0}\right)}. \tag{217}$$

It is crucial that this constraint is attainable when z_0 tends to 0, as we are interested in the dynamics near the homoclinic orbit, but as z_0 goes to 0, the right hand side of the above inequality is unbounded, hence it is not possible to find fixed α and μ which satisfy the constraint for all $z_0 < z_1$. This means that there

are points in Σ_0 that never reach Σ_1. Therefore, through this kind of construction we will fail to observe horseshoes for the return map around the homoclinic orbit.

A very similar case can be found by taking a power of z,

$$\begin{aligned} \begin{pmatrix} \dot{x} \\ \dot{y} \end{pmatrix} &= A \begin{pmatrix} x \\ y \end{pmatrix} \\ \dot{z} &= \mu(x^2+y^2)^N z^2 \end{aligned} \tag{218}$$

which has the solution

$$\begin{pmatrix} x \\ y \\ z \end{pmatrix}(t) = \begin{pmatrix} e^{\alpha t}(x_0 \cos\beta t - y_0 \sin\beta t) \\ e^{\alpha t}(x_0 \sin\beta t + y_0 \cos\beta t) \\ \frac{z_0}{1-\frac{z_0(x_0^2+y_0^2)\mu}{2N\alpha}(e^{2N\alpha t}-1)} \end{pmatrix}. \tag{219}$$

With the exact same construction as before, if we try to solve $z_1 = z(t)$ for z, we have

$$\begin{aligned} z_1 &= \frac{z_0}{1-\frac{z_0(x_0^2+y_0^2\mu)}{2N\alpha}(e^{2N\alpha t}-1)} \\ \left(\frac{1}{z_0}-\frac{1}{z_1}\right)\frac{2N\alpha}{\mu(x_0^2+y_0^2)^N} + 1 &= e^{2N\alpha t}. \end{aligned} \tag{220}$$

In the second equality, the left-hand side must be positive in order to be able to apply the logarithm to isolate t. This is equivalent to,

$$\frac{\alpha}{\mu} > \frac{-(x_0^2+y_0^2)^N}{2N\left(\frac{1}{z_0}-\frac{1}{z_1}\right)}. \tag{221}$$

The right-hand side of this inequality tends to 0 as z_0 tends to 0, so taking $\frac{\alpha}{\mu}$ greater than the supremum in z_0 is enough. We therefore apply logarithms on the equation for t and obtain

$$\frac{1}{2N\alpha}\log\left(\left(\frac{1}{z_0}-\frac{1}{z_1}\right)\frac{2N\alpha}{\mu(x_0^2+y_0^2)^N}+1\right) = t. \tag{222}$$

In the above equality the first factor is negative, $\frac{1}{2N\alpha} < 0$, so we need the second factor to be also negative in order to have a positive time of flight. This is if and only if

$$\left(\frac{1}{z_0}-\frac{1}{z_1}\right)\frac{2N\alpha}{\mu(x_0^2+y_0^2)^N}+1 < 1 \tag{223}$$

which is in turn equivalent to $\frac{1}{z_0} < \frac{1}{z_1}$, which is a contradiction because $z_0 < z_1$. So in this case the time of flight from Σ_0 to Σ_1 does not exist. Hence, we will not encounter horseshoes around the homoclinic orbit due to this construction.

9.3 Future Work

This section has briefly shown that in some cases, parabolic systems can be remitted to hyperbolic systems or solved in order to prove the existence or lack of horseshoes due to Sil'nikov-like constructions. We are therefore left with a wide open door to future investigations on the field of parabolic systems. This would

include studying generalised versions of Equation (199). One generalisation can be obtained by adding higher order terms to the equation,

$$\begin{aligned} \begin{pmatrix} \dot{x} \\ \dot{y} \end{pmatrix} &= A \begin{pmatrix} x \\ y \end{pmatrix} + O_2(x, y, z) \\ \dot{z} &= \mu z^N + O_{N+1}(x, y, x). \end{aligned} \tag{224}$$

Another generalisation can be obtained by multiplication of the z-component by a scalar function,

$$\begin{aligned} \begin{pmatrix} \dot{x} \\ \dot{y} \end{pmatrix} &= A \begin{pmatrix} x \\ y \end{pmatrix} \\ \dot{z} &= f(x, y, z)\mu z^N. \end{aligned} \tag{225}$$

We can also think in a generalization of (199) by considering

$$\begin{aligned} \begin{pmatrix} \dot{x} \\ \dot{y} \end{pmatrix} &= f_1(x, y, z) \left[A \begin{pmatrix} x \\ y \end{pmatrix} + O_2(x, y, z) \right] \\ \dot{z} &= f_2(x, y, z)[\mu z^N + O_{N+1}(x, y, z)]. \end{aligned} \tag{226}$$

It is not known in general under which conditions these systems present horseshoes. This leaves us with many open questions.

10. Bibliography

References

[1] D. K. Arrowsmith and C. M. Place, *An Introduction to Dynamical Systems*, Cambridge University Press, 1990.

[2] Inma Baldomá Barraca i Pau Martín de la Torre, *Introducció als Sistemes Dinàmics*, Facultat de Matemàtiques i Estadística, 2018.

[3] Bo Deng, *The Sil'nikov Problem, Exponential Expansion, Strong λ-Lemma, C^1-Linearization and Homoclinic Bifurcation*, Journal of Differential Equations, Vol. 79, No. 2, June 1989.

[4] Bo Deng, *On Silnikov's Homoclinic-Saddle-Focus Theorem*. Journal of Differential Equations, Vol. 102, pages 305-329, 1993.

[5] Bo Deng website `www.math.unl.edu/~bdeng1/`

[6] Robert L. Devaney, *An Introduction to Chaotic Dynamical Systems* Addison-Wesley Redwood City, Calif 1989.

[7] John Guckenheimer and Philip Holmes, *Nonlinear Oscillations, Dynamical Systems and Bifurcations of Vector Fields*, Applied Mathematical Sciences 42, Springer, 1983.

[8] Yuri A. Kuznetsov, *Elements of Applied Bifurcation Theory*, Applied Mathematical Sciences 112, Springer, 1998.

[9] Leonid P. Sil'nikov, *A Case of the Existence of a Countable Number of Periodic Motions*, Soviet Math. Dokl. 6, pages 163-166, 1965.